UNIVERSITY OF AMSTERDAM

UvA-DARE (Digital Academic Repository)

Measurement of the electroweak production of dijets in association with a Z-boson and distributions sensitive to vector boson fusion in proton-proton collisions at √s = 8 TeV using the ATLAS detector

Aad, G.; et al., [Unknown]; Aben, R.; Beemster, L.J.; Bentvelsen, S.; Berge, D.; Berglund, E.; Bobbink, G.J.; Bos, K.; Boterenbrood, H.; Castelli, A.; Colijn, A.P.; de Jong, P.; de Nooij, L.; Deigaard, I.; Deluca, C.; Deviveiros, P.O.; Dhaliwal, S.; Ferrari, P.; Gadatsch, S.; Geerts, D.A.A.; Hartjes, F.; Hessey, N.P.; Hod, N.; Igonkina, O.; Kluit, P.; Koffeman, E.; Lee, H.; Lenz, T.; Linde, F.; Mahlstedt, J.; Mechnich, J.; Oussoren, K.P.; Pani, P.; Salek, D.; Valencic, N.; van der Deijl, P.C.; van der Geer, R.; van der Graaf, H.; van der Leeuw, R.; van Vulpen, I.; Verkerke, W.; Vermeulen, J.C.; Vranjes Milosavljevic, M.; Vreeswijk, M.; Weits, H.

DOI
10.1007/JHEP04(2014)031

Publication date
2014

Document Version
Final published version

Published in
The Journal of High Energy Physics

Link to publication

Citation for published version (APA):
Aad, G., et al., U., Aben, R., Beemster, L. J., Bentvelsen, S., Berge, D., Berglund, E., Bobbink, G. J., Bos, K., Boterenbrood, H., Castelli, A., Colijn, A. P., de Jong, P., de Nooij, L., Deigaard, I., Deluca, C., Deviveiros, P. O., Dhaliwal, S., Ferrari, P., ... Weits, H. (2014). Measurement of the electroweak production of dijets in association with a Z-boson and distributions sensitive to vector boson fusion in proton-proton collisions at √s = 8 TeV using the ATLAS detector. *The Journal of High Energy Physics*, *2014*(4), Article 31. https://doi.org/10.1007/JHEP04(2014)031

General rights
It is not permitted to download or to forward/distribute the text or part of it without the consent of the author(s) and/or copyright holder(s), other than for strictly personal, individual use, unless the work is under an open content license (like Creative Commons).

UvA-DARE is a service provided by the library of the University of Amsterdam (https://dare.uva.nl)

Disclaimer/Complaints regulations
If you believe that digital publication of certain material infringes any of your rights or (privacy) interests, please let the Library know, stating your reasons. In case of a legitimate complaint, the Library will make the material inaccessible and/or remove it from the website. Please Ask the Library: https://uba.uva.nl/en/contact, or a letter to: Library of the University of Amsterdam, Secretariat, P.O. Box 19185, 1000 GD Amsterdam, The Netherlands. You will be contacted as soon as possible.

Download date:15 Oct 2026

Published for SISSA by Springer

Received: *January 30, 2014*
Accepted: *March 5, 2014*
Published: *April 7, 2014*

Measurement of the electroweak production of dijets in association with a Z-boson and distributions sensitive to vector boson fusion in proton-proton collisions at $\sqrt{s} = 8$ TeV using the ATLAS detector

The ATLAS collaboration

E-mail: atlas.publications@cern.ch

Abstract: Measurements of fiducial cross sections for the electroweak production of two jets in association with a Z-boson are presented. The measurements are performed using 20.3 fb^{-1} of proton-proton collision data collected at a centre-of-mass energy of $\sqrt{s} = 8$ TeV by the ATLAS experiment at the Large Hadron Collider. The electroweak component is extracted by a fit to the dijet invariant mass distribution in a fiducial region chosen to enhance the electroweak contribution over the dominant background in which the jets are produced via the strong interaction. The electroweak cross sections measured in two fiducial regions are in good agreement with the Standard Model expectations and the background-only hypothesis is rejected with significance above the 5σ level. The electroweak process includes the vector boson fusion production of a Z-boson and the data are used to place limits on anomalous triple gauge boson couplings. In addition, measurements of cross sections and differential distributions for inclusive Z-boson-plus-dijet production are performed in five fiducial regions, each with different sensitivity to the electroweak contribution. The results are corrected for detector effects and compared to predictions from the `Sherpa` and `Powheg` event generators.

Keywords: Electroweak interaction, Jets, Hadron-Hadron Scattering

ArXiv ePrint: 1401.7610

Open Access, Copyright CERN,
for the benefit of the ATLAS Collaboration.
Article funded by SCOAP^3.

doi:10.1007/JHEP04(2014)031

Contents

1 Introduction **2**

2 The ATLAS detector **3**

3 Event reconstruction and selection **4**

4 Theoretical predictions **5**

5 Monte Carlo simulation **6**

6 Fiducial cross-section measurements of inclusive Zjj production **7**
- 6.1 Backgrounds 9
- 6.2 Systematic uncertainties 9
- 6.3 Comparison of data and simulation 11
- 6.4 Cross section determination 11

7 Differential distributions of inclusive Zjj production **13**
- 7.1 Analysis methodology and unfolding to particle level 14
- 7.2 Systematic uncertainties 15
- 7.3 Unfolded differential distributions 16

8 Extraction of the electroweak Zjj fiducial cross section **21**
- 8.1 Template construction and fit results 21
- 8.2 Validation of the control region constraint procedure 23
- 8.3 Systematic uncertainties on the fit procedure 25
- 8.4 Measurement of fiducial cross section 27
- 8.5 Estimate of signal significance 28
- 8.6 Limits on anomalous triple gauge couplings 29

9 Summary **30**

A Additional inclusive Zjj differential distributions **32**

The ATLAS collaboration **40**

JHEP04(2014)031

1 Introduction

The dominant production mechanism for a leptonically decaying Z/γ^*-boson[1] in association with two jets (Zjj) at the Large Hadron Collider (LHC) is via the Drell-Yan process, with the additional jets arising as a result of the strong interaction. Production of Zjj events via the t-channel exchange of an electroweak gauge boson is a purely electroweak process and is therefore much rarer. Electroweak Zjj production in the leptonic decay channel is defined to include all contributions to $\ell^+\ell^- jj$ production for which there is a t-channel exchange of an electroweak gauge boson [1, 2]. These contributions include Z-boson production via vector boson fusion (VBF), Z-boson bremsstrahlung and non-resonant production, as shown in figure 1. The VBF process is of particular interest because of the similarity to the VBF production of a Higgs boson and the sensitivity to anomalous WWZ triple gauge couplings.[2]

This paper presents two measurements of Zjj production using 20.3 fb^{-1} of proton-proton collision data collected by the ATLAS experiment [3] at a centre-of-mass energy of $\sqrt{s} = 8$ TeV:

1. Measurements of fiducial cross sections and differential distributions of inclusive Zjj production. These measurements are performed in five fiducial regions with different sensitivity to the electroweak component. Inclusive Zjj production is dominated by the strong production process, an example of which is shown in figure 2(a). The data therefore provide important constraints on the theoretical modelling of QCD-initiated processes that produce VBF-like topologies.[3]

2. Observation of electroweak Zjj production and measurements of the cross section in two fiducial regions. Limits are also placed on anomalous WWZ couplings.

These measurements are performed using a combination of the $Z \to e^+e^-$ and $Z \to \mu^+\mu^-$ decay channels.

Using electroweak Zjj production as a probe of colour-singlet exchange and as a validation of the vector boson fusion process has been discussed extensively in the literature [1, 4, 5]. A previous measurement by the CMS Collaboration showed evidence for electroweak Zjj production using proton-proton collisions at $\sqrt{s} = 7$ TeV [6]. However, due to large experimental and theoretical uncertainties associated with the modelling of strong Zjj production, the background-only hypothesis could be rejected only at the 2.6σ level. The measurement presented in this paper constrains the modelling of strong Zjj production using a data-driven technique. This allows the background-only hypothesis to be rejected at greater than 5σ significance and leads to a more precise cross section measurement for electroweak Zjj production.

[1] The contribution from γ^* production in association with two jets is substantially reduced in this analysis by an invariant mass cut on the Z/γ^* decay products.

[2] The VBF process cannot be isolated due to a large destructive interference with the electroweak Z-boson bremsstrahlung process. The contribution to the electroweak cross section from non-resonant $\ell^+\ell^- jj$ production is less than 1% after applying the selection criteria used in this analysis.

[3] Inclusive Zjj production contains a small (percent-level) contribution from diboson events (figure 2(b)).

JHEP04(2014)031

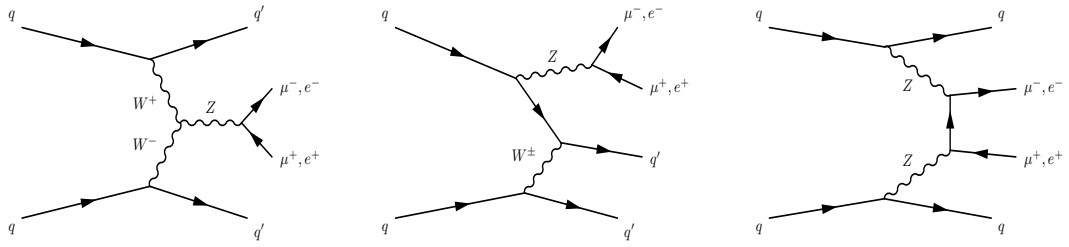

(a) vector boson fusion (b) Z-boson bremsstrahlung (c) non-resonant $\ell^+\ell^- jj$

Figure 1. Representative leading-order Feynman diagrams for electroweak Zjj production at the LHC: (a) vector boson fusion (b) Z-boson bremsstrahlung and (c) non-resonant $\ell^+\ell^- jj$ production.

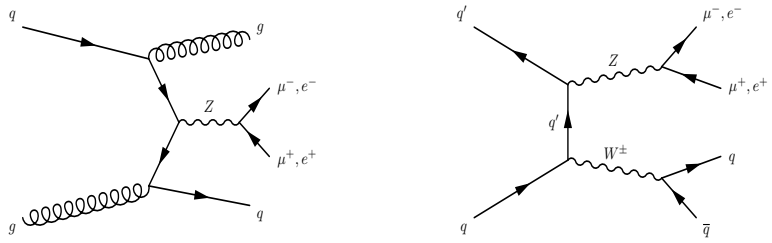

(a) strong Zjj production (b) diboson-initiated

Figure 2. Examples of leading-order Feynman diagrams for (a) strong Zjj production and (b) diboson-initiated Zjj production.

2 The ATLAS detector

The ATLAS detector is described in detail in ref. [3]. Tracks and interaction vertices are reconstructed with the inner detector tracking system, which consists of a silicon pixel detector, a silicon microstrip detector and a transition radiation tracker, all immersed in a 2 T axial magnetic field, providing charged-particle tracking in the pseudorapidity range $|\eta| < 2.5$.[4] The ATLAS calorimeter system provides fine-grained measurements of shower energy depositions over a wide range of η. An electromagnetic liquid-argon sampling calorimeter covers the region $|\eta| < 3.2$. It is divided into a barrel part ($|\eta| < 1.475$) and an endcap part ($1.375 < |\eta| < 3.2$). The hadronic barrel calorimeter ($|\eta| < 1.7$) consists of steel absorbers and active scintillator tiles. The hadronic endcap calorimeter ($1.5 < |\eta| < 3.2$) and forward electromagnetic and hadronic calorimeters ($3.1 < |\eta| < 4.9$) use liquid argon as

[4] ATLAS uses a right-handed coordinate system with its origin at the nominal interaction point (IP) in the centre of the detector and the z-axis along the beam pipe. The x-axis points from the IP to the centre of the LHC ring, and the y-axis points upward. Cylindrical coordinates (r, ϕ) are used in the transverse plane, ϕ being the azimuthal angle around the beam pipe. The pseudorapidity is defined in terms of the polar angle θ as $\eta = -\ln\tan(\theta/2)$. The rapidity is defined as $y = 0.5 \ln\left((E + p_z)\,/\,(E - p_z)\right)$, where E and p_z refer to energy and longitudinal momentum, respectively.

JHEP04(2014)031

the active medium. The muon spectrometer comprises separate trigger and high-precision tracking chambers measuring the deflection of muons in a magnetic field generated by superconducting air-core toroids. The precision chamber system covers the region $|\eta| < 2.7$ with three layers of monitored drift tube chambers, complemented by cathode strip chambers in the forward region, where the background is highest. The muon trigger system covers the range $|\eta| < 2.4$ with resistive plate chambers in the barrel, and thin gap chambers in the endcap regions. A three-level trigger system is used to select interesting events [7]. The Level-1 trigger reduces the event rate to less than 75 kHz using hardware-based trigger algorithms acting on a subset of detector information. Two software-based trigger levels further reduce the event rate to about 400 Hz using the complete detector information.

3 Event reconstruction and selection

The measurement is performed using proton-proton collision data recorded at $\sqrt{s} = 8\,\text{TeV}$. The data were collected between April and December 2012 and correspond to an integrated luminosity of 20.3 fb^{-1}. Events containing a Z-candidate in the $\mu^+\mu^-$ decay channel were retained for further analysis using a single-muon trigger, with muon transverse momentum, p_{T}, greater than 24 GeV or 36 GeV (isolation criteria are applied at the lower threshold). Events containing a Z-candidate in the e^+e^- decay channel were retained using a dielectron trigger with both electrons having $p_{\text{T}} > 12\,\text{GeV}$.

In both decay channels, events are required to have a reconstructed collision vertex, defined by at least three associated inner detector tracks with $p_{\text{T}} > 400\,\text{MeV}$. The primary vertex for each event is then defined as the collision vertex with the highest sum of squared transverse momenta of associated inner detector tracks. Finally, the event is required to be in a data-taking period in which the detector was fully operational.

Muon candidates are identified as tracks in the inner detector matched and combined with track segments in the muon spectrometer [8]. They are required to have $p_{\text{T}} > 25\,\text{GeV}$ and $|\eta| < 2.4$. In order to suppress backgrounds, track quality requirements are imposed for muon identification, and impact parameter requirements ensure that the muon candidates originate from the primary vertex. The muon candidates are also required to be isolated: the scalar sum of the p_{T} of tracks with $\Delta R < 0.2$ around the muon track is required to be less than 10% of the p_{T} of the muon. The radius parameter is defined as $(\Delta R)^2 = (\Delta\eta)^2 + (\Delta\phi)^2$.

Electron candidates are reconstructed from clusters of energy in the electromagnetic calorimeter matched to inner detector tracks. They are required to have $p_{\text{T}} > 25\,\text{GeV}$ and $|\eta| < 2.47$, but excluding the transition regions between the barrel and endcap electromagnetic calorimeters, $1.37 < |\eta| < 1.52$. The electron candidates must satisfy a set of 'medium' selection criteria [9] that have been reoptimised for the higher rate of proton-proton collisions per beam crossing (pileup) observed in the 2012 data. Impact parameter requirements ensure the electron candidates originate from the primary vertex.

Jets are reconstructed with the anti-k_t jet algorithm [10] with a jet-radius parameter of 0.4. The input objects to the jet algorithm are three-dimensional topological clusters of energy in the calorimeter [11]. The resultant jet energies are initially corrected to account

JHEP04(2014)031

for soft energy arising from pileup [12]. The energy and direction of each jet is then corrected for calorimeter non-compensation, detector material and the transition between calorimeter regions, using a combination of MC-derived calibration constants and in situ data-driven calibration constants [13, 14]. Jets are required to have $p_{\mathrm{T}} > 25\,\mathrm{GeV}$ and $|y| < 4.4$, where y is the rapidity. Additional data quality requirements are imposed to minimise the effect of noisy calorimeter cells. To suppress jets from overlapping proton-proton collisions, the jet vertex fraction (JVF) is used to identify jets from the primary interaction. Tracks are associated with jets using ghost-association [15], where tracks are assigned negligible momentum and clustered to the jet using the anti-k_t algorithm. The JVF is subsequently defined as the scalar summed transverse momentum of associated tracks from the primary vertex divided by the summed transverse momentum of associated tracks from all vertices. Each jet with $p_{\mathrm{T}} < 50\,\mathrm{GeV}$ and $|\eta| < 2.4$ is required to have JVF > 0.5. Finally, jets are required to be well separated from any of the selected leptons (jets within a cone of radius $\Delta R < 0.3$ in η–ϕ space around any lepton are removed from the analysis).

4 Theoretical predictions

Theoretical predictions for strong and electroweak Zjj production are obtained using the `Powheg Box` [16–18] and `Sherpa` v1.4.3 [19] event generators. The small contribution from diboson events is estimated using `Sherpa`.

`Sherpa` is a matrix-element plus parton-shower generator that provides $Z + n$-parton predictions ($n = 0, 1, 2\ldots$) at leading-order (LO) accuracy in perturbative QCD. The CKKW method is used to combine the various final-state topologies and match to the parton shower [20]. Electroweak Zjj production is accurate at LO for two and three partons in the final state. Strong Zjj production is accurate at LO for two, three and four partons in the final state, and the Z-boson plus zero and one parton configurations are also produced (at LO accuracy) to allow contributions from double parton scattering to be included. Diboson-initiated Zjj production (ZV) is generated with up to three partons in addition to the partonically decaying boson. For all production channels, parton-shower, hadronisation and multiple parton interaction (MPI) algorithms create the fully hadronic final state. The `Sherpa` predictions are produced using the `CT10` [21] parton distribution functions (PDFs) and the default generator tune for underlying event activity.

The `Powheg Box` provides Zjj predictions at next-to-leading-order (NLO) accuracy in perturbative QCD for both electroweak and strong production [22–25]. The fully hadronic final state is produced by interfacing the `Powheg Box` to `PYTHIA 6` [26], which provides parton showering, hadronisation and MPI. These particle level-predictions are referred to as `Powheg` in the remainder of this paper. The `Powheg` predictions are produced using the `CT10` PDFs and the Perugia 2011 tune [27] for underlying event activity. The strong Zjj sample was generated with the MiNLO feature [28], which also produces Z plus zero and one jet events at LO accuracy and allows contributions to Zjj production from double parton scattering to be evaluated.

JHEP04(2014)031

Theoretical uncertainties are estimated for the strong and electroweak Zjj predictions from Sherpa and Powheg. Scale uncertainties on all theoretical predictions are estimated by varying the renormalisation and factorisation scales (separately) by a factor of 0.5 and 2.0. Additional modelling uncertainties in the Sherpa prediction arise from the choice of CKKW matching scale, the choice of parton-shower scheme, and the MPI-modelling.[5] Similar modelling uncertainties in the Powheg prediction are estimated using the suite of Perugia 2011 tunes [27], with the largest effects coming from those tunes with increased/decreased parton-shower activity or increased MPI activity.

The use of independent strong and electroweak Zjj samples relies on the fact that interference between the two processes is colour and kinematically suppressed, and therefore negligible. Interference between the strong and electroweak processes has been proven to be negligible for the production of the Higgs boson in association with two jets (Hjj) [32–35]. Although no such studies have been performed for the electroweak production of a Zjj system, the interference effects arise from the same sources as Hjj production and should therefore be small. The assumption of negligible interference is checked for this measurement using a combined strong/electroweak Sherpa sample that is accurate to leading order for Zjj production. This combined sample includes electroweak and strong Zjj matrix elements at the amplitude level and thereby calculates the interference between them. The interference contribution is established by subtracting the strong-only and electroweak-only Zjj components. The impact of interference on inclusive Zjj cross sections and distributions is found to be negligible. The impact of interference on the extraction of the electroweak Zjj component is at the few-percent level and is discussed in more detail in section 8.

5 Monte Carlo simulation

Event generator samples are passed through GEANT4 [36, 37] for a full simulation [38] of the ATLAS detector and reconstructed with the same analysis chain as used for the data. Pileup is simulated by overlaying inelastic proton-proton interactions produced with PYTHIA 8 [39], tune A2 [40] with the MSTW2008LO PDF set [41].

Strong and electroweak Zjj simulated events are produced using the Sherpa samples discussed in section 4. The samples are normalised to reproduce the NLO calculations for Zjj production obtained from Powheg; the NLO K-factors are 1.23 and 1.02 for the strong and electroweak samples, respectively. The contribution from ZV events is also produced using Sherpa. To cross-check aspects of the theoretical modelling of strong Zjj production at the detector level, a small simulated sample of Zjj events is produced using ALPGEN [42]. ALPGEN is a leading-order matrix-element generator that produces Z-boson

[5] The uncertainty in the CKKW matching is determined by increasing the matching scale by a factor of two. Uncertainties associated with the parton shower are estimated by changing the recoil strategy for dipoles with initial-state emitter and final-state spectator, from the default [29] to that proposed in ref. [30]. The uncertainty due to a potential mismodelling of the underlying event is estimated by increasing the MPI activity uniformly by 10% [31], or changing the shape of the MPI spectrum such that more jets from double parton scattering are produced. The parameter variations for the latter are: SIGMA_ND_FACTOR=0.14 and SCALE_MIN=4.0

JHEP04(2014)031

events with up to five additional partons in the final state and is interfaced to HERWIG [43, 44] and JIMMY [45] to add the parton shower, hadronisation and MPI (AUET2 tune [46]).

Background events stemming from $t\bar{t}$ and single-top production are produced using MC@NLO v4.03 [47] interfaced to HERWIG and JIMMY (AUET2 tune). The generator modelling of $t\bar{t}$ events is cross-checked with a simulated sample produced using the Powheg Box interfaced to PYTHIA 6 (Perugia 2011 tune). The $t\bar{t}$ samples are normalised to a next-to-next-to-leading-order (NNLO) calculation in QCD including resummation of next-to-next-to-leading-logarithmic (NNLL) soft gluon terms [48]. The backgrounds arising from WW and W+jets events are produced using Sherpa.

6 Fiducial cross-section measurements of inclusive Zjj production

The cross section for inclusive Zjj production, σ_{fid}, is defined by

$$\sigma_{\text{fid}} = \frac{N_{\text{obs}} - N_{\text{bkg}}}{\int L\,\mathrm{d}t \cdot \mathcal{C}} \tag{6.1}$$

where N_{obs} is the number of events observed in the data passing the reconstruction-level selection criteria, N_{bkg} is the expected number of background events, $\int L\,\mathrm{d}t$ is the integrated luminosity and $\mathcal{C}$ is a correction factor accounting for differences in event yields at reconstruction and particle level due to detector inefficiencies and resolutions.

The particle-level prediction is constructed using final-state particles with mean lifetime ($c\tau$) longer than 10 mm. Leptons are defined as objects constructed from the four-momentum combination of an electron (or muon) and all nearby photons in a cone of radius $\Delta R = 0.1$ in η–ϕ space centred on the lepton (so-called 'dressed leptons'). Leptons are required to have $p_{\text{T}} > 25\,\text{GeV}$ and $|\eta| < 2.47$. Jets are reconstructed using the anti-k_t algorithm with a jet-radius parameter of 0.4. Jets are required to have $p_{\text{T}} > 25\,\text{GeV}$, $|y| < 4.4$ and $\Delta R_{j,\ell} \geq 0.3$, where $\Delta R_{j,\ell}$ is the distance in η–ϕ space between the jet and the selected leptons.

The cross section for inclusive Zjj production is measured in five fiducial regions, each with different sensitivity to the electroweak component of Zjj production. A summary of the selection criteria for each fiducial region is given in table 1. The *search* region is chosen to optimise the expected significance when extracting the electroweak Zjj component, and is defined as:

- A Z-boson candidate, defined as exactly two oppositely charged, same-flavour leptons with a dilepton invariant mass of $81 \leq m_{\ell\ell} < 101\,\text{GeV}$.
- The transverse momentum of the dilepton pair must satisfy $p_{\text{T}}^{\ell\ell} > 20\,\text{GeV}$.
- At least two jets that satisfy $p_{\text{T}}^{j_1} > 55\,\text{GeV}$, $p_{\text{T}}^{j_2} > 45\,\text{GeV}$, where j_1 and j_2 label the highest and second highest transverse momentum jets in the event.
- The invariant mass of the two leading jets is required to satisfy $m_{jj} > 250\,\text{GeV}$.
- No additional jets with $p_{\text{T}} > 25\,\text{GeV}$ in the rapidity interval between the two leading jets.

JHEP04(2014)031

Object	*baseline*	*high-mass*	*search*	*control*	*high-p_{T}*
Leptons	$\lvert\eta^{\ell}\rvert < 2.47$, $p_{\mathrm{T}}^{\ell} > 25\,\mathrm{GeV}$				
Dilepton pair	$81 \le m_{\ell\ell} \le 101\,\mathrm{GeV}$				
	—		$p_{\mathrm{T}}^{\ell\ell} > 20\,\mathrm{GeV}$		—
Jets	$\lvert y^{j}\rvert < 4.4$, $\Delta R_{j,\ell} \ge 0.3$				
	$p_{\mathrm{T}}^{j_1} > 55\,\mathrm{GeV}$				$p_{\mathrm{T}}^{j_1} > 85\,\mathrm{GeV}$
	$p_{\mathrm{T}}^{j_2} > 45\,\mathrm{GeV}$				$p_{\mathrm{T}}^{j_2} > 75\,\mathrm{GeV}$
Dijet system	—	$m_{jj} > 1\,\mathrm{TeV}$	$m_{jj} > 250\,\mathrm{GeV}$		—
Interval jets	—		$N_{\mathrm{jet}}^{\mathrm{gap}} = 0$	$N_{\mathrm{jet}}^{\mathrm{gap}} \ge 1$	—
Zjj system	—		$p_{\mathrm{T}}^{\mathrm{balance}} < 0.15$	$p_{\mathrm{T}}^{\mathrm{balance},3} < 0.15$	—

Table 1. Summary of the selection criteria that define the fiducial regions. 'Interval jets' refer to the selection criteria applied to the jets that lie in the rapidity interval bounded by the dijet system.

- The normalised transverse-momentum balance between the two leptons and the two highest transverse momentum jets, $p_{\mathrm{T}}^{\mathrm{balance}}$, is required to be less than 0.15. The $p_{\mathrm{T}}^{\mathrm{balance}}$ is defined as

$$p_{\mathrm{T}}^{\mathrm{balance}} = \frac{\left|\vec{p}_{\mathrm{T}}^{\,\ell_1} + \vec{p}_{\mathrm{T}}^{\,\ell_2} + \vec{p}_{\mathrm{T}}^{\,j_1} + \vec{p}_{\mathrm{T}}^{\,j_2}\right|}{\left|\vec{p}_{\mathrm{T}}^{\,\ell_1}\right| + \left|\vec{p}_{\mathrm{T}}^{\,\ell_2}\right| + \left|\vec{p}_{\mathrm{T}}^{\,j_1}\right| + \left|\vec{p}_{\mathrm{T}}^{\,j_2}\right|}, \tag{6.2}$$

  where $\vec{p}_{\mathrm{T}}^{\,i}$ is the transverse momentum vector of object i, and ℓ_1 and ℓ_2 label the two leptons that define the Z-boson candidate.

The tight cut on the dilepton invariant mass is chosen to suppress backgrounds from events that do not contain a Z-boson. The high-p_{T} requirement on the two leading jets and the veto on additional jet activity preferentially suppress strong Zjj production with respect to electroweak Zjj production. The dijet invariant mass criterion removes a large fraction of diboson events. The $p_{\mathrm{T}}^{\mathrm{balance}}$ and $p_{\mathrm{T}}^{\ell\ell}$ requirements reduce the impact of those events containing jets that originate from pileup interactions or multiple parton interactions. Events with poorly measured jets are also removed by the $p_{\mathrm{T}}^{\mathrm{balance}}$ requirement.

The *control* region criteria are chosen in order to suppress the electroweak Zjj contribution, allowing the theoretical modelling of strong Zjj production to be evaluated. The selection criteria are similar to the *search* region, with two modifications: (i) at least one additional jet with $p_{\mathrm{T}} > 25\,\mathrm{GeV}$ must be present in the rapidity interval between the two leading jets. (ii) the transverse-momentum balancing variable is redefined to use the two leptons, the two highest transverse momentum jets, and the highest transverse momentum jet in the rapidity interval bounded by the two leading jets. This variable, $p_{\mathrm{T}}^{\mathrm{balance},3}$, is defined in an analogous way to the $p_{\mathrm{T}}^{\mathrm{balance}}$ variable in eq. (6.2), but incorporating the additional jet in the numerator and denominator.

JHEP04(2014)031

The remaining three fiducial regions are chosen with fewer selection criteria, in order to study inclusive Zjj production in simpler topologies. The *baseline* region is defined as containing a Z-boson candidate plus at least two jets with $p_{\mathrm{T}}^{j_1} > 55\,\mathrm{GeV}$ and $p_{\mathrm{T}}^{j_2} > 45\,\mathrm{GeV}$. This is the most inclusive fiducial region examined and contains the events in all other fiducial regions. The *high-mass* region is chosen as the subset of these events that have $m_{jj} > 1\,\mathrm{TeV}$. The *high-p_{T}* region is defined as containing a Z-boson candidate plus at least two jets with $p_{\mathrm{T}}^{j_1} > 85\,\mathrm{GeV}$ and $p_{\mathrm{T}}^{j_2} > 75\,\mathrm{GeV}$. The *high-mass* and *high-p_{T}* regions are useful to probe the impact of the electroweak Zjj process, which produces a harder jet transverse momentum and harder dijet invariant mass than the strong Zjj process.

The simulation-based correction factor ($\mathcal{C}$) used to correct the measurement to the particle level is estimated using the `Sherpa` Zjj samples. The correction factor is found to lie between 0.80 and 0.92 in the muon channel, and between 0.64 and 0.71 in the electron channel, depending on the fiducial region. The difference between the channels arises primarily from the different efficiency in reconstructing and identifying electrons and muons in the detector.

6.1 Backgrounds

The contributions from the $t\bar{t}$, WW, tW and W+jets background processes are obtained by applying the analysis chain to the dedicated simulated samples introduced in section 5. The multijet background contributes if two jets are misidentified as leptons or contain leptons from b- or c-hadron decays. A multijet sample is obtained from the data by reversing some of the electron identification criteria for the analysis in the electron channel, or reversing the muon isolation criteria for the analysis in the muon channel. The normalisation of the multijet sample in each fiducial region is then obtained by a two-component template fit to the dilepton invariant mass distributions, using the multijet template and a template formed from all other processes.

Table 2 shows the composition by percentage of the predicted signal and background processes in each of the five fiducial regions. The event sample is dominated by processes producing a Z-boson in the final state. The dominant background to inclusive Zjj production is from $t\bar{t}$ production.

6.2 Systematic uncertainties

The systematic uncertainties on the lepton reconstruction, identification, isolation and trigger efficiencies, as well as the lepton momentum scale and resolution, are defined in refs. [9, 49]. The total impact of the lepton-based systematic uncertainties on the cross-section measurement in each fiducial region is typically 3% in the electron channel and 2% in the muon channel. The uncertainty on the integrated luminosity is estimated to be 2.8%, using the methodology detailed in ref. [50] for beam-separation scans performed in November 2012.

The jet energy scale (JES) and jet energy resolution (JER) uncertainties account for differences between the calorimeter response in simulation and data [13, 14, 51]. The JES uncertainty for 2012 data includes components for the soft-energy pileup corrections, the MC-based/data-driven calibration constants, the calibration of forward jets, and the

JHEP04(2014)031

	Composition (%)				
Process	*baseline*	*high-p_{T}*	*search*	*control*	*high-mass*
Strong Zjj	95.8	94.0	94.7	96.0	85
Electroweak Zjj	1.1	2.1	4.0	1.4	12
WZ and ZZ	1.0	1.3	0.7	1.4	1
$t\bar{t}$	1.8	2.2	0.6	1.0	2
Single top	0.1	0.1	< 0.1	< 0.1	< 0.1
Multijet	0.1	0.2	< 0.1	0.2	< 0.1
WW, W+jets	< 0.1	< 0.1	< 0.1	< 1.1	< 0.1

Table 2. Process composition (%) for each fiducial region for the combined muon and electron channels. The strong Zjj, electroweak Zjj, diboson, $t\bar{t}$, W+jets and tW rates are estimated by running the analysis chain over MC samples fully simulated in the ATLAS detector. The multijet background is estimated using a data-driven technique.

unknown jet flavour.[6] The uncertainty due to JES is the dominant systematic uncertainty, ranging from 7.5% in the *search* region to 19% in the *high-mass* region. The uncertainty due to JER is much smaller, ranging from 0.1% in the *high-p_{T}* region to 5% in the *high-mass* region.

The JVF cut removes a fraction of the jets associated with the primary vertex in addition to the jets originating from pileup interactions. Any mismodelling of the JVF distribution therefore introduces a possible bias in the shape and normalisation of the distributions. A systematic uncertainty is determined after repeating the full analysis using modified JVF cuts that cover possible differences in efficiency between data and simulation. The JVF cuts are varied by ± 0.03 and the uncertainty due to JVF modelling is found to be between 0.2% and 2.8% in the *baseline* and *control* regions, respectively.

Hard jets originating from the additional (pileup) interactions are also reconstructed in the event and any mismodelling of pileup jets in the simulation is a source of systematic uncertainty. In the central calorimeter region, the JVF cut removes a large fraction of these jets. In the forward calorimeter regions (outside the inner detector acceptance), no track-based cut can be applied to remove these pileup jets. To estimate the impact of a possible mismodelling of the jets originating from pileup, the analysis is repeated using the simulated samples after removing pileup jets, defined as those reconstruction-level jets that are not matched ($\Delta R \leq 0.3$) to a particle-level jet from the hard scattering process with $p_{\mathrm{T}} > 10\,\mathrm{GeV}$. The effect of pileup on each cross section measurement is then determined by comparing the reconstruction-level event yield obtained in simulation after applying jet matching to that obtained with no matching applied. Studies of the central jet transverse momentum in a pileup-enhanced sample (JVF < 0.1), and the transverse energy density in the forward region of the detector [52], indicate that the simulation could be mismodelling the number of pileup jets by up to 35%. The difference between the reconstruction-level event yields obtained with and without jet matching is therefore scaled by 0.35 and taken

[6] The jet flavour uncertainty refers to the different calorimeter response for quark-initiated and gluon-initiated jets.

JHEP04(2014)031

as a two-sided systematic uncertainty on the fiducial cross section. The impact on the final measurement is not large, ranging from less than 0.1% in the *search* region to 2.3% in the *baseline* region.

In addition to the experimental uncertainties discussed above, systematic uncertainties on the correction factor, $\mathcal{C}$, due to possible event generator mismodelling are evaluated. These generator modelling uncertainties are estimated by reweighting the events, at reconstruction level and particle level, such that the kinematic distributions in the simulation match those observed in the data. The reweighting is carried out for the two lepton transverse momenta and pseudorapidities, the two leading jet transverse momenta and pseudorapidities, and the variables used to define the fiducial regions. The correction factor is re-evaluated for each reweighting and the difference with respect to the nominal correction factor is taken as a theory modelling uncertainty. The uncertainty on the correction factor from theoretical modelling ranges from 1% in the *baseline* region to 6.6% in the *high-mass* region.

The uncertainty due to background subtraction is found to be between 0.2% in the *search* region and 0.5% in the *high-mass* region. This accounts for the uncertainty in the normalisation of the inclusive $t\bar{t}$ sample, generator modelling differences in $t\bar{t}$ events predicted by `MC@NLO` and `Powheg`, and the uncertainty in the data-driven method used to determine the multijet background.

The total systematic uncertainty on the inclusive Zjj cross-section measurement in each fiducial region is defined as the quadrature sum of all sources of experimental and theoretical uncertainty.

6.3 Comparison of data and simulation

Figure 3 shows data compared to MC simulation in the *baseline* region, as a function of the leading jet transverse momentum and rapidity, the subleading jet transverse momentum and rapidity, and the invariant mass and rapidity separation of the two leading jets. The uncertainty on the simulation due to the experimental systematic uncertainties is shown in the ratio as a hatched (blue) band. In general, the simulation gives an adequate description of the data, although there are indications of generator mismodelling at high jet transverse momentum and high dijet invariant mass. The contribution from $t\bar{t}$ and multijet events remains small in each bin of the distributions.

6.4 Cross section determination

The cross sections are measured in the muon and electron decay channels separately. The cross-section measured in each fiducial region is found to be compatible between the two channels, with a maximum difference of 1.1σ after accounting for those uncertainties that are uncorrelated between channels. The results are then combined[7] to obtain a weighted average, with each channel's weight set to the inverse squared uncorrelated uncertainty. Table 3 presents the measured inclusive Zjj cross sections in the five fiducial regions together

[7]The individual- and combined-channel cross sections are defined using dressed leptons as discussed in section 6. Cross sections defined using 'Born' leptons (which originate directly from the Z-boson decay and before final state QED radiation) would differ by 2–3%.

JHEP04(2014)031

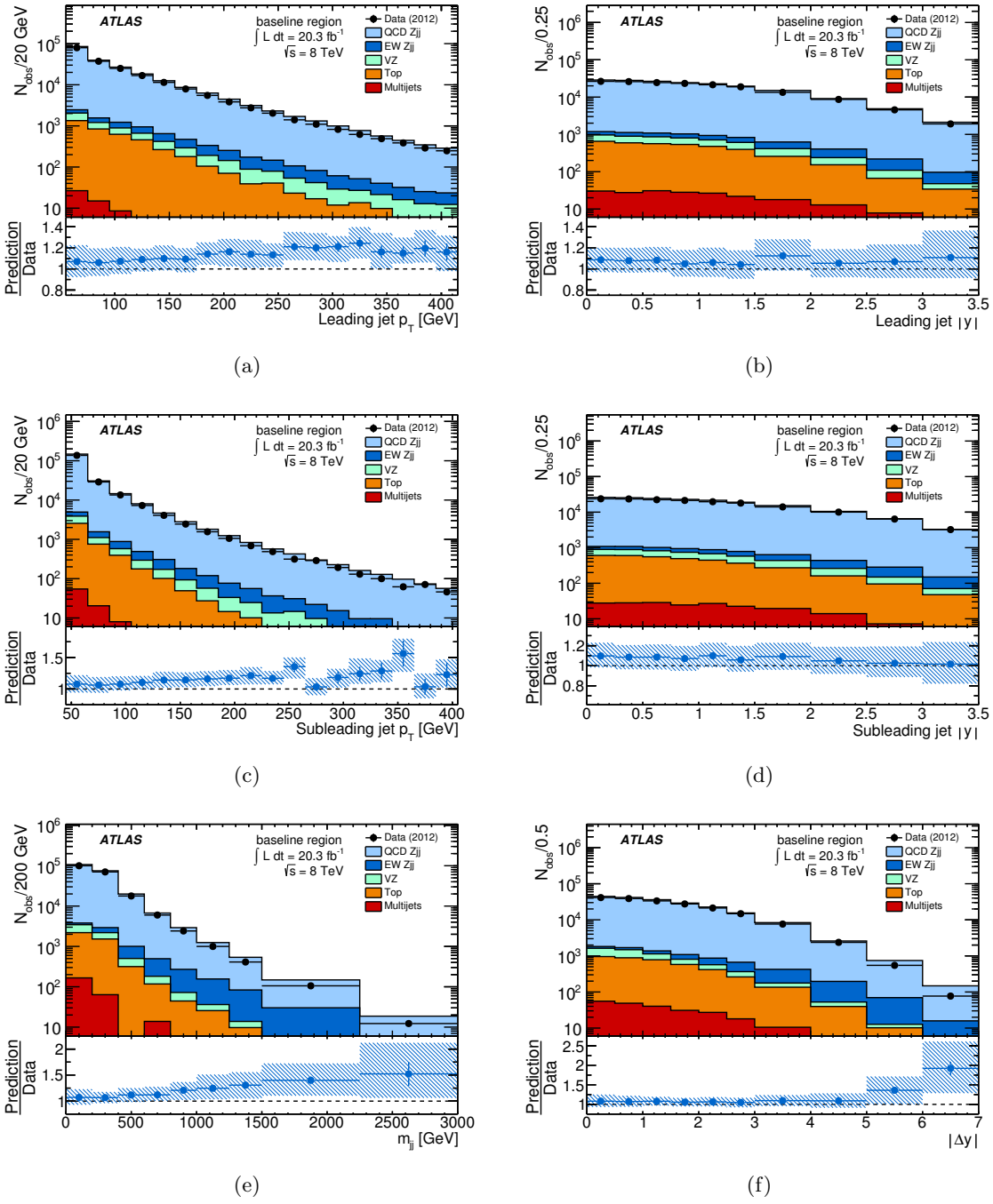

Figure 3. Comparison of data and simulation in the *baseline* region for (a,b) the leading jet transverse momentum and rapidity, (c,d) the subleading jet transverse momentum and rapidity, (e,f) the invariant mass and rapidity span of the dijet system. The simulated samples are normalised to the cross-section predictions discussed in section 5 and then stacked. The error bars reflect the statistical uncertainties of the data. The hatched band in the ratio reflects the total experimental systematic uncertainty on the simulation.

JHEP04(2014)031

Fiducial region	σ_{fid} (pb)
baseline	5.88 ± 0.01 (stat) ± 0.62 (syst) ± 0.17 (lumi)
high-p_{T}	1.82 ± 0.01 (stat) ± 0.17 (syst) ± 0.05 (lumi)
high-mass	0.066 ± 0.001 (stat) ± 0.012 (syst) ± 0.002 (lumi)
search	1.10 ± 0.01 (stat) ± 0.09 (syst) ± 0.03 (lumi)
control	0.447 ± 0.004 (stat) ± 0.059 (syst) ± 0.013 (lumi)

Table 3. Fiducial cross sections for inclusive Zjj production, measured in the $Z \to \ell^+\ell^-$ decay channel.

Fiducial region	σ_{theory} (pb)
baseline	6.26 ± 0.06 (stat) $^{+0.50}_{-0.60}$ (scale) $^{+0.29}_{-0.35}$ (PDF) $^{+0.19}_{-0.25}$ (model)
high-p_{T}	1.92 ± 0.02 (stat) $^{+0.17}_{-0.20}$ (scale) $^{+0.09}_{-0.10}$ (PDF) $^{+0.05}_{-0.07}$ (model)
high-mass	0.068 ± 0.001 (stat) $^{+0.009}_{-0.009}$ (scale) $^{+0.004}_{-0.003}$ (PDF) $^{+0.004}_{-0.002}$ (model)
search	1.23 ± 0.01 (stat) $^{+0.11}_{-0.13}$ (scale) $^{+0.06}_{-0.07}$ (PDF) $^{+0.03}_{-0.04}$ (model)
control	0.444 ± 0.005 (stat) $^{+0.051}_{-0.054}$ (scale) $^{+0.021}_{-0.025}$ (PDF) $^{+0.032}_{-0.034}$ (model)

Table 4. Theory predictions for inclusive Zjj production cross sections in the $Z \to \ell^+\ell^-$ decay channel. The strong Zjj and electroweak Zjj events are produced using `Powheg`. A small contribution of ZV events, produced by `Sherpa`, is also included. The PDF uncertainty is estimated from the CT10 eigenvectors using the procedure described in ref. [21]. Scale and modelling uncertainties are each estimated from the envelope of `Powheg` sample variations discussed in section 4.

with their statistical and systematic uncertainties. Table 4 presents the `Powheg` prediction for strong and electroweak Zjj production, combined with the `Sherpa` prediction for the small contribution from diboson processes. Uncertainties on the theoretical predictions are broken down into statistical, scale, PDF and generator modelling uncertainties. Good agreement between data and theory is observed in all fiducial regions and a summary is shown in figure 4.

7 Differential distributions of inclusive Zjj production

In this section, inclusive Zjj differential distributions are measured in the five fiducial regions presented in the previous section. The theoretical modelling of strong Zjj production is therefore confronted in regions with differing sensitivity to the electroweak Zjj component. The data are fully corrected for detector effects and are provided in HEPDATA [53] with full correlation information. The distributions sensitive to the kinematics of the two tagging jets are:

- $\frac{1}{\sigma} \cdot \frac{\mathrm{d}\sigma}{\mathrm{d}m_{jj}}$: the normalised distribution of the dijet invariant mass of the two leading jets, m_{jj}.
- $\frac{1}{\sigma} \cdot \frac{\mathrm{d}\sigma}{\mathrm{d}|\Delta y|}$: the normalised distribution of the difference in rapidity between the two leading jets, $|\Delta y|$.

JHEP04(2014)031

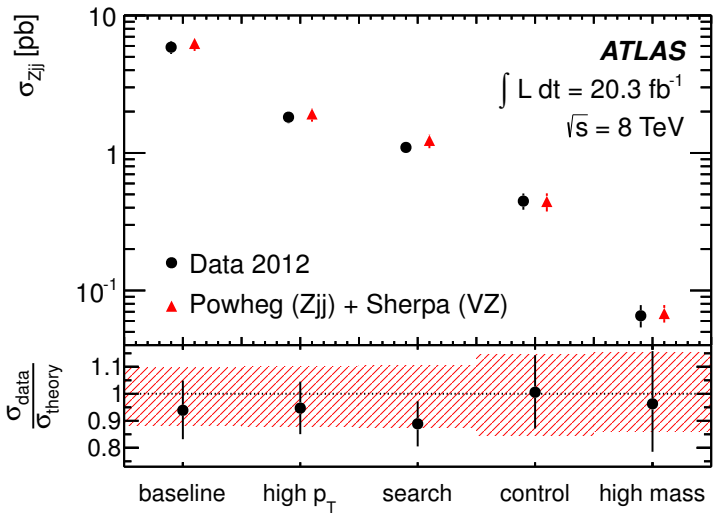

Figure 4. Fiducial cross-section measurements for inclusive Zjj production in the $Z \to \ell^+\ell^-$ decay channel, compared to the `Powheg` prediction for strong and electroweak Zjj production and the small contribution from ZV production predicted by `Sherpa`. The (black) circles represent the data and the associated error bar is the total uncertainty in the measurement. The (red) triangles represent the theoretical prediction, the associated error bar (or hatched band in the lower plot) is the total theoretical uncertainty on the prediction.

- $\frac{1}{\sigma} \cdot \frac{\mathrm{d}\sigma}{\mathrm{d}|\Delta\phi(j,j)|}$: the normalised distribution of the difference in azimuthal angle between the two leading jets, $\Delta\phi(j,j)$.

The distributions sensitive to the difference in t-channel colour flow between electroweak and strong production of Zjj events include:

- $\frac{1}{\sigma} \cdot \frac{\mathrm{d}\sigma}{\mathrm{d}N_{\mathrm{jet}}^{\mathrm{gap}}}$: the normalised distribution of the number of jets, $N_{\mathrm{jet}}^{\mathrm{gap}}$, with $p_{\mathrm{T}} > 25\,\mathrm{GeV}$ in the rapidity interval bounded by the two highest-p_{T} jets.
- $\frac{1}{\sigma} \cdot \frac{\mathrm{d}\sigma}{\mathrm{d}p_{\mathrm{T}}^{\mathrm{balance}}}$: the normalised distribution of the p_{T}-balancing distribution, $p_{\mathrm{T}}^{\mathrm{balance}}$ (see eq. (6.2)).
- The fraction of events that contain no additional jets with $p_{\mathrm{T}} > 25\,\mathrm{GeV}$ in the rapidity interval bounded by the two highest-p_{T} jets (the *jet veto efficiency*) as a function of m_{jj} and $|\Delta y|$.
- The average number of jets with $p_{\mathrm{T}} > 25\,\mathrm{GeV}$ in the rapidity interval bounded by the two highest-p_{T} jets, $\langle N_{\mathrm{jet}}^{\mathrm{gap}} \rangle$, as a function of m_{jj} and $|\Delta y|$.
- The fraction of events with $p_{\mathrm{T}}^{\mathrm{balance}} < 0.15$ ($p_{\mathrm{T}}^{\mathrm{balance}}$ *cut efficiency*) as a function of m_{jj} and $|\Delta y|$.

7.1 Analysis methodology and unfolding to particle level

The differential distributions are normalised to unity after subtracting the small background contributions from $t\bar{t}$ and multijet events in each bin of the distributions. An

JHEP04(2014)031

iterative Bayesian unfolding procedure [54, 55] is then applied to the data to produce distributions at the particle level. This procedure uses a detector response matrix to reverse the bin migration caused by finite detector resolution. The response matrix is constructed from the strong and electroweak Zjj simulated samples for each distribution. Events that pass the reconstruction-level but not the particle-level selection criteria (or vice versa) are also corrected for as part of the unfolding procedure.

The Bayesian unfolding procedure relies on knowledge of the underlying particle-level distribution. This 'prior' distribution is taken to be the particle-level prediction from `Sherpa`. After the first unfolding iteration, the input prior is replaced with the unfolded distribution from the data and the unfolding process is repeated. It is found that two iterations are sufficient to ensure convergence of the results.

The statistical uncertainty on the data after unfolding is computed using pseudo-experiments. The statistical correlation between the numerator and the denominator in the jet veto distributions is retained by unfolding two-dimensional distributions constructed from the dijet observable $(m_{jj}, |\Delta y|)$ and information as to whether events passed or failed the efficiency criterion. The $p_{\mathrm{T}}^{\mathrm{balance}}$ *cut efficiency* distribution is unfolded in a similar way. Correlations in the $\langle N_{\mathrm{jet}}^{\mathrm{gap}} \rangle$ distributions are retained by unfolding a two-dimensional distribution constructed from the dijet observable and the number of jets in the rapidity interval between the two leading jets. Statistical correlations between bins from different unfolded distributions are estimated using a bootstrap method [56].

7.2 Systematic uncertainties

The sources of experimental and theoretical uncertainty include all of those present in the measurement of the inclusive Zjj fiducial cross section (section 6.2). The impact of lepton-based and luminosity systematic uncertainties on the measured distributions is negligible and the experimental systematic uncertainties therefore arise from JES, JER, JVF, as well as pileup jet modelling. The theoretical modelling uncertainties are again estimated by reweighting the simulation, such that the kinematic distributions of the variables used to define the fiducial regions match those observed in the data. An additional uncertainty associated with the closure of the Bayesian iterative procedure is estimated by reweighting the simulated events such that the reconstruction-level distribution being unfolded better matches the one observed in the data. The reweighting functions applied at the particle level are taken to be the ratio of the reconstruction-level distributions in data and simulation.

For all sources of systematic uncertainty, the data are unfolded using a new response matrix constructed after shifting and smearing the MC events and objects. The shift in the unfolded spectrum is taken as the systematic uncertainty on the final result. The dominant uncertainties arise from the JES and JER, with small additional uncertainties from JVF, pileup modelling and theoretical modelling. The systematic uncertainties are presented in figure 5 for the $\frac{1}{\sigma} \cdot \frac{\mathrm{d}\sigma}{\mathrm{d}|\Delta y|}$ distribution and the jet veto efficiency as a function of $|\Delta y|$, in the *baseline* region. The total systematic uncertainty in each bin is defined as the quadrature sum of the individual sources of experimental and theoretical uncertainty.

JHEP04(2014)031

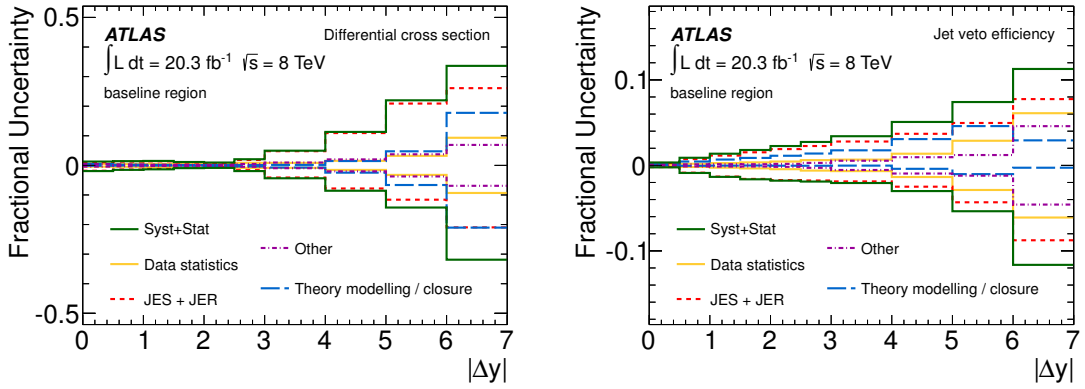

(a) (b)

Figure 5. Example systematic uncertainty breakdown for the $\frac{1}{\sigma}\cdot\frac{\mathrm{d}\sigma}{\mathrm{d}|\Delta y|}$ distribution and the jet veto efficiency as a function of $|\Delta y|$ in the *baseline* region. The effect of MC statistics, pileup modelling and JVF modelling are combined into one uncertainty labelled 'other'.

The unfolding procedure is cross-checked using the simulated ALPGEN sample in place of the Sherpa strong Zjj sample. The data are unfolded using the new response matrix formed from these simulated events. The data unfolded using the ALPGEN- and Sherpa-based response matrices are found to agree, after accounting for the larger statistical uncertainty in the ALPGEN sample in addition to the theory modelling and closure uncertainties assigned to the nominal result.

7.3 Unfolded differential distributions

The unfolded data are compared to particle-level predictions from Powheg and Sherpa in figures 6–10. The theoretical predictions are shown for combined electroweak and strong Zjj production and for strong Zjj production only. The theoretical uncertainty on the combined electroweak and strong Zjj prediction is estimated using the envelope of theory modelling uncertainties discussed in section 4. The contribution from diboson production is neglected for the theoretical predictions as the impact on the distributions is negligible.

The unfolded $\frac{1}{\sigma}\cdot\frac{\mathrm{d}\sigma}{\mathrm{d}m_{jj}}$ and $\frac{1}{\sigma}\cdot\frac{\mathrm{d}\sigma}{\mathrm{d}|\Delta y|}$ distributions are shown in figure 6 and 7, respectively, for the *baseline* and *search* regions (corresponding distributions in the *high-*p_{T} and *control* regions are provided in appendix A). Both of these distributions are sensitive to the difference between electroweak and strong production of Zjj events, especially at large m_{jj} or $|\Delta y|$. In the electroweak process, the masses of the exchanged electroweak bosons lead to jets produced preferentially at large rapidities with sizeable transverse momentum. Furthermore, strong Zjj production typically involves the t-channel exchange of a spin-1/2 quark, which leads to steeper m_{jj} and $|\Delta y|$ spectra than the spin-1 exchange that is present in electroweak Zjj production.

In the *baseline* region, the Powheg prediction is accurate to NLO in perturbative QCD and better describes the data at the highest values of m_{jj} and $|\Delta y|$ than Sherpa, which is accurate to LO. In particular, Sherpa predicts too large a fraction of events at large m_{jj} and $|\Delta y|$, a feature also seen in previous measurements at the LHC and Tevatron [57, 58].

JHEP04(2014)031

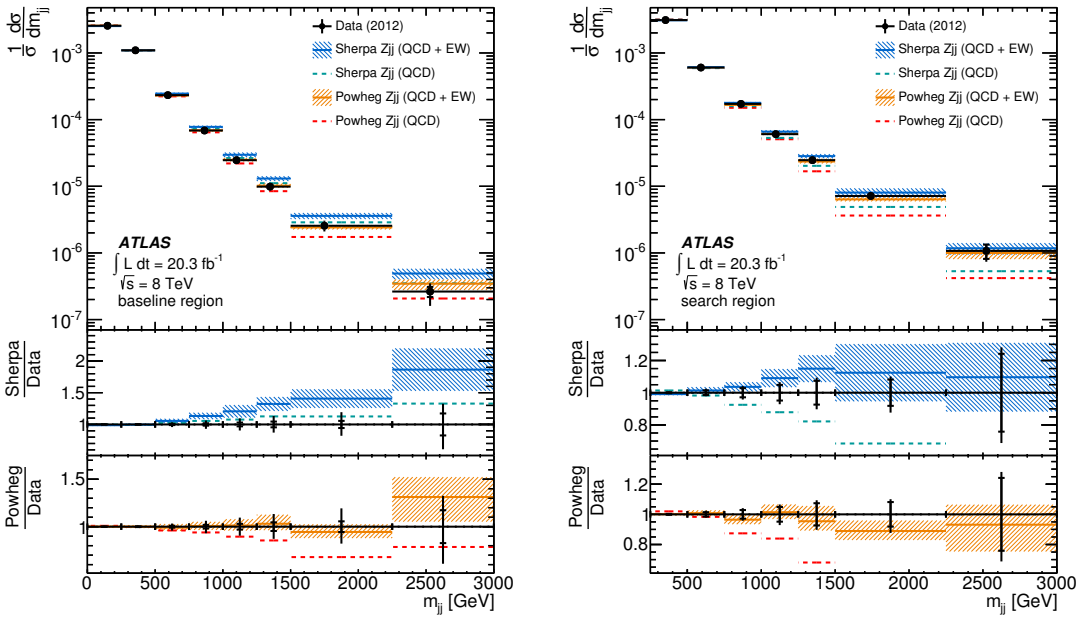

(a) (b)

Figure 6. Unfolded $\frac{1}{\sigma} \cdot \frac{\mathrm{d}\sigma}{\mathrm{d}m_{jj}}$ distribution in the (a) *baseline* and (b) *search* regions. The data are shown as filled (black) circles. The vertical error bars show the size of the total uncertainty on the measurement, with tick marks used to reflect the size of the statistical uncertainty only. Particle-level predictions from `Sherpa` and `Powheg` are shown for combined strong and electroweak Zjj production (labelled as QCD+EW) by hatched bands, denoting the model uncertainty, around the central prediction, which is shown as a solid line. The predictions from `Sherpa` and `Powheg` for strong Zjj production (labelled QCD) are shown as dashed lines.

In the *search* region, the veto on additional jet activity means that both `Sherpa` and `Powheg` are accurate only to LO. Despite this, both predictions give a satisfactory description of the data if both strong and electroweak Zjj production are included. The contribution from electroweak Zjj production is evident at high m_{jj} and high $|\Delta y|$ in the *search* region for both event generators.

The unfolded $\frac{1}{\sigma} \cdot \frac{\mathrm{d}\sigma}{\mathrm{d}N_{\mathrm{jet}}^{\mathrm{gap}}}$, $\frac{1}{\sigma} \cdot \frac{\mathrm{d}\sigma}{\mathrm{d}p_{\mathrm{T}}^{\mathrm{balance}}}$ and $\frac{1}{\sigma} \cdot \frac{\mathrm{d}\sigma}{\mathrm{d}|\Delta\phi(j,j)|}$ distributions are shown in the *high-mass* region in figure 8. Quark/gluon radiation from the electroweak Zjj process is much less likely than in the strong Zjj process because there is no colour flow between the two jets. The contribution from electroweak Zjj production is clear in the low-multiplicity region of the $\frac{1}{\sigma} \cdot \frac{\mathrm{d}\sigma}{\mathrm{d}N_{\mathrm{jet}}^{\mathrm{gap}}}$ distribution for both `Powheg` and `Sherpa`, demonstrating the effectiveness of the jet veto at separating the strong and electroweak components of Zjj production. Both `Powheg` and `Sherpa` adequately describe the data for the $\frac{1}{\sigma} \cdot \frac{\mathrm{d}\sigma}{\mathrm{d}p_{\mathrm{T}}^{\mathrm{balance}}}$ and $\frac{1}{\sigma} \cdot \frac{\mathrm{d}\sigma}{\mathrm{d}|\Delta\phi(j,j)|}$ distributions; the latter distribution has little sensitivity to the electroweak process.[8]

[8] Although the azimuthal angle between the jets is not sensitive to the differences between strong and electroweak Zjj production, it is of interest in Higgs-plus-two-jet studies, as the vector boson fusion and gluon fusion production channels have very different azimuthal structure [59–61].

JHEP04(2014)031

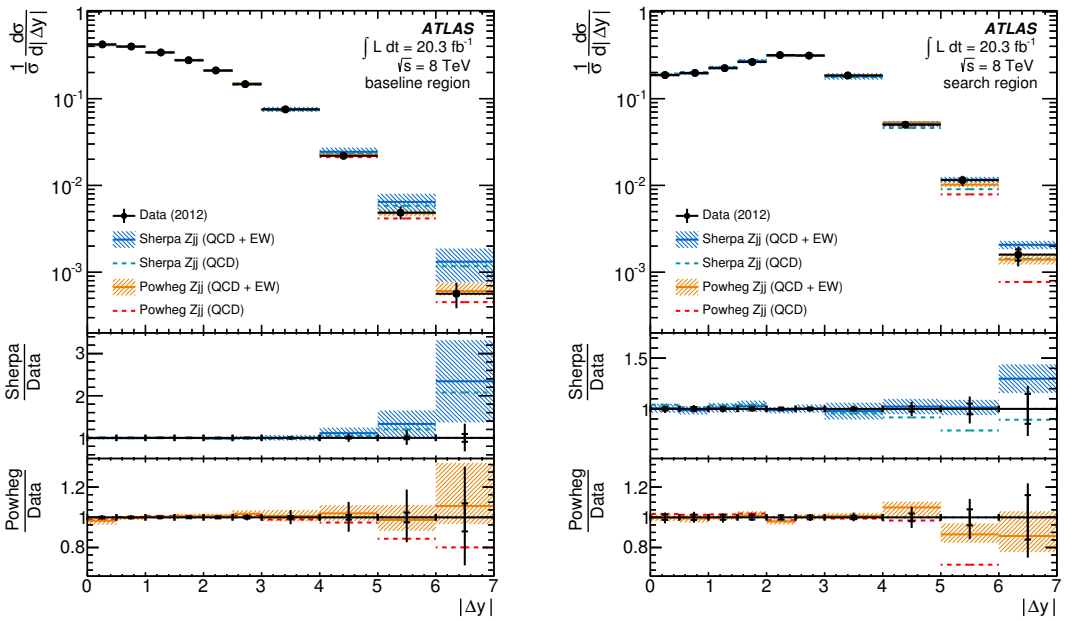

(a) (b)

Figure 7. Unfolded $\frac{1}{\sigma} \cdot \frac{\mathrm{d}\sigma}{\mathrm{d}|\Delta y|}$ distribution in the (a) *baseline* and (b) *search* regions. The data and theoretical predictions are presented in the same way as in figure 6.

Figure 9 shows the unfolded jet veto efficiency and $\langle N_{\text{jet}}^{\text{gap}} \rangle$ distributions as a function of m_{jj} and $|\Delta y|$ in the *baseline* region (corresponding distributions in the *high-*p_{T} region are provided in appendix A). These variables probe the theoretical description of wide-angle quark and gluon radiation in strong Zjj events as a function of the energy scale of the dijet system. For the electroweak process, quark and gluon radiation into the rapidity interval is suppressed and little jet activity is expected. This is evident at medium-to-high values of m_{jj}, for which the strong Zjj prediction has more jet activity than the combined strong and electroweak Zjj prediction. In general, both theoretical predictions give a good description of the data (for combined strong and electroweak Zjj production), although `Sherpa` gives a slightly better description than `Powheg` when compared across both the m_{jj} and $|\Delta y|$ distributions. `Sherpa` and `Powheg` have previously provided a good description of the jet activity in the rapidity interval bounded by a dijet system in purely dijet topologies [31, 62].

The unfolded $p_{\text{T}}^{\text{balance}}$ *cut efficiency* as a function of m_{jj} and $|\Delta y|$ in the *baseline* region is shown in figure 10 (the corresponding distribution in the *high-*p_{T} region is provided in appendix A). Again, with less quark/gluon radiation from the electroweak process, it is expected that the two jets are better balanced against the Z-boson for the electroweak Zjj process than for the strong Zjj process. This is apparent at high m_{jj} and high $|\Delta y|$, where the strong Zjj prediction falls below the data. For this distribution, `Powheg` describes the data poorly at low values of m_{jj} or $|\Delta y|$, whereas `Sherpa` gives a good description of the data over the full range of the distributions.

In general, neither `Sherpa` nor `Powheg` is able to fully reproduce the data for all distributions in all fiducial regions. `Powheg` gives a better description of the data than `Sherpa`

JHEP04(2014)031

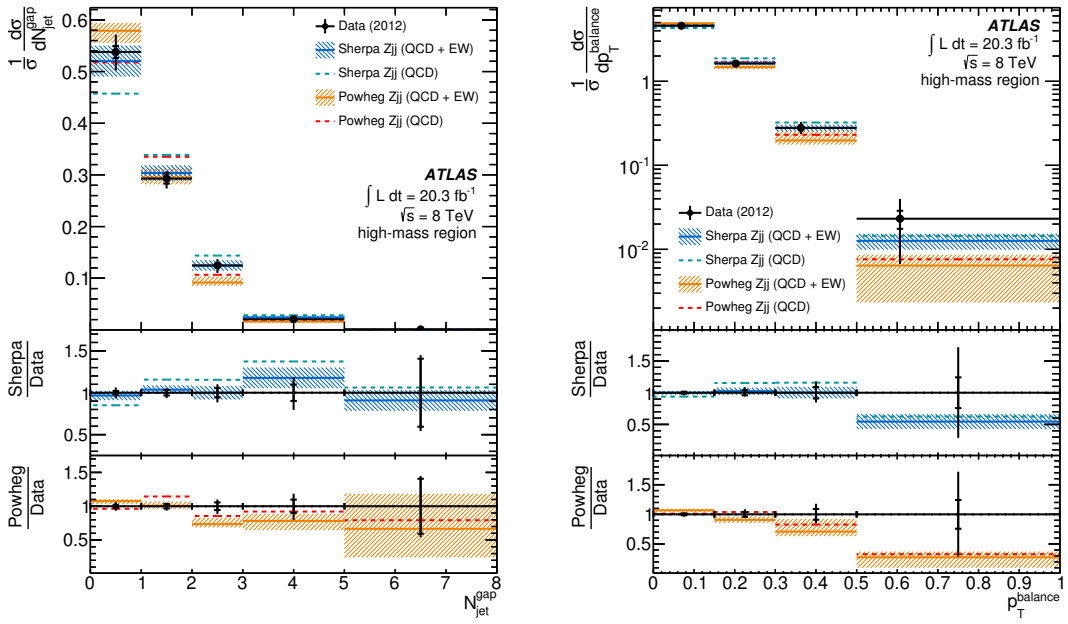

(a) (b)

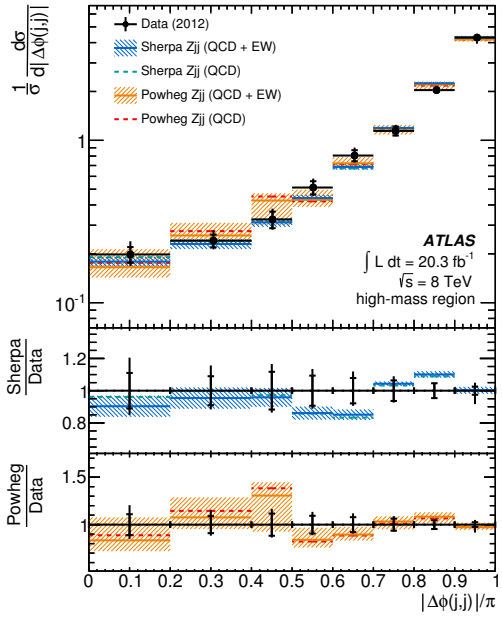

(c)

Figure 8. Unfolded (a) $\frac{1}{\sigma}\cdot\frac{\mathrm{d}\sigma}{\mathrm{d}N_{\mathrm{jet}}^{\mathrm{gap}}}$, (b) $\frac{1}{\sigma}\cdot\frac{\mathrm{d}\sigma}{\mathrm{d}p_{\mathrm{T}}^{\mathrm{balance}}}$ and (c) $\frac{1}{\sigma}\cdot\frac{\mathrm{d}\sigma}{\mathrm{d}|\Delta\phi(j,j)|}$ distributions in the *high-mass* region. The data and theoretical predictions are presented in the same way as in figure 6.

for the m_{jj} and $|\Delta y|$ distributions, with `Sherpa` predicting too large a cross section at the highest values of m_{jj} or $|\Delta y|$. However, `Sherpa` gives a better description for variables sensitive to the additional jet activity in the event, with `Powheg` predicting too little jet ac-

JHEP04(2014)031

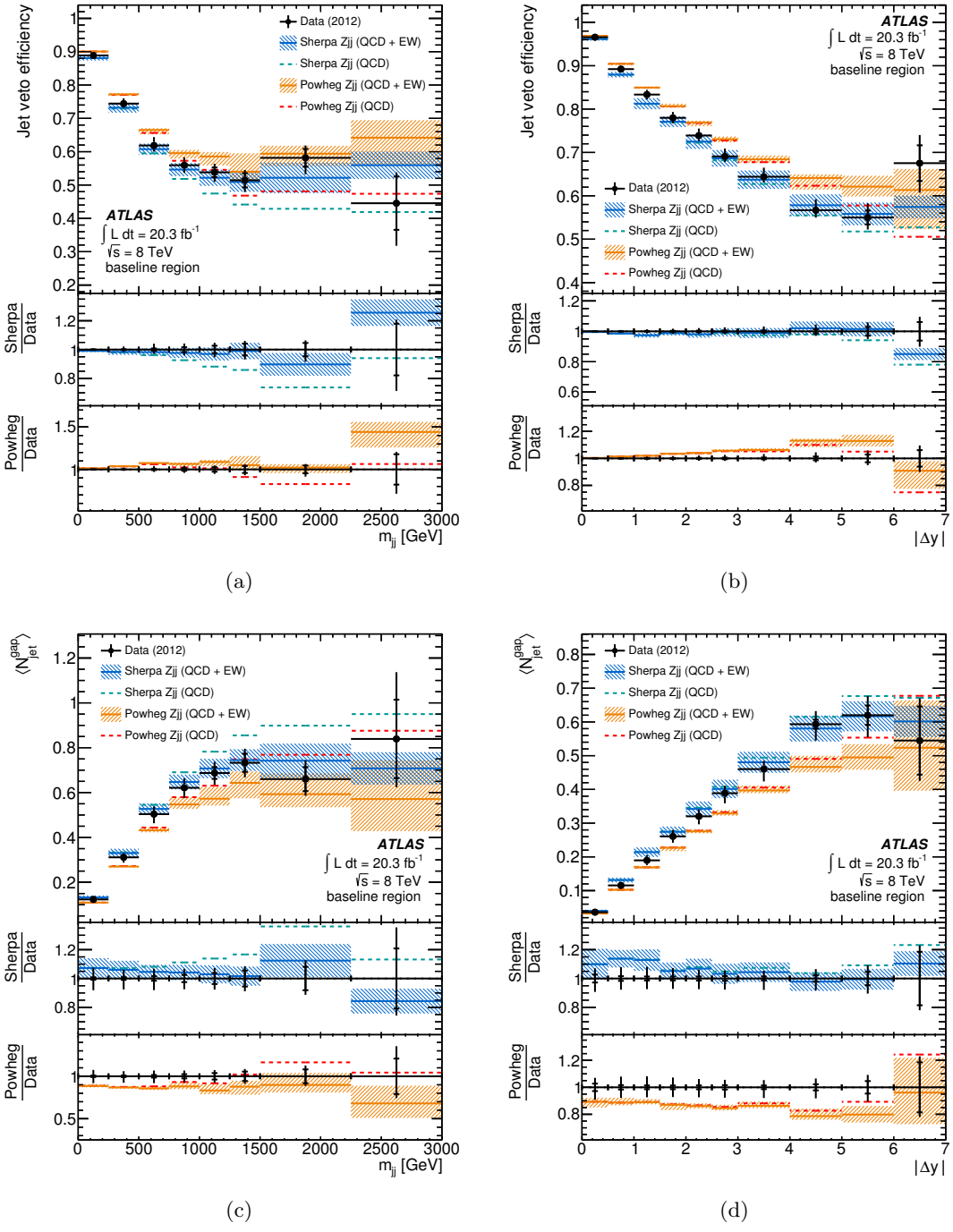

Figure 9. Unfolded *jet veto efficiency* versus (a) m_{jj} and (b) $|\Delta y|$, and unfolded $\langle N_{\text{jet}}^{\text{gap}} \rangle$ versus (c) m_{jj} and (d) $|\Delta y|$. All distributions are measured in the *baseline* region. The data and theoretical predictions are presented in the same way as in figure 6.

tivity in the rapidity interval bounded by the dijet system. The unfolded data can be used to constrain the modelling of Zjj production in the extreme phase-space regions probed in this measurement. The unfolded data are provided in HEPDATA with statistical and sys-

JHEP04(2014)031

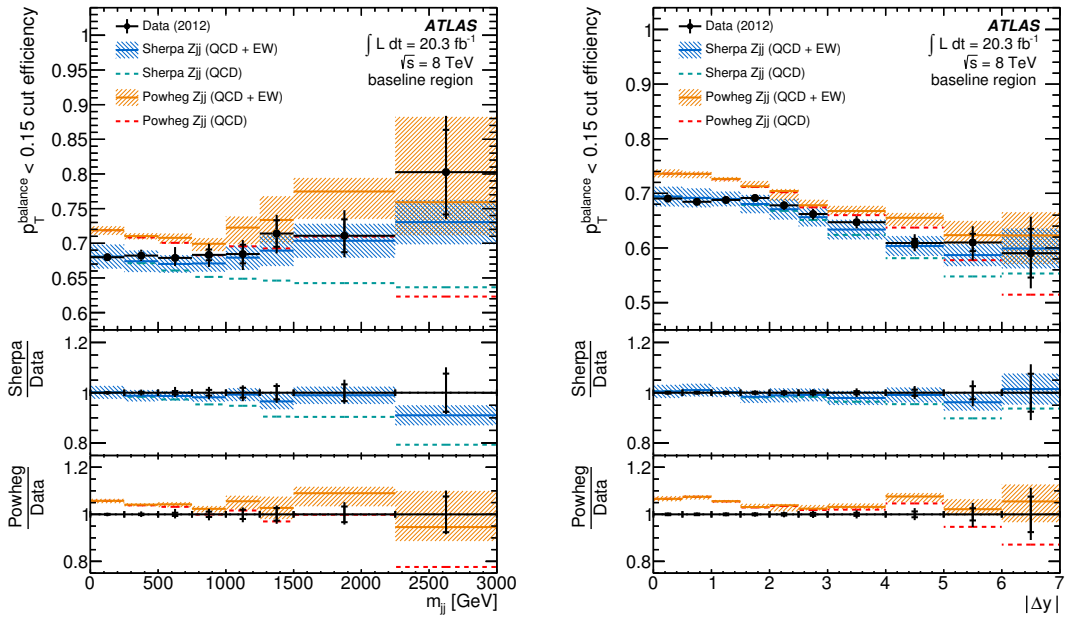

(a) (b)

Figure 10. Unfolded $p_{\mathrm{T}}^{\mathrm{balance}}$ *cut efficiency* versus (a) m_{jj} and (b) $|\Delta y|$ in the *baseline* region. The data and theoretical predictions are presented in the same way as in figure 6.

tematic uncertainties. Furthermore, the correlation between bins of different distributions is provided, allowing the quantitative comparison of all distributions simultaneously.

8 Extraction of the electroweak Zjj fiducial cross section

The electroweak Zjj component is extracted by fitting the dijet invariant mass reconstructed in the *search* region. Templates are formed for the signal and background processes and a fit to the dijet invariant mass distribution in the data is performed, allowing the normalisation of each template to float. The fit is performed using a log-likelihood maximisation [63] and the number of signal and background events is extracted. The number of signal events is then converted into a fiducial cross section, using a correction factor to convert from the reconstruction-level event selection to the particle-level event selection.

8.1 Template construction and fit results

The signal template is obtained from the `Sherpa` electroweak Zjj sample. The background template is constructed from the `Sherpa` strong Zjj sample plus the small contribution from the diboson and $t\bar{t}$ samples (the other background sources are found to have negligible impact on the results). The background template is then constrained using the following data-driven technique. The dijet invariant mass distributions are constructed for data and MC simulation in the *control* region and a reweighting function is defined by fitting the ratio of the data to MC simulation with a second-order polynomial. This reweighting function is then applied directly to the background template in the *search* region. The

JHEP04(2014)031

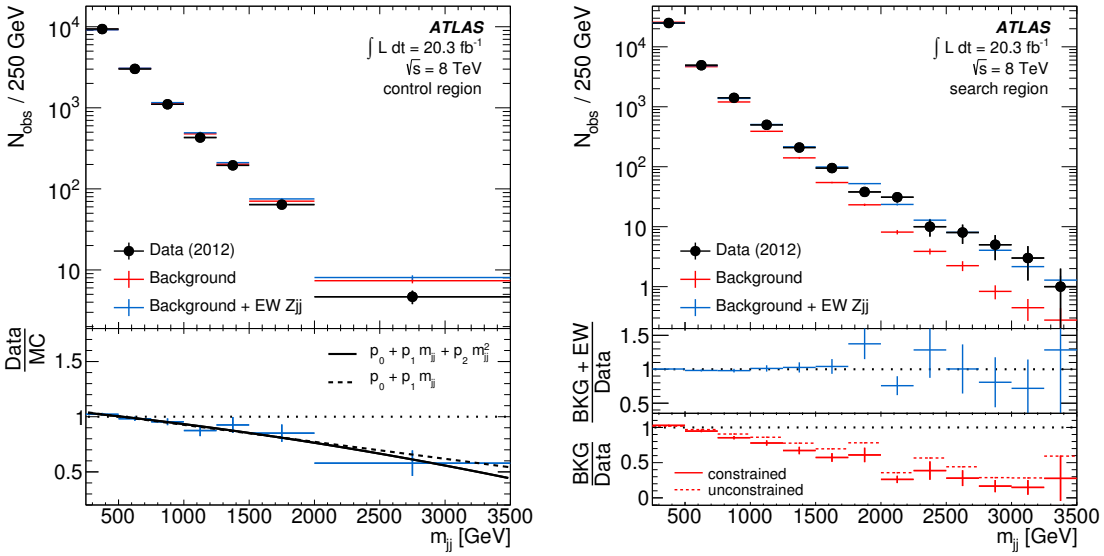

(a) (b)

Figure 11. (a) The dijet invariant mass distribution in the *control* region. The simulation has been normalised to match the number of events observed in the data. The lower panel shows the reweighting function used to constrain the shape of the background template. (b) The dijet invariant mass distribution in the *search* region. The signal and (constrained) background templates are scaled to match the number of events obtained in the fit. The lowest panel shows the ratio of constrained and unconstrained background templates to the data.

data are therefore used to constrain the generator modelling of the background m_{jj} shape, and the MC simulation is used only to extrapolate this constraint between the *control* and *search* regions. This procedure has the advantage of minimising both the experimental and theoretical systematic uncertainties on the background template. Figure 11(a) shows the dijet invariant mass distribution in the *control* region for the data and the MC simulation for the electron and muon channels combined. The reweighting function is shown in the lower panel. The use of the *control* region to constrain the background template is validated in section 8.2 and corresponding systematic uncertainties are presented in section 8.3.

Figure 11(b) shows the dijet invariant mass distribution in the *search* region for the electron and muon channels combined. The signal and background templates are normalised to the values obtained from the fit. The background template is presented after the data-driven reweighting using the second-order polynomial in figure 11 (a). The unconstrained background template is also compared to the data in the lowest panel, demonstrating that the background-only prediction always falls below the data at high-m_{jj}.

Table 5 summarises the fit results, giving the number of signal (N_{EW}) and background (N_{bkg}) events expected by the MC simulation and the number obtained from the fit, together with the statistical uncertainties from the data (first uncertainty) and MC templates (second uncertainty). The results are shown for electrons and muons separately and also with both channels combined, where the latter result is obtained by combining the two

JHEP04(2014)031

	Electron	Muon	Electron+muon
Data	14248	17938	32186
MC predicted N_{bkg}	$13700 \pm 1200\,^{+1400}_{-1700}$	$18600 \pm 1500\,^{+1900}_{-2300}$	$32600 \pm 2600\,^{+3400}_{-4000}$
MC predicted N_{EW}	$602 \pm 27 \pm 18$	$731 \pm 29 \pm 22$	$1333 \pm 50 \pm 40$
Fitted N_{bkg}	$13351 \pm 144 \pm 29$	$17201 \pm 161 \pm 31$	$30530 \pm 216 \pm 40$
Fitted N_{EW}	$897 \pm 92 \pm 27$	$737 \pm 98 \pm 28$	$1657 \pm 134 \pm 40$

Table 5. The number of strong (N_{bkg}) and electroweak (N_{EW}) Zjj events as predicted by the MC simulation and obtained from a fit to the data. The number of events in data is also given. The first and second uncertainties on the fitted yields are due to statistical uncertainties in data and simulation, respectively. The first and second uncertainties in the MC prediction are the experimental and theoretical systematic uncertainties, respectively.

channels for the data and for the MC templates before fitting. For the purpose of measuring the fiducial cross section, the yields from the fits to electrons and muons are used. For the purpose of determining systematic uncertainties on N_{EW}, which are correlated between the two channels, the fractional shift in the number of events obtained from the fit combining both channels is used.

8.2 Validation of the control region constraint procedure

The data-driven background constraint derived in the control region is an important component of the analysis as it improves the modelling of the background m_{jj} spectrum and constrains the impact of experimental and theoretical uncertainties. Several cross-checks are performed to validate the method.

The choice of polynomial used to describe the reweighting function is investigated by using a first-order polynomial instead of a second-order polynomial. The lower panel of figure 11(a) shows that both choices of polynomial give very similar reweighting functions at low m_{jj} and differ only at the highest values of m_{jj}. The change in N_{EW} is less than 2% if the first-order polynomial is used to reweight the background template in place of the second-order polynomial.

The choice of event generator is examined by reweighting the simulated dijet invariant mass distribution for strong Zjj production using the ratio of the `Powheg` and `Sherpa` particle-level predictions. This reweighting is carried out in the *search* and *control* regions separately. `Powheg` has been shown to give a much better description of the data for the dijet invariant mass in figure 6 for all fiducial regions. The reweighting to `Powheg` improves the description of the data in the *control* region. The data-driven reweighting function then becomes much flatter and repeating the full analysis procedure with the new templates produces a result consistent at 0.8% with the analysis based on the `Sherpa` samples alone.

The choice of control region is studied by splitting it into six subregions that probe the additional jet activity in the rapidity interval between the two leading jets. The *control*

JHEP04(2014)031

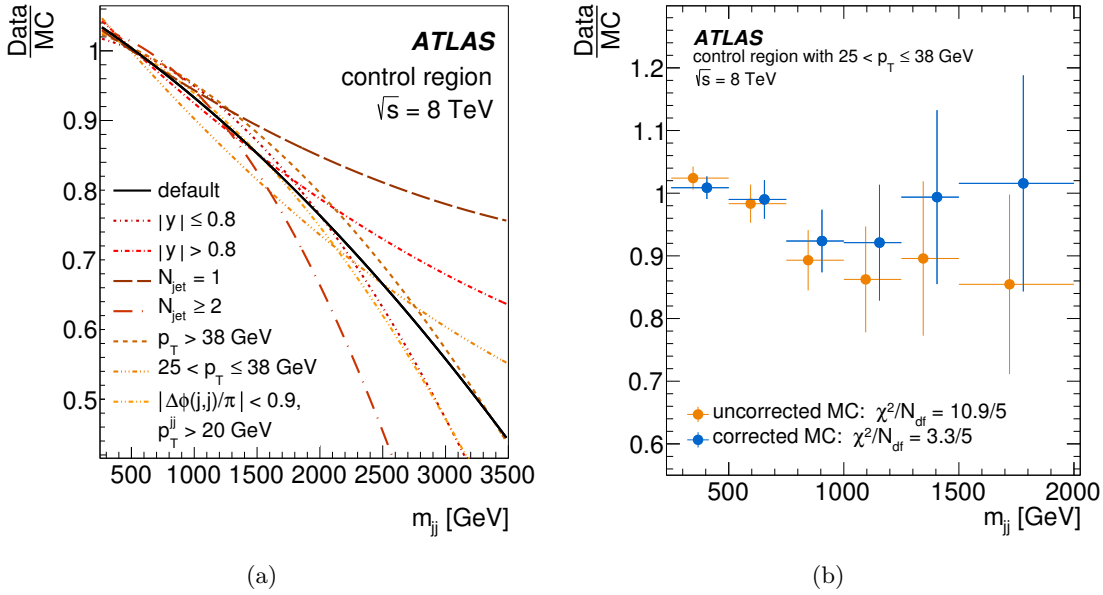

(a) (b)

Figure 12. (a) Background reweighting functions obtained for different choices of *control* region. (b) The agreement between data and simulation in the $25 < p_{\mathrm{T}} \leq 38\,\mathrm{GeV}$ subregion both before and after applying a background reweighting function derived in the $p_{\mathrm{T}} > 38\,\mathrm{GeV}$ subregion.

and *search* regions are distinguished by this additional jet activity and these subregions allow the impact of any mismodelling in the simulation to be explored. Two subregions are defined by the transverse momentum of the leading jet in the rapidity interval ($25 < p_{\mathrm{T}} \leq 38\,\mathrm{GeV}$ and $p_{\mathrm{T}} > 38\,\mathrm{GeV}$), two subregions are defined by the rapidity of the jet ($|y| \leq 0.8$ and $|y| > 0.8$), and two subregions are defined by the number of jets in the rapidity interval ($N_{\mathrm{jet}} = 1$ and $N_{\mathrm{jet}} \geq 2$). In addition to these six regions, an MPI-suppressed subregion is defined by the requirements $|\Delta\phi(j,j)/\pi| < 0.9$ and $p_{\mathrm{T}}^{jj} > 20\,\mathrm{GeV}$, where p_{T}^{jj} is the transverse momentum of the dijet system. This region allows the impact of MPI on the control region constraint to be examined.

Figure 12(a) shows the background reweighting functions obtained from these subregions, compared to the default function obtained from the default *control* region. The extraction of the electroweak signal is cross-checked using each of these constraints. The values of N_{EW} are consistent, with a maximum 5% spread between subregions. This spread is likely to be statistical in origin, as the values of N_{EW} obtained from reweighting functions derived in orthogonal subregions are found to agree to better than 1σ when considering only the statistical uncertainty associated with the reweighting functions. Although the spread of reweighting functions in figure 12(a) is large at high m_{jj}, the background modelling in this region has only a small impact on the extracted number of electroweak Zjj events. The background modelling shape has most impact at values of m_{jj} around 1–1.5 TeV, for which the spread of reweighting functions is just a few percent.

The orthogonal subregions are also used to test the agreement between data and the corrected simulation directly. The reweighting function derived in the $p_{\mathrm{T}} > 38\,\mathrm{GeV}$ subregion is used to correct the simulation in the $25 < p_{\mathrm{T}} \leq 38\,\mathrm{GeV}$ subregion, as shown

JHEP04(2014)031

in figure 12(b). The corrected simulation gives a better description of the data than the uncorrected simulation. Similar tests are performed for the subregions split by jet rapidity or jet multiplicity. In all cases, the corrected simulation gives a better description of data than the uncorrected simulation.

8.3 Systematic uncertainties on the fit procedure

Systematic uncertainties on N_{EW} arise from the background template reweighting function, the jet-based experimental systematic uncertainties, and the theoretical modelling uncertainties on the Zjj samples. The uncertainty due to the lepton-based systematic uncertainties is negligible. A summary of the systematic uncertainties discussed in this section is presented in table 6. The systematic uncertainty due to the limited number of events in the control region is obtained using pseudo-experiments, and is found to be 8.9% and 11.2% in the electron and muon channels, respectively. The remaining experimental systematic uncertainties affect the extracted value of N_{EW} by changing the shape of the signal template and/or the shape of the background template. The experimental systematic uncertainties that change the template shape are due to JES, JER, JVF, as well as pileup jet modelling, as discussed in section 6.2. The effect on the number of fitted events due to each source of uncertainty is evaluated simultaneously for signal and background templates in order to account for correlations.

Systematic variations in the signal template are evaluated by taking the ratio of the template formed with a systematic shift to the nominal template, fitting that ratio with a second-order polynomial, applying that polynomial as a reweighting function to the signal template, and repeating the fit for the number of electroweak events. The use of the polynomial to estimate the systematic shift reduces the impact of statistical fluctuations at large m_{jj}.

For the systematic variations in the background template, the data provide a constraint in the *control* region, meaning that only the effect of each systematic variation on the extrapolation between the *control* and *search* regions needs to be evaluated. A double ratio is formed from the systematic-shifted to nominal ratios in the *search* and *control* regions and fitted with a first-order polynomial function. If the gradient of the fitted function is statistically significant, defined as the parameter value being greater than 1.64 times the parameter uncertainty, then this component is considered as a significant source of systematic uncertainty. This significance requirement is chosen to remove 90% of statistical fluctuations and avoid double counting statistical uncertainties in the simulated samples.[9] For each significant source of systematic uncertainty, the first-order polynomial is applied as an additional reweighting to the background template in the *search* region and the fit is repeated.

The dominant systematic uncertainty on the extracted value of N_{EW} from experimental sources is from the JES (5.6%). This uncertainty comes almost entirely from the uncertainty on the signal template shape, because the shape of the background template

[9]The choice of significance requirement was investigated by changing the requirement to 1.0 or 2.0. The resultant systematic uncertainties were unchanged from the nominal choice of 1.64.

JHEP04(2014)031

is constrained using the *control* region. The uncertainty due to the JVF is modest (1.1%), whereas the uncertainty from JER and pileup modelling is effectively negligible (0.4% and 0.3%, respectively).

Additional uncertainties on the extraction of the electroweak component arise from the theoretical modelling in the MC generators. Again, these affect the signal template as well as the extrapolation between the *control* and *search* region for the background template. The uncertainties due to theoretical modelling are split into two components: PDF modelling and generator modelling.

Uncertainties due to PDF modelling are obtained as follows. The nominal value of N_{EW} is obtained using the `CT10` PDF set. The full analysis is then repeated using simulated samples created using (i) the `CT10` uncertainties and (ii) the central values and uncertainties of two other PDF sets, `MSTW2008nlo` [41] and `NNPDF2.3` [64]. Each PDF variation is applied to the signal and background simultaneously. For each PDF set, the uncertainty on N_{EW} is then calculated using the recommended procedure from each collaboration [65, 66], with the `CT10` results scaled to reflect 68% probability. The α_s uncertainty is found to be negligible. The overall uncertainty due to PDF modelling is found to be $^{+1.5}_{-3.9}$% from the envelope of uncertainties obtained from each PDF set.

The generator modelling uncertainties are determined using the dedicated `Sherpa` sample variations discussed in section 4, by varying the factorisation and renormalisation scale, varying the activity from multiple parton interactions (MPI), and changing the parton-shower scheme or CKKW matching parameters. To evaluate the generator modelling uncertainty, the analysis is repeated for each sample variation independently to obtain a shift in N_{EW}. The standard deviation in the shifted values for each sample variation is obtained using a pseudo-experiment approach. The effect of the signal modelling uncertainty on N_{EW} is found to be 8.9% from the envelope of the shifts (mean plus standard deviation) produced from the eight dedicated signal templates. A separate uncertainty on N_{EW} is obtained from the envelope of the shifts (mean plus standard deviation) produced from the eight dedicated background templates. The uncertainty due to background modelling is found to be 7.5%. The uncertainties in the signal and background generator modelling are taken as uncorrelated.

The uncertainties on the signal and background modelling are cross-checked by reweighting the simulated dijet invariant mass distribution for strong and electroweak Zjj production, using the ratio of the `Powheg` and `Sherpa` particle-level predictions. As discussed in section 8.2, reweighting the strong Zjj sample produces a change in N_{EW} of just 0.8%. This is covered by the background modelling uncertainty determined from the `Sherpa` systematic variations. Reweighting the electroweak Zjj sample produces a change in N_{EW} of 4.6%, which is also covered by the signal modelling uncertainty assigned from the `Sherpa` systematic variations.

The systematic uncertainty associated with possible interference between electroweak and strong Zjj production is estimated by reweighting the background template to account for the interference contribution. The interference is determined using the dedicated `Sherpa` samples discussed in section 4. These samples use only leading-order matrix elements for Zjj production and the change in the background template is therefore estimated prior to

JHEP04(2014)031

Source	ΔN_{EW}		$\Delta \mathcal{C}_{\mathrm{EW}}$	
	Electrons	Muons	Electrons	Muons
Lepton systematics	—	—	±3.2 %	±2.5%
Control region statistics	±8.9 %	±11.2 %	—	—
JES	±5.6 %		$^{+2.7}_{-3.4}$ %	
JER	±0.4 %		±0.8 %	
Pileup jet modelling	±0.3 %		±0.3 %	
JVF	±1.1 %		$^{+0.4}_{-1.0}$ %	
Signal modelling	±8.9 %		$^{+0.6}_{-1.0}$ %	
Background modelling	±7.5 %		—	
Signal/background interference	±6.2 %		—	
PDF	$^{+1.5}_{-3.9}$ %		±0.1 %	

Table 6. Systematic uncertainties, expressed in percentages, on (i) the number of fitted signal events in the *search* region, N_{EW}, and (ii) the correction factor to the particle-level, $\mathcal{C}_{\mathrm{EW}}$. The uncertainties are anti-correlated between N_{EW} and $\mathcal{C}_{\mathrm{EW}}$.

applying the jet veto. The impact of interference is determined by repeating the full fitting procedure after reweighting the background template in either the *search* region or the *control* region alone. This approach assumes the interference affects only one of the two regions and therefore has a maximal impact on the analysis. If the background template is reweighted only in the *search* region, the extracted value of N_{EW} is reduced by 6.2%. Alternatively, if the background template is reweighted only in the *control* region, the value of N_{EW} increases by 6.2%. A conservative systematic uncertainty of ±6.2% is assigned to the final measurement.

8.4 Measurement of fiducial cross section

The fitted values of N_{EW} for the electron and muon channels are converted to a fiducial cross section, defined as:

$$\sigma_{\mathrm{EW}} = \frac{N_{\mathrm{EW}}}{\int L\,\mathrm{d}t \cdot \mathcal{C}_{\mathrm{EW}}} \tag{8.1}$$

where $\mathcal{C}_{\mathrm{EW}}$ is a correction factor based on the reconstruction- to particle-level ratio of the `Sherpa` prediction for electroweak Zjj production in the *search* region.

The correction factors are 0.80 and 0.66 in the muon and electron channels, respectively. The difference in correction factor between the two channels arises primarily from the different reconstruction and identification efficiencies for muons and electrons. The systematic uncertainties on the correction factor are divided into those that are uncorrelated between the electron and muon channels (MC sample statistics, lepton reconstruction, identification, trigger, energy scale and energy smearing) and those that are correlated (JES, JER, JVF, pileup jet modelling, generator modelling and PDFs). The generator

JHEP04(2014)031

modelling can affect the correction factor due to differences in the kinematics of final-state particles. This uncertainty is determined by reweighting the nominal MC simulation such that the particle-level distributions match those of the dedicated `Sherpa` model variations discussed in section 4. This is carried out for all kinematic distributions for which a cut is made in defining the *search* region and the resulting uncertainties are added in quadrature. A breakdown of the uncertainties on the correction factor is given in table 6. The JES and lepton identification are the largest sources of uncertainty.

For each source of systematic uncertainty, the impact on N_{EW} and $\mathcal{C}_{\mathrm{EW}}$ is found to be anti-correlated, and the fractional uncertainty on the measured cross section is therefore obtained from a linear combination of the fractional uncertainties on N_{EW} and $\mathcal{C}_{\mathrm{EW}}$. The total systematic uncertainty on the measured cross section is then taken to be the quadrature sum of the individual sources of systematic uncertainty.

The fiducial cross sections in the electron and muon channels are

$$\begin{aligned}\sigma_{\mathrm{EW}}^{ee} &= 67.2 \pm 6.9\,(\mathrm{stat})\,^{+12.7}_{-13.4}\,(\mathrm{syst}) \pm 1.9\,(\mathrm{lumi})\,\mathrm{fb} \qquad \text{and}\\ \sigma_{\mathrm{EW}}^{\mu\mu} &= 45.6 \pm 6.1\,(\mathrm{stat})\,^{+9.1}_{-9.6}\,(\mathrm{syst}) \pm 1.3\,(\mathrm{lumi})\,\mathrm{fb}.\end{aligned}$$

These measurements are consistent at the 1.7σ level, accounting for only those uncertainties that are uncorrelated between the two channels. The channels are then combined using a weighted average, with the weight of each channel defined as the squared inverse of the uncorrelated uncertainties. The combined fiducial cross section is

$$\sigma_{\mathrm{EW}} = 54.7 \pm 4.6\,(\mathrm{stat})\,^{+9.8}_{-10.4}\,(\mathrm{syst}) \pm 1.5\,(\mathrm{lumi})\,\mathrm{fb}.$$

The theoretical prediction from `Powheg` for the electroweak Zjj cross section is $46.1 \pm 0.2\,(\mathrm{stat})\,^{+0.3}_{-0.2}\,(\mathrm{scale}) \pm 0.8\,(\mathrm{PDF}) \pm 0.5\,(\mathrm{model})\,\mathrm{fb}$, which is in good agreement with the data.

A detector-corrected fiducial cross section for electroweak Zjj production is also determined for the *search* region with $m_{jj} > 1\,\mathrm{TeV}$, using the integral of the fitted signal template. In this region, electroweak production accounts for approximately 35% of the events. The region at large dijet invariant mass is therefore the part of the spectrum that is most sensitive to the electroweak Zjj component and the least sensitive to the background normalisation. The measured cross section for electroweak Zjj production in the *search* region with $m_{jj} > 1\,\mathrm{TeV}$ is

$$\sigma_{\mathrm{EW}}\,(m_{jj} > 1\,\mathrm{TeV}) = 10.7 \pm 0.9\,(\mathrm{stat}) \pm 1.9\,(\mathrm{syst}) \pm 0.3\,(\mathrm{lumi})\,\mathrm{fb},$$

which is again in good agreement with the theoretical prediction from `Powheg`, $9.38 \pm 0.05\,(\mathrm{stat})\,^{+0.15}_{-0.24}\,(\mathrm{scale}) \pm 0.24\,(\mathrm{PDF}) \pm 0.09\,(\mathrm{model})\,\mathrm{fb}$.

8.5 Estimate of signal significance

The significance of the measurement is estimated using pseudo-experiments. Pseudo-data are created for the *search* and *control* regions from the constrained background templates, after scaling the simulation such that the integral of the template in the *control* region

JHEP04(2014)031

matches the number of events observed in the data. Each bin in the pseudo-data is randomly generated from a Poisson distribution with its mean set to the expected number of events in the normalised constrained templates. Signal and background templates are constructed from the nominal templates by smearing the template shape according to experimental and theoretical systematic uncertainties, which are taken to be Gaussian-distributed. The complete analysis procedure is then performed, including the use of the pseudo-data in the *control* region to construct the reweighting function to apply to the background template in the *search* region. The pseudo-data in the *search* region are subsequently fitted with the new signal and background templates and a value of N_{EW} is extracted. The process is repeated one billion times and none of the pseudo-experiments produce a value of N_{EW} greater than (or equal to) the 1657 events observed in data. The background-only hypothesis is therefore rejected at greater than 5σ significance.[10]

8.6 Limits on anomalous triple gauge couplings

The observation of electroweak Zjj production allows limits to be placed on anomalous triple gauge couplings (aTGCs). The potential benefits of using the electroweak Zjj channel as a probe of aTGCs have been discussed previously in the literature [67]. In the standard hadron collider analyses, aTGC limits are set by measuring vector boson pair production, for which all three gauge bosons entering the WWZ vertex have time-like four-momentum. In the VBF diagram, however, two of the gauge bosons entering the WWZ vertex have space-like four-momentum transfer. Electroweak Zjj production therefore offers a complementary test of aTGCs, because the effects of boson propagators present in electroweak Zjj production are different from those in vector boson pair production. Reference [67] emphasises that full information on triple gauge boson couplings can be obtained only if electroweak vector boson production is measured in addition to vector boson pair production.

The effective Lagrangian, $\mathcal{L}$, for aTGCs can be written as

$$\frac{\mathcal{L}}{g_{WWZ}} = i\left[g_{1,Z}\left(W^{\dagger}_{\mu\nu}W^{\mu}Z^{\nu} - W_{\mu\nu}W^{\dagger\mu}Z^{\nu}\right) + \kappa_Z W^{\dagger}_{\mu}W_{\nu}Z^{\mu\nu} + \frac{\lambda_Z}{m_W^2}W^{\dagger}_{\rho\mu}W^{\mu}_{\nu}Z^{\nu\rho}\right] \quad (8.2)$$

if only those terms that conserve charge conjugation and parity are retained from the general expression [68]. Here, $g_{WWZ} = -e\cot\theta_{\mathrm{W}}$, e is the electric charge, θ_W is the weak mixing angle, W^{μ} and Z^{μ} are the W-boson and Z-boson fields, $X_{\mu\nu} = \partial_{\mu}X_{\nu} - \partial_{\nu}X_{\mu}$ for $X = W$ or Z, and $g_{1,Z}$, κ_Z and λ_Z are dimensionless couplings. The SM values of these dimensionless couplings are $g_{1,Z}^{SM} = 1$, $\kappa_Z^{SM} = 1$ and $\lambda_Z^{SM} = 0$.

The tree-level S-matrix for this effective Lagrangian violates unitarity at large energy scales. Unitarity is restored in the full theory by propagator (form factor) effects. A typical approach is to modify the couplings by a dipole form factor

$$a(\hat{s}) = \frac{a_0}{(1+\hat{s}/\Lambda^2)^2} \quad (8.3)$$

[10] To cross-check the possible impact of non-Gaussian tails in the systematic uncertainties, the pseudo-experiments are repeated using templates smeared (for each source of systematic uncertainty) according to a uniform distribution in the range -5 to $+5$ times the systematic uncertainty. In this extremely conservative approach, the background-only hypothesis is still rejected at greater than 5σ significance.

JHEP04(2014)031

aTGC	$\Lambda = 6$ TeV (obs)	$\Lambda = 6$ TeV (exp)	$\Lambda = \infty$ (obs)	$\Lambda = \infty$ (exp)
$\Delta g_{1,Z}$	$[-0.65, 0.33]$	$[-0.58, 0.27]$	$[-0.50, 0.26]$	$[-0.45, 0.22]$
λ_Z	$[-0.22, 0.19]$	$[-0.19, 0.16]$	$[-0.15, 0.13]$	$[-0.14, 0.11]$

Table 7. The 95% confidence intervals obtained on the aTGC parameters from counting the number of events with $m_{jj} > 1$ TeV in the *search* region. Observed and expected intervals, labelled 'obs' and 'exp' respectively, are presented for unitarisation scales of $\Lambda = 6$ TeV and $\Lambda = \infty$. The parameter $\Delta g_{1,Z}$ refers to the deviation of $g_{1,Z}$ from the SM value.

where a_0 is the bare coupling, $\hat{s}$ is the partonic centre-of-mass energy and Λ is a unitarisation scale. In this measurement, limits are placed on the aTGC parameters for unitarisation scales set to $\Lambda = 6$ TeV and $\Lambda = \infty$. The unitarisation scale of 6 TeV is chosen as the largest common value allowed by unitarity considerations [69, 70] for all anomalous couplings probed in the measurement.

The extracted number of events in the *search* region with $m_{jj} > 1$ TeV is used to place limits on the aTGCs as this region is the least affected by the background normalisation and signal template shape. There are 900 events observed in the data in this region. The expected number of electroweak Zjj events in the SM is 261, estimated using the `Sherpa` sample. The expected number of background events is 592, estimated after fitting the m_{jj} spectrum with signal and background templates. Note that the normalisation of the background template is effectively governed by the low-m_{jj} region, thus limiting the impact of background modelling in the aTGC limit setting in the high m_{jj} tail. The aTGC parameters (and form factors) are varied within the `Sherpa` event generator, allowing the change in the number of electroweak Zjj events to be estimated.

Frequentist confidence intervals are set for the anomalous couplings by performing a profile likelihood test [71]. A Poisson likelihood function is constructed from the observed number of events, the expected signal as a function of the anomalous couplings and the estimated number of background events. The systematic uncertainties are included in the likelihood function as nuisance parameters with correlated Gaussian constraints. A given aTGC parameter point is rejected at 95% confidence level if more than 95% of randomly generated pseudo-experiments exhibit a value of the profile likelihood ratio larger than that observed in data.

The limits presented in this paper are sensitive to the momentum transfer in the t-channel due to the high-m_{jj} requirement and, therefore, most sensitive to the terms in the Lagrangian that contain a derivative of the W-boson field. Table 7 shows the 95% confidence intervals obtained on the anomalous coupling parameters λ_Z and $g_{1,Z}$. The limits are not as stringent as those set in WZ production [72], which are approximately a factor of three smaller in the λ_Z coupling, for example.

9 Summary

Fiducial cross sections for electroweak Zjj production have been presented for proton-proton collisions at $\sqrt{s} = 8$ TeV, using a dataset corresponding to an integrated luminos-

JHEP04(2014)031

ity of $20.3\,\text{fb}^{-1}$ collected by the ATLAS experiment at the Large Hadron Collider. The background-only model has been rejected above the 5σ level and these measurements constitute observation of the electroweak Zjj process. The measured cross sections are in good agreement with the Standard Model expectation and limits have been set on anomalous triple gauge couplings. In addition, cross sections and differential distributions have been measured for inclusive Zjj production in five fiducial regions. The cross-section measurements are all in good agreement with the prediction from `Powheg` for Zjj production. The differential distributions are sensitive to the electroweak component of Zjj production, as well as the modelling of strong Zjj production in the extreme phase-space regions probed. The data are compared to theoretical predictions from the `Sherpa` and `Powheg` event generators. Neither prediction is able to fully reproduce the data for all distributions and the data can be used to constrain the theoretical modelling in these extreme phase-space regions.

Acknowledgments

We thank CERN for the very successful operation of the LHC, as well as the support staff from our institutions without whom ATLAS could not be operated efficiently. We also thank Stefan Hoeche and Frank Krauss for insight and cross-checks related to the interference between electroweak and strong Zjj production as predicted by the Sherpa event generator.

We acknowledge the support of ANPCyT, Argentina; YerPhI, Armenia; ARC, Australia; BMWF and FWF, Austria; ANAS, Azerbaijan; SSTC, Belarus; CNPq and FAPESP, Brazil; NSERC, NRC and CFI, Canada; CERN; CONICYT, Chile; CAS, MOST and NSFC, China; COLCIENCIAS, Colombia; MSMT CR, MPO CR and VSC CR, Czech Republic; DNRF, DNSRC and Lundbeck Foundation, Denmark; EPLANET, ERC and NSRF, European Union; IN2P3-CNRS, CEA-DSM/IRFU, France; GNSF, Georgia; BMBF, DFG, HGF, MPG and AvH Foundation, Germany; GSRT and NSRF, Greece; ISF, MINERVA, GIF, DIP and Benoziyo Center, Israel; INFN, Italy; MEXT and JSPS, Japan; CNRST, Morocco; FOM and NWO, Netherlands; BRF and RCN, Norway; MNiSW and NCN, Poland; GRICES and FCT, Portugal; MNE/IFA, Romania; MES of Russia and ROSATOM, Russian Federation; JINR; MSTD, Serbia; MSSR, Slovakia; ARRS and MIZŠ, Slovenia; DST/NRF, South Africa; MINECO, Spain; SRC and Wallenberg Foundation, Sweden; SER, SNSF and Cantons of Bern and Geneva, Switzerland; NSC, Taiwan; TAEK, Turkey; STFC, the Royal Society and Leverhulme Trust, United Kingdom; DOE and NSF, United States of America.

The crucial computing support from all WLCG partners is acknowledged gratefully, in particular from CERN and the ATLAS Tier-1 facilities at TRIUMF (Canada), NDGF (Denmark, Norway, Sweden), CC-IN2P3 (France), KIT/GridKA (Germany), INFN-CNAF (Italy), NL-T1 (Netherlands), PIC (Spain), ASGC (Taiwan), RAL (U.K.) and BNL (U.S.A.) and in the Tier-2 facilities worldwide.

JHEP04(2014)031

A Additional inclusive Zjj differential distributions

In this section, unfolded inclusive Zjj distributions are presented in fiducial regions that complement the data presented in section 7. These additional data are fully corrected for detector effects and available in HEPDATA. The unfolded $\frac{1}{\sigma}\cdot\frac{\mathrm{d}\sigma}{\mathrm{d}m_{jj}}$ and $\frac{1}{\sigma}\cdot\frac{\mathrm{d}\sigma}{\mathrm{d}|\Delta y|}$ distributions are shown in figure 13 and 14, respectively, for the *high-*p_{T} and *control* regions. Figure 15 shows the unfolded jet veto efficiency and $\langle N_{\mathrm{jet}}^{\mathrm{gap}}\rangle$ distributions as a function of m_{jj} and $|\Delta y|$ in the *high-*p_{T} region. Finally, the unfolded $p_{\mathrm{T}}^{\mathrm{balance}}$ *cut efficiency* as a function of m_{jj} and $|\Delta y|$ in the *high-*p_{T} region is shown in figure 16.

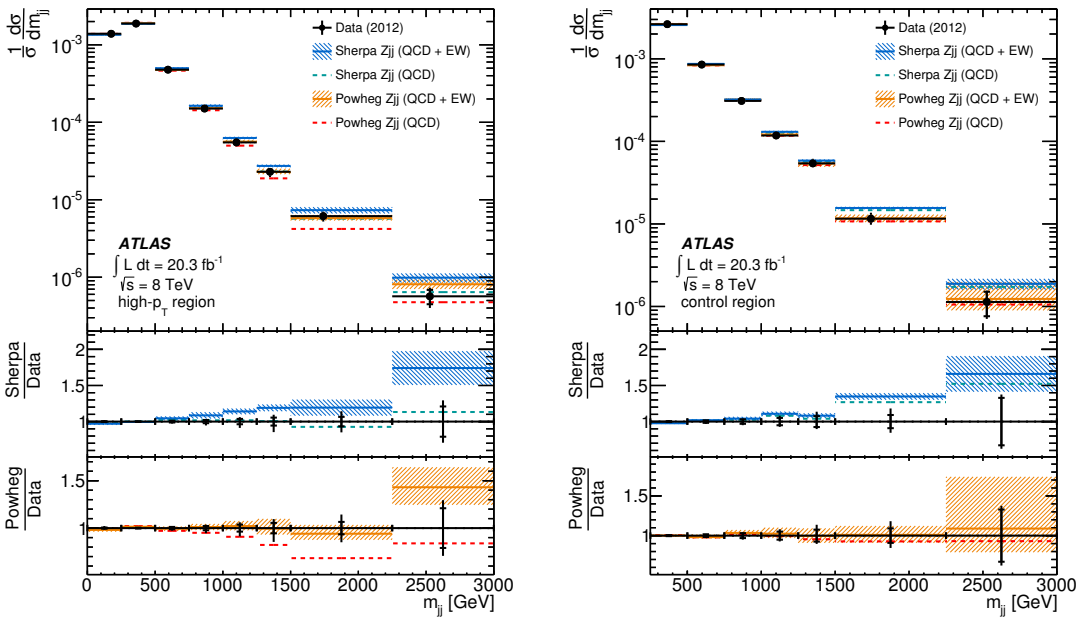

(a) (b)

Figure 13. Unfolded $\frac{1}{\sigma}\cdot\frac{\mathrm{d}\sigma}{\mathrm{d}m_{jj}}$ distribution in (a) the *high-*p_{T} and (b) *control* regions. The data and theoretical predictions are presented in the same way as in figure 6.

JHEP04(2014)031

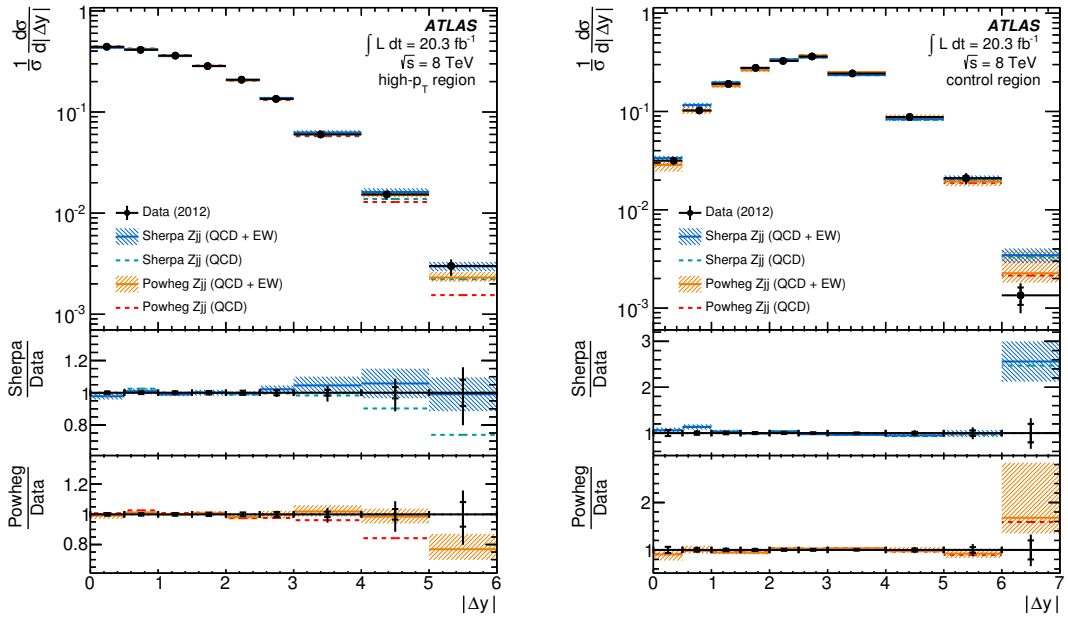

(a) (b)

Figure 14. Unfolded $\frac{1}{\sigma} \cdot \frac{\mathrm{d}\sigma}{\mathrm{d}|\Delta y|}$ distribution in (a) the *high-*p_{T} and (b) *control* regions. The data and theoretical predictions are presented in the same way as in figure 6.

JHEP04(2014)031

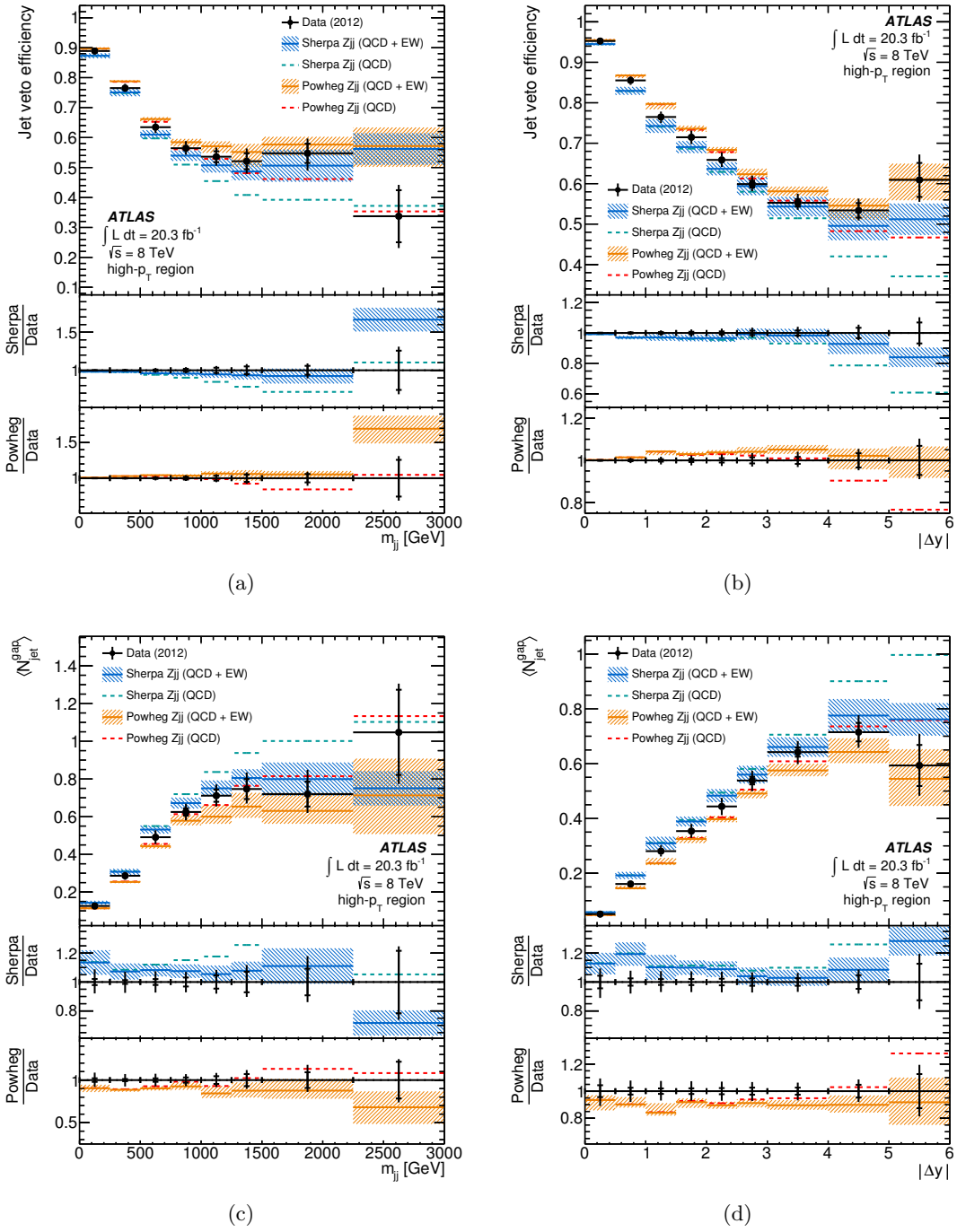

Figure 15. Unfolded *jet veto efficiency* versus (a) m_{jj} and (b) $|\Delta y|$ in the *high-*p_{T} region. Unfolded $\langle N_{\mathrm{jet}}^{\mathrm{gap}} \rangle$ versus (c) m_{jj} and (d) $|\Delta y|$ in the *high-*p_{T} region. The data and theoretical predictions are presented in the same way as in figure 6.

JHEP04(2014)031

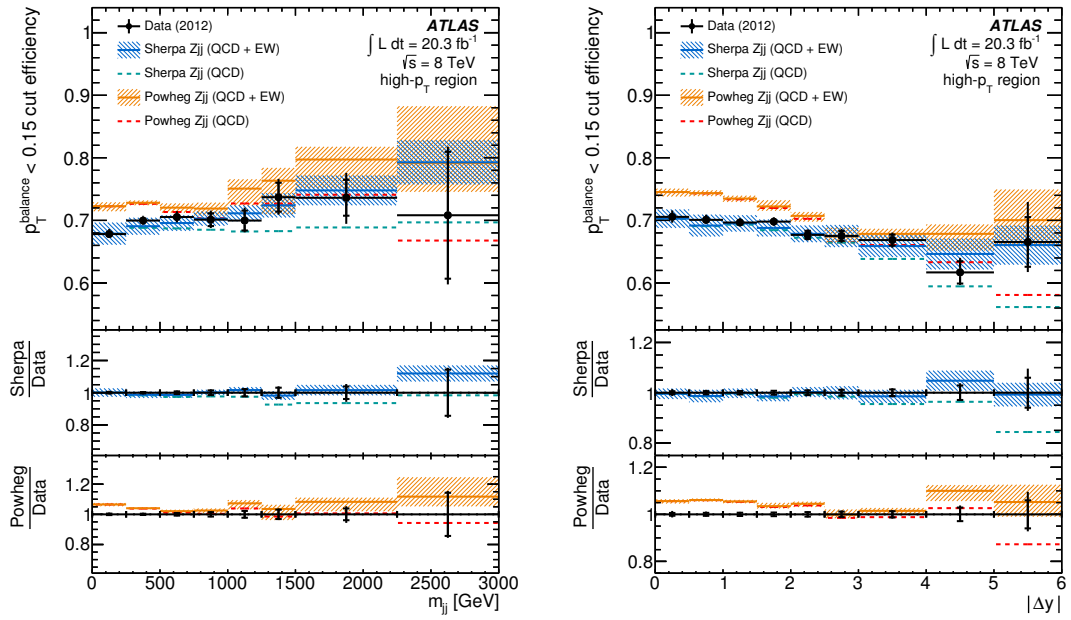

(a) (b)

Figure 16. Unfolded $p_{\mathrm{T}}^{\mathrm{balance}}$ *cut efficiency* versus (a) m_{jj} and (b) $|\Delta y|$ in the *high-*p_{T} region. The data and theoretical predictions are presented in the same way as in figure 6.

Open Access. This article is distributed under the terms of the Creative Commons Attribution License (CC-BY 4.0), which permits any use, distribution and reproduction in any medium, provided the original author(s) and source are credited.

References

[1] C. Oleari and D. Zeppenfeld, *QCD corrections to electroweak $\nu_\ell jj$ and $\ell^+\ell^- jj$ production*, *Phys. Rev.* **D 69** (2004) 093004 [hep-ph/0310156] [INSPIRE].

[2] K. Arnold, J. Bellm, G. Bozzi, M. Brieg, F. Campanario et al., *VBFNLO: A parton level Monte Carlo for processes with electroweak bosons – Manual for version 2.5.0*, arXiv:1107.4038 [INSPIRE].

[3] ATLAS collaboration, *The ATLAS experiment at the CERN Large Hadron Collider*, 2008 *JINST* **3** S08003 [INSPIRE].

[4] D.L. Rainwater, R. Szalapski and D. Zeppenfeld, *Probing color singlet exchange in Z + two jet events at the CERN LHC*, *Phys. Rev.* **D 54** (1996) 6680 [hep-ph/9605444] [INSPIRE].

[5] V. Khoze, M. Ryskin, W. Stirling and P. Williams, *A Z monitor to calibrate Higgs production via vector boson fusion with rapidity gaps at the LHC*, *Eur. Phys. J.* **C 26** (2003) 429 [hep-ph/0207365] [INSPIRE].

[6] CMS collaboration, *Measurement of the hadronic activity in events with a Z and two jets and extraction of the cross section for the electroweak production of a Z with two jets in pp collisions at $\sqrt{s} = 7$ TeV*, *JHEP* **10** (2013) 101 [arXiv:1305.7389] [INSPIRE].

JHEP04(2014)031

[7] ATLAS collaboration, *Performance of the ATLAS trigger system in 2010*, *Eur. Phys. J.* **C 72** (2012) 1849 [arXiv:1110.1530] [INSPIRE].

[8] ATLAS collaboration, *Measurement of the $W \to \ell\nu$ and $Z/\gamma^* \to \ell\ell$ production cross sections in proton-proton collisions at $\sqrt{s} = 7$ TeV with the ATLAS detector*, *JHEP* **12** (2010) 060 [arXiv:1010.2130] [INSPIRE].

[9] ATLAS collaboration, *Electron performance measurements with the ATLAS detector using the 2010 LHC proton-proton collision data*, *Eur. Phys. J.* **C 72** (2012) 1909 [arXiv:1110.3174] [INSPIRE].

[10] M. Cacciari, G.P. Salam and G. Soyez, *The anti-k_t jet clustering algorithm*, *JHEP* **04** (2008) 063 [arXiv:0802.1189] [INSPIRE].

[11] ATLAS collaboration, *Calorimeter clustering algorithms: description and performance*, ATLAS-LARG-PUB-2008-002 (2008).

[12] ATLAS collaboration, *Pile-up subtraction and suppression for jets in ATLAS*, ATLAS-CONF-2013-083 (2013).

[13] ATLAS collaboration, *Jet energy measurement with the ATLAS detector in proton-proton collisions at $\sqrt{s} = 7$ TeV*, *Eur. Phys. J.* **C 73** (2013) 2304 [arXiv:1112.6426] [INSPIRE].

[14] ATLAS collaboration, *Jet energy scale and its systematic uncertainty in proton-proton collisions at $\sqrt{s} = 7$ TeV with ATLAS 2011 data*, ATLAS-CONF-2013-004 (2013).

[15] M. Cacciari, G.P. Salam and G. Soyez, *The catchment area of jets*, *JHEP* **04** (2008) 005 [arXiv:0802.1188] [INSPIRE].

[16] P. Nason, *A new method for combining NLO QCD with shower Monte Carlo algorithms*, *JHEP* **11** (2004) 040 [hep-ph/0409146] [INSPIRE].

[17] S. Frixione, P. Nason and C. Oleari, *Matching NLO QCD computations with Parton Shower simulations: the POWHEG method*, *JHEP* **11** (2007) 070 [arXiv:0709.2092] [INSPIRE].

[18] S. Alioli, P. Nason, C. Oleari and E. Re, *A general framework for implementing NLO calculations in shower Monte Carlo programs: the POWHEG BOX*, *JHEP* **06** (2010) 043 [arXiv:1002.2581] [INSPIRE].

[19] T. Gleisberg et al., *Event generation with SHERPA 1.1*, *JHEP* **02** (2009) 007 [arXiv:0811.4622] [INSPIRE].

[20] S. Catani, F. Krauss, R. Kuhn and B. Webber, *QCD matrix elements + parton showers*, *JHEP* **11** (2001) 063 [hep-ph/0109231] [INSPIRE].

[21] H.-L. Lai et al., *New parton distributions for collider physics*, *Phys. Rev.* **D 82** (2010) 074024 [arXiv:1007.2241] [INSPIRE].

[22] B. Jager, S. Schneider and G. Zanderighi, *Next-to-leading order QCD corrections to electroweak Zjj production in the POWHEG BOX*, *JHEP* **09** (2012) 083 [arXiv:1207.2626] [INSPIRE].

[23] F. Schissler and D. Zeppenfeld, *Parton shower effects on W and Z production via vector boson fusion at NLO QCD*, *JHEP* **04** (2013) 057 [arXiv:1302.2884] [INSPIRE].

[24] E. Re, *NLO corrections merged with parton showers for $Z + 2$ jets production using the POWHEG method*, *JHEP* **10** (2012) 031 [arXiv:1204.5433] [INSPIRE].

[25] J.M. Campbell, R.K. Ellis, P. Nason and G. Zanderighi, *W and Z bosons in association with two jets using the POWHEG method*, *JHEP* **08** (2013) 005 [arXiv:1303.5447] [INSPIRE].

JHEP04(2014)031

[26] T. Sjöstrand, S. Mrenna and P.Z. Skands, *PYTHIA 6.4 physics and manual*, *JHEP* **05** (2006) 026 [hep-ph/0603175] [INSPIRE].

[27] P.Z. Skands, *Tuning Monte Carlo generators: the Perugia tunes*, *Phys. Rev.* **D 82** (2010) 074018 [arXiv:1005.3457] [INSPIRE].

[28] K. Hamilton, P. Nason and G. Zanderighi, *MINLO: Multi-scale Improved NLO*, *JHEP* **10** (2012) 155 [arXiv:1206.3572] [INSPIRE].

[29] S. Hoeche, S. Schumann and F. Siegert, *Hard photon production and matrix-element parton-shower merging*, *Phys. Rev.* **D 81** (2010) 034026 [arXiv:0912.3501] [INSPIRE].

[30] S. Schumann and F. Krauss, *A parton shower algorithm based on Catani-Seymour dipole factorisation*, *JHEP* **03** (2008) 038 [arXiv:0709.1027] [INSPIRE].

[31] S. Hoeche and M. Schonherr, *Uncertainties in next-to-leading order plus parton shower matched simulations of inclusive jet and dijet production*, *Phys. Rev.* **D 86** (2012) 094042 [arXiv:1208.2815] [INSPIRE].

[32] J.R. Andersen and J.M. Smillie, *QCD and electroweak interference in Higgs production by gauge boson fusion*, *Phys. Rev.* **D 75** (2007) 037301 [hep-ph/0611281] [INSPIRE].

[33] M. Ciccolini, A. Denner and S. Dittmaier, *Electroweak and QCD corrections to Higgs production via vector-boson fusion at the LHC*, *Phys. Rev.* **D 77** (2008) 013002 [arXiv:0710.4749] [INSPIRE].

[34] J. Andersen, T. Binoth, G. Heinrich and J. Smillie, *Loop induced interference effects in Higgs Boson plus two jet production at the LHC*, *JHEP* **02** (2008) 057 [arXiv:0709.3513] [INSPIRE].

[35] A. Bredenstein, K. Hagiwara and B. Jager, *Mixed QCD-electroweak contributions to Higgs-plus-dijet production at the LHC*, *Phys. Rev.* **D 77** (2008) 073004 [arXiv:0801.4231] [INSPIRE].

[36] S. Agostinelli et al., *GEANT4 — A simulation toolkit*, *Nucl. Instrum. Meth.* **506** (2003) 250.

[37] J. Allison et al., *GEANT4 developments and applications*, *IEEE Trans. Nucl. Sci.* **53** (2006) 270 [INSPIRE].

[38] ATLAS collaboration, *The ATLAs simulation infrastructure*, *Eur. Phys. J.* **C 70** (2010) 823 [arXiv:1005.4568] [INSPIRE].

[39] T. Sjöstrand, S. Mrenna and P.Z. Skands, *A brief introduction to PYTHIA 8.1*, *Comput. Phys. Commun.* **178** (2008) 852 [arXiv:0710.3820] [INSPIRE].

[40] ATLAS Collaboration, *Further ATLAS tunes of PYTHIA 6 and Pythia 8*, ATLAS-PHYS-PUB-2011-014 (2011).

[41] A. Martin, W. Stirling, R. Thorne and G. Watt, *Parton distributions for the LHC*, *Eur. Phys. J.* **C 63** (2009) 189 [arXiv:0901.0002] [INSPIRE].

[42] M.L. Mangano, M. Moretti, F. Piccinini, R. Pittau and A.D. Polosa, *ALPGEN, a generator for hard multiparton processes in hadronic collisions*, *JHEP* **07** (2003) 001 [hep-ph/0206293] [INSPIRE].

[43] G. Corcella et al., *HERWIG 6: an event generator for hadron emission reactions with interfering gluons (including supersymmetric processes)*, *JHEP* **01** (2001) 010 [hep-ph/0011363] [INSPIRE].

[44] G. Corcella et al., *HERWIG 6.5 release note*, hep-ph/0210213 [INSPIRE].

JHEP04(2014)031

[45] J. Butterworth, J.R. Forshaw and M. Seymour, *Multiparton interactions in photoproduction at HERA*, *Z. Phys.* **C 72** (1996) 637 [hep-ph/9601371] [INSPIRE].

[46] ATLAS collaboration, *New ATLAS event generator tunes to 2010 data*, ATL-PHYS-PUB-2011-008 (2011).

[47] S. Frixione and B.R. Webber, *Matching NLO QCD computations and parton shower simulations*, *JHEP* **06** (2002) 029 [hep-ph/0204244] [INSPIRE].

[48] M. Czakon and A. Mitov, *Top++: a program for the calculation of the top-pair cross-section at hadron colliders*, arXiv:1112.5675 [INSPIRE].

[49] ATLAS collaboration, *Preliminary results on the muon reconstruction efficiency, momentum resolution and momentum scale in ATLAS 2012 pp collision data*, ATLAS-CONF-2013-088 (2013).

[50] ATLAS collaboration, *Improved luminosity determination in pp collisions at $\sqrt{s} = 7$ TeV using the ATLAS detector at the LHC*, *Eur. Phys. J.* **C 73** (2013) 2518 [arXiv:1302.4393] [INSPIRE].

[51] ATLAS collaboration, *Jet energy resolution in proton-proton collisions at $\sqrt{s} = 7$ TeV recorded in* 2010 *with the ATLAS detector*, *Eur. Phys. J.* **C 73** (2013) 2306 [arXiv:1210.6210] [INSPIRE].

[52] ATLAS collaboration, *Measurements of the pseudorapidity dependence of the total transverse energy in proton-proton collisions at $\sqrt{s} = 7$ TeV with ATLAS*, *JHEP* **11** (2012) 033 [arXiv:1208.6256] [INSPIRE].

[53] http://hepdata.cedar.ac.uk/.

[54] G. D'Agostini, *A multidimensional unfolding method based on Bayes' theorem*, *Nucl. Instrum. Meth.* **A 362** (1995) 487 [INSPIRE].

[55] T. Adye, *Unfolding algorithms and tests using RooUnfold*, arXiv:1105.1160 [INSPIRE].

[56] K. Hayes, M.L. Perl and B. Efron, *Application of the bootstrap statistical method to the τ decay mode problem*, *Phys. Rev.* **D 39** (1989) 274 [INSPIRE].

[57] ATLAS collaboration, *Measurement of the production cross section of jets in association with a Z boson in pp collisions at $\sqrt{s} = 7$ TeV with the ATLAS detector*, *JHEP* **07** (2013) 032 [arXiv:1304.7098] [INSPIRE].

[58] D0 collaboration, V.M. Abazov et al., *Studies of W boson plus jets production in $p\bar{p}$ collisions at $\sqrt{s} = 1.96$ TeV*, *Phys. Rev.* **D 88** (2013) 092001 [arXiv:1302.6508] [INSPIRE].

[59] T. Plehn, D.L. Rainwater and D. Zeppenfeld, *Determining the structure of Higgs couplings at the LHC*, *Phys. Rev. Lett.* **88** (2002) 051801 [hep-ph/0105325] [INSPIRE].

[60] G. Klamke and D. Zeppenfeld, *Higgs plus two jet production via gluon fusion as a signal at the CERN LHC*, *JHEP* **04** (2007) 052 [hep-ph/0703202] [INSPIRE].

[61] J.R. Andersen, K. Arnold and D. Zeppenfeld, *Azimuthal angle correlations for Higgs boson plus multi-jet events*, *JHEP* **06** (2010) 091 [arXiv:1001.3822] [INSPIRE].

[62] ATLAS collaboration, *Measurement of dijet production with a veto on additional central jet activity in pp collisions at $\sqrt{s} = 7$ TeV using the ATLAS detector*, *JHEP* **09** (2011) 053 [arXiv:1107.1641] [INSPIRE].

[63] W. Verkerke and D.P. Kirkby, *The RooFit toolkit for data modeling*, *eConf* **C 0303241** (2003) MOLT007 [physics/0306116] [INSPIRE].

JHEP04(2014)031

[64] R.D. Ball et al., *Parton distributions with LHC data*, *Nucl. Phys.* **B 867** (2013) 244 [arXiv:1207.1303] [INSPIRE].

[65] J.M. Campbell, J. Huston and W. Stirling, *HArd interactions of quarks and gluons: a primer for LHC physics*, *Rept. Prog. Phys.* **70** (2007) 89 [hep-ph/0611148] [INSPIRE].

[66] A. Martin, W. Stirling, R. Thorne and G. Watt, *Uncertainties on α_s in global PDF analyses and implications for predicted hadronic cross sections*, *Eur. Phys. J.* **C 64** (2009) 653 [arXiv:0905.3531] [INSPIRE].

[67] U. Baur and D. Zeppenfeld, *Measuring three vector boson couplings in $qq \to qqW$ at the SSC*, hep-ph/9309227 [INSPIRE].

[68] K. Hagiwara, R. Peccei, D. Zeppenfeld and K. Hikasa, *Probing the weak boson sector in $e^+e^- \to W^+W^-$*, *Nucl. Phys.* **B 282** (1987) 253 [INSPIRE].

[69] U. Baur and D. Zeppenfeld, *Unitarity constraints on the electroweak three vector boson vertices*, *Phys. Lett.* **B 201** (1988) 383 [INSPIRE].

[70] H. Aihara et al., *Anomalous gauge boson interactions*, hep-ph/9503425 [INSPIRE].

[71] G. Cowan, K. Cranmer, E. Gross and O. Vitells, *Asymptotic formulae for likelihood-based tests of new physics*, *Eur. Phys. J.* **C 71** (2011) 1554 [arXiv:1007.1727] [INSPIRE].

[72] ATLAS collaboration, *Measurement of WZ production in proton-proton collisions at $\sqrt{s} = 7$ TeV with the ATLAS detector*, *Eur. Phys. J.* **C 72** (2012) 2173 [arXiv:1208.1390] [INSPIRE].

JHEP04(2014)031

The ATLAS collaboration

G. Aad[84], T. Abajyan[21], B. Abbott[112], J. Abdallah[152], S. Abdel Khalek[116], O. Abdinov[11], R. Aben[106], B. Abi[113], M. Abolins[89], O.S. AbouZeid[159], H. Abramowicz[154], H. Abreu[137], Y. Abulaiti[147a,147b], B.S. Acharya[165a,165b,a], L. Adamczyk[38a], D.L. Adams[25], T.N. Addy[56], J. Adelman[177], S. Adomeit[99], T. Adye[130], T. Agatonovic-Jovin[13b], J.A. Aguilar-Saavedra[125f,125a], M. Agustoni[17], S.P. Ahlen[22], A. Ahmad[149], F. Ahmadov[64,b], G. Aielli[134a,134b], T.P.A. Åkesson[80], G. Akimoto[156], A.V. Akimov[95], J. Albert[170], S. Albrand[55], M.J. Alconada Verzini[70], M. Aleksa[30], I.N. Aleksandrov[64], C. Alexa[26a], G. Alexander[154], G. Alexandre[49], T. Alexopoulos[10], M. Alhroob[165a,165c], G. Alimonti[90a], L. Alio[84], J. Alison[31], B.M.M. Allbrooke[18], L.J. Allison[71], P.P. Allport[73], S.E. Allwood-Spiers[53], J. Almond[83], A. Aloisio[103a,103b], R. Alon[173], A. Alonso[36], F. Alonso[70], C. Alpigiani[75], A. Altheimer[35], B. Alvarez Gonzalez[89], M.G. Alviggi[103a,103b], K. Amako[65], Y. Amaral Coutinho[24a], C. Amelung[23], V.V. Ammosov[129,*], S.P. Amor Dos Santos[125a,125c], A. Amorim[125a,125b], S. Amoroso[48], N. Amram[154], G. Amundsen[23], C. Anastopoulos[140], L.S. Ancu[17], N. Andari[30], T. Andeen[35], C.F. Anders[58b], G. Anders[58a], K.J. Anderson[31], A. Andreazza[90a,90b], V. Andrei[58a], X.S. Anduaga[70], S. Angelidakis[9], P. Anger[44], A. Angerami[35], F. Anghinolfi[30], A.V. Anisenkov[108], N. Anjos[125a], A. Annovi[47], A. Antonaki[9], M. Antonelli[47], A. Antonov[97], J. Antos[145b], F. Anulli[133a], M. Aoki[65], L. Aperio Bella[18], R. Apolle[119,c], G. Arabidze[89], I. Aracena[144], Y. Arai[65], A.T.H. Arce[45], J-F. Arguin[94], S. Argyropoulos[42], M. Arik[19a], A.J. Armbruster[88], O. Arnaez[82], V. Arnal[81], O. Arslan[21], A. Artamonov[96], G. Artoni[23], S. Asai[156], N. Asbah[94], S. Ask[28], B. Åsman[147a,147b], L. Asquith[6], K. Assamagan[25], R. Astalos[145a], M. Atkinson[166], N.B. Atlay[142], B. Auerbach[6], E. Auge[116], K. Augsten[127], M. Aurousseau[146b], G. Avolio[30], G. Azuelos[94,d], Y. Azuma[156], M.A. Baak[30], C. Bacci[135a,135b], A.M. Bach[15], H. Bachacou[137], K. Bachas[155], M. Backes[30], M. Backhaus[21], J. Backus Mayes[144], E. Badescu[26a], P. Bagiacchi[133a,133b], P. Bagnaia[133a,133b], Y. Bai[33a], D.C. Bailey[159], T. Bain[35], J.T. Baines[130], O.K. Baker[177], S. Baker[77], P. Balek[128], F. Balli[137], E. Banas[39], Sw. Banerjee[174], D. Banfi[30], A. Bangert[151], V. Bansal[170], H.S. Bansil[18], L. Barak[173], S.P. Baranov[95], T. Barber[48], E.L. Barberio[87], D. Barberis[50a,50b], M. Barbero[84], T. Barillari[100], M. Barisonzi[176], T. Barklow[144], N. Barlow[28], B.M. Barnett[130], R.M. Barnett[15], Z. Barnovska[5], A. Baroncelli[135a], G. Barone[49], A.J. Barr[119], F. Barreiro[81], J. Barreiro Guimarães da Costa[57], R. Bartoldus[144], A.E. Barton[71], P. Bartos[145a], V. Bartsch[150], A. Bassalat[116], A. Basye[166], R.L. Bates[53], L. Batkova[145a], J.R. Batley[28], M. Battistin[30], F. Bauer[137], H.S. Bawa[144,e], T. Beau[79], P.H. Beauchemin[162], R. Beccherle[123a,123b], P. Bechtle[21], H.P. Beck[17], K. Becker[176], S. Becker[99], M. Beckingham[139], A.J. Beddall[19c], A. Beddall[19c], S. Bedikian[177], V.A. Bednyakov[64], C.P. Bee[149], L.J. Beemster[106], T.A. Beermann[176], M. Begel[25], K. Behr[119], C. Belanger-Champagne[86], P.J. Bell[49], W.H. Bell[49], G. Bella[154], L. Bellagamba[20a], A. Bellerive[29], M. Bellomo[85], A. Belloni[57], O.L. Beloborodova[108,f], K. Belotskiy[97], O. Beltramello[30], O. Benary[154], D. Benchekroun[136a], K. Bendtz[147a,147b], N. Benekos[166], Y. Benhammou[154], E. Benhar Noccioli[49], J.A. Benitez Garcia[160b], D.P. Benjamin[45], J.R. Bensinger[23], K. Benslama[131], S. Bentvelsen[106], D. Berge[106], E. Bergeaas Kuutmann[16], N. Berger[5], F. Berghaus[170], E. Berglund[106], J. Beringer[15], C. Bernard[22], P. Bernat[77], C. Bernius[78], F.U. Bernlochner[170], T. Berry[76], P. Berta[128], C. Bertella[84], F. Bertolucci[123a,123b], M.I. Besana[90a], G.J. Besjes[105], O. Bessidskaia[147a,147b], N. Besson[137], C. Betancourt[48], S. Bethke[100], W. Bhimji[46], R.M. Bianchi[124], L. Bianchini[23], M. Bianco[30], O. Biebel[99], S.P. Bieniek[77], K. Bierwagen[54], J. Biesiada[15], M. Biglietti[135a], J. Bilbao De Mendizabal[49], H. Bilokon[47], M. Bindi[20a,20b], S. Binet[116], A. Bingul[19c], C. Bini[133a,133b], C.W. Black[151], J.E. Black[144], K.M. Black[22], D. Blackburn[139], R.E. Blair[6], J.-B. Blanchard[137], T. Blazek[145a], I. Bloch[42], C. Blocker[23], W. Blum[82,*], U. Blumenschein[54], G.J. Bobbink[106], V.S. Bobrovnikov[108], S.S. Bocchetta[80], A. Bocci[45], C.R. Boddy[119], M. Boehler[48], J. Boek[176], T.T. Boek[176], J.A. Bogaerts[30], A.G. Bogdanchikov[108], A. Bogouch[91,*], C. Bohm[147a], J. Bohm[126], V. Boisvert[76], T. Bold[38a], V. Boldea[26a], A.S. Boldyrev[98], N.M. Bolnet[137], M. Bomben[79], M. Bona[75], M. Boonekamp[137], A. Borisov[129], G. Borissov[71], M. Borri[83], S. Borroni[42], J. Bortfeldt[99], V. Bortolotto[135a,135b], K. Bos[106], D. Boscherini[20a], M. Bosman[12], H. Boterenbrood[106], J. Boudreau[124], J. Bouffard[2],

JHEP04(2014)031

E.V. Bouhova-Thacker[71], D. Boumediene[34], C. Bourdarios[116], N. Bousson[84], S. Boutouil[136d], A. Boveia[31], J. Boyd[30], I.R. Boyko[64], I. Bozovic-Jelisavcic[13b], J. Bracinik[18], P. Branchini[135a], A. Brandt[8], G. Brandt[15], O. Brandt[58a], U. Bratzler[157], B. Brau[85], J.E. Brau[115], H.M. Braun[176,*], S.F. Brazzale[165a,165c], B. Brelier[159], K. Brendlinger[121], A.J. Brennan[87], R. Brenner[167], S. Bressler[173], K. Bristow[146c], T.M. Bristow[46], D. Britton[53], F.M. Brochu[28], I. Brock[21], R. Brock[89], C. Bromberg[89], J. Bronner[100], G. Brooijmans[35], T. Brooks[76], W.K. Brooks[32b], J. Brosamer[15], E. Brost[115], G. Brown[83], J. Brown[55], P.A. Bruckman de Renstrom[39], D. Bruncko[145b], R. Bruneliere[48], S. Brunet[60], A. Bruni[20a], G. Bruni[20a], M. Bruschi[20a], L. Bryngemark[80], T. Buanes[14], Q. Buat[143], F. Bucci[49], P. Buchholz[142], R.M. Buckingham[119], A.G. Buckley[53], S.I. Buda[26a], I.A. Budagov[64], F. Buehrer[48], L. Bugge[118], M.K. Bugge[118], O. Bulekov[97], A.C. Bundock[73], H. Burckhart[30], S. Burdin[73], B. Burghgrave[107], S. Burke[130], I. Burmeister[43], E. Busato[34], V. Büscher[82], P. Bussey[53], C.P. Buszello[167], B. Butler[57], J.M. Butler[22], A.I. Butt[3], C.M. Buttar[53], J.M. Butterworth[77], W. Buttinger[28], A. Buzatu[53], M. Byszewski[10], S. Cabrera Urbán[168], D. Caforio[20a,20b], O. Cakir[4a], P. Calafiura[15], G. Calderini[79], P. Calfayan[99], R. Calkins[107], L.P. Caloba[24a], D. Calvet[34], S. Calvet[34], R. Camacho Toro[49], P. Camarri[134a,134b], D. Cameron[118], L.M. Caminada[15], R. Caminal Armadans[12], S. Campana[30], M. Campanelli[77], A. Campoverde[149], V. Canale[103a,103b], A. Canepa[160a], J. Cantero[81], R. Cantrill[76], T. Cao[40], M.D.M. Capeans Garrido[30], I. Caprini[26a], M. Caprini[26a], M. Capua[37a,37b], R. Caputo[82], R. Cardarelli[134a], T. Carli[30], G. Carlino[103a], L. Carminati[90a,90b], S. Caron[105], E. Carquin[32a], G.D. Carrillo-Montoya[146c], A.A. Carter[75], J.R. Carter[28], J. Carvalho[125a,125c], D. Casadei[77], M.P. Casado[12], E. Castaneda-Miranda[146b], A. Castelli[106], V. Castillo Gimenez[168], N.F. Castro[125a], P. Catastini[57], A. Catinaccio[30], J.R. Catmore[71], A. Cattai[30], G. Cattani[134a,134b], S. Caughron[89], V. Cavaliere[166], D. Cavalli[90a], M. Cavalli-Sforza[12], V. Cavasinni[123a,123b], F. Ceradini[135a,135b], B. Cerio[45], K. Cerny[128], A.S. Cerqueira[24b], A. Cerri[150], L. Cerrito[75], F. Cerutti[15], M. Cerv[30], A. Cervelli[17], S.A. Cetin[19b], A. Chafaq[136a], D. Chakraborty[107], I. Chalupkova[128], K. Chan[3], P. Chang[166], B. Chapleau[86], J.D. Chapman[28], D. Charfeddine[116], D.G. Charlton[18], C.A. Chavez Barajas[30], S. Cheatham[86], A. Chegwidden[89], S. Chekanov[6], S.V. Chekulaev[160a], G.A. Chelkov[64], M.A. Chelstowska[88], C. Chen[63], H. Chen[25], K. Chen[149], L. Chen[33d,g], S. Chen[33c], X. Chen[146c], Y. Chen[35], H.C. Cheng[88], Y. Cheng[31], A. Cheplakov[64], R. Cherkaoui El Moursli[136e], V. Chernyatin[25,*], E. Cheu[7], L. Chevalier[137], V. Chiarella[47], G. Chiefari[103a,103b], J.T. Childers[6], A. Chilingarov[71], G. Chiodini[72a], A.S. Chisholm[18], R.T. Chislett[77], A. Chitan[26a], M.V. Chizhov[64], S. Chouridou[9], B.K.B. Chow[99], I.A. Christidi[77], D. Chromek-Burckhart[30], M.L. Chu[152], J. Chudoba[126], L. Chytka[114], G. Ciapetti[133a,133b], A.K. Ciftci[4a], R. Ciftci[4a], D. Cinca[62], V. Cindro[74], A. Ciocio[15], P. Cirkovic[13b], Z.H. Citron[173], M. Citterio[90a], M. Ciubancan[26a], A. Clark[49], P.J. Clark[46], R.N. Clarke[15], W. Cleland[124], J.C. Clemens[84], B. Clement[55], C. Clement[147a,147b], Y. Coadou[84], M. Cobal[165a,165c], A. Coccaro[139], J. Cochran[63], L. Coffey[23], J.G. Cogan[144], J. Coggeshall[166], B. Cole[35], S. Cole[107], A.P. Colijn[106], C. Collins-Tooth[53], J. Collot[55], T. Colombo[58c], G. Colon[85], G. Compostella[100], P. Conde Muiño[125a,125b], E. Coniavitis[167], M.C. Conidi[12], I.A. Connelly[76], S.M. Consonni[90a,90b], V. Consorti[48], S. Constantinescu[26a], C. Conta[120a,120b], G. Conti[57], F. Conventi[103a,h], M. Cooke[15], B.D. Cooper[77], A.M. Cooper-Sarkar[119], N.J. Cooper-Smith[76], K. Copic[15], T. Cornelissen[176], M. Corradi[20a], F. Corriveau[86,i], A. Corso-Radu[164], A. Cortes-Gonzalez[12], G. Cortiana[100], G. Costa[90a], M.J. Costa[168], D. Costanzo[140], D. Côté[8], G. Cottin[28], G. Cowan[76], B.E. Cox[83], K. Cranmer[109], G. Cree[29], S. Crépé-Renaudin[55], F. Crescioli[79], M. Crispin Ortuzar[119], M. Cristinziani[21], G. Crosetti[37a,37b], C.-M. Cuciuc[26a], C. Cuenca Almenar[177], T. Cuhadar Donszelmann[140], J. Cummings[177], M. Curatolo[47], C. Cuthbert[151], H. Czirr[142], P. Czodrowski[3], Z. Czyczula[177], S. D'Auria[53], M. D'Onofrio[73], M.J. Da Cunha Sargedas De Sousa[125a,125b], C. Da Via[83], W. Dabrowski[38a], A. Dafinca[119], T. Dai[88], O. Dale[14], F. Dallaire[94], C. Dallapiccola[85], M. Dam[36], A.C. Daniells[18], M. Dano Hoffmann[36], V. Dao[105], G. Darbo[50a], G.L. Darlea[26c], S. Darmora[8], J.A. Dassoulas[42], W. Davey[21], C. David[170], T. Davidek[128], E. Davies[119,c], M. Davies[94], O. Davignon[79], A.R. Davison[77], P. Davison[77], Y. Davygora[58a], E. Dawe[143], I. Dawson[140],

JHEP04(2014)031

R.K. Daya-Ishmukhametova[23], K. De[8], R. de Asmundis[103a], S. De Castro[20a,20b], S. De Cecco[79], J. de Graat[99], N. De Groot[105], P. de Jong[106], C. De La Taille[116], H. De la Torre[81], F. De Lorenzi[63], L. De Nooij[106], D. De Pedis[133a], A. De Salvo[133a], U. De Sanctis[165a,165c], A. De Santo[150], J.B. De Vivie De Regie[116], G. De Zorzi[133a,133b], W.J. Dearnaley[71], R. Debbe[25], C. Debenedetti[46], B. Dechenaux[55], D.V. Dedovich[64], J. Degenhardt[121], I. Deigaard[106], J. Del Peso[81], T. Del Prete[123a,123b], T. Delemontex[55], F. Deliot[137], M. Deliyergiyev[74], A. Dell'Acqua[30], L. Dell'Asta[22], M. Della Pietra[103a,h], D. della Volpe[49], M. Delmastro[5], P.A. Delsart[55], C. Deluca[106], S. Demers[177], M. Demichev[64], A. Demilly[79], S.P. Denisov[129], D. Derendarz[39], J.E. Derkaoui[136d], F. Derue[79], P. Dervan[73], K. Desch[21], C. Deterre[42], P.O. Deviveiros[106], A. Dewhurst[130], S. Dhaliwal[106], A. Di Ciaccio[134a,134b], L. Di Ciaccio[5], A. Di Domenico[133a,133b], C. Di Donato[103a,103b], A. Di Girolamo[30], B. Di Girolamo[30], A. Di Mattia[153], B. Di Micco[135a,135b], R. Di Nardo[47], A. Di Simone[48], R. Di Sipio[20a,20b], D. Di Valentino[29], M.A. Diaz[32a], E.B. Diehl[88], J. Dietrich[42], T.A. Dietzsch[58a], S. Diglio[87], A. Dimitrievska[13a], J. Dingfelder[21], C. Dionisi[133a,133b], P. Dita[26a], S. Dita[26a], F. Dittus[30], F. Djama[84], T. Djobava[51b], M.A.B. do Vale[24c], A. Do Valle Wemans[125a,125g], T.K.O. Doan[5], D. Dobos[30], E. Dobson[77], C. Doglioni[49], T. Doherty[53], T. Dohmae[156], J. Dolejsi[128], Z. Dolezal[128], B.A. Dolgoshein[97,*], M. Donadelli[24d], S. Donati[123a,123b], P. Dondero[120a,120b], J. Donini[34], J. Dopke[30], A. Doria[103a], A. Dos Anjos[174], A. Dotti[123a,123b], M.T. Dova[70], A.T. Doyle[53], M. Dris[10], J. Dubbert[88], S. Dube[15], E. Dubreuil[34], E. Duchovni[173], G. Duckeck[99], O.A. Ducu[26a], D. Duda[176], A. Dudarev[30], F. Dudziak[63], L. Duflot[116], L. Duguid[76], M. Dührssen[30], M. Dunford[58a], H. Duran Yildiz[4a], M. Düren[52], M. Dwuznik[38a], J. Ebke[99], W. Edson[2], N.C. Edwards[46], W. Ehrenfeld[21], T. Eifert[144], G. Eigen[14], K. Einsweiler[15], T. Ekelof[167], M. El Kacimi[136c], M. Ellert[167], S. Elles[5], F. Ellinghaus[82], K. Ellis[75], N. Ellis[30], J. Elmsheuser[99], M. Elsing[30], D. Emeliyanov[130], Y. Enari[156], O.C. Endner[82], M. Endo[117], R. Engelmann[149], J. Erdmann[177], A. Ereditato[17], D. Eriksson[147a], G. Ernis[176], J. Ernst[2], M. Ernst[25], J. Ernwein[137], D. Errede[166], S. Errede[166], E. Ertel[82], M. Escalier[116], H. Esch[43], C. Escobar[124], X. Espinal Curull[12], B. Esposito[47], A.I. Etienvre[137], E. Etzion[154], H. Evans[60], L. Fabbri[20a,20b], G. Facini[30], R.M. Fakhrutdinov[129], S. Falciano[133a], Y. Fang[33a], M. Fanti[90a,90b], A. Farbin[8], A. Farilla[135a], T. Farooque[12], S. Farrell[164], S.M. Farrington[171], P. Farthouat[30], F. Fassi[168], P. Fassnacht[30], D. Fassouliotis[9], A. Favareto[50a,50b], L. Fayard[116], P. Federic[145a], O.L. Fedin[122], W. Fedorko[169], M. Fehling-Kaschek[48], S. Feigl[30], L. Feligioni[84], C. Feng[33d], E.J. Feng[6], H. Feng[88], A.B. Fenyuk[129], S. Fernandez Perez[30], W. Fernando[6], S. Ferrag[53], J. Ferrando[53], V. Ferrara[42], A. Ferrari[167], P. Ferrari[106], R. Ferrari[120a], D.E. Ferreira de Lima[53], A. Ferrer[168], D. Ferrere[49], C. Ferretti[88], A. Ferretto Parodi[50a,50b], M. Fiascaris[31], F. Fiedler[82], A. Filipčič[74], M. Filipuzzi[42], F. Filthaut[105], M. Fincke-Keeler[170], K.D. Finelli[151], M.C.N. Fiolhais[125a,125c], L. Fiorini[168], A. Firan[40], J. Fischer[176], M.J. Fisher[110], W.C. Fisher[89], E.A. Fitzgerald[23], M. Flechl[48], I. Fleck[142], P. Fleischmann[175], S. Fleischmann[176], G.T. Fletcher[140], G. Fletcher[75], T. Flick[176], A. Floderus[80], L.R. Flores Castillo[174], A.C. Florez Bustos[160b], M.J. Flowerdew[100], A. Formica[137], A. Forti[83], D. Fortin[160a], D. Fournier[116], H. Fox[71], P. Francavilla[12], M. Franchini[20a,20b], S. Franchino[30], D. Francis[30], M. Franklin[57], S. Franz[61], M. Fraternali[120a,120b], S. Fratina[121], S.T. French[28], C. Friedrich[42], F. Friedrich[44], D. Froidevaux[30], J.A. Frost[28], C. Fukunaga[157], E. Fullana Torregrosa[128], B.G. Fulsom[144], J. Fuster[168], C. Gabaldon[55], O. Gabizon[173], A. Gabrielli[20a,20b], A. Gabrielli[133a,133b], S. Gadatsch[106], S. Gadomski[49], G. Gagliardi[50a,50b], P. Gagnon[60], C. Galea[105], B. Galhardo[125a,125c], E.J. Gallas[119], V. Gallo[17], B.J. Gallop[130], P. Gallus[127], G. Galster[36], K.K. Gan[110], R.P. Gandrajula[62], J. Gao[33b,g], Y.S. Gao[144,e], F.M. Garay Walls[46], F. Garberson[177], C. García[168], J.E. García Navarro[168], M. Garcia-Sciveres[15], R.W. Gardner[31], N. Garelli[144], V. Garonne[30], C. Gatti[47], G. Gaudio[120a], B. Gaur[142], L. Gauthier[94], P. Gauzzi[133a,133b], I.L. Gavrilenko[95], C. Gay[169], G. Gaycken[21], E.N. Gazis[10], P. Ge[33d,j], Z. Gecse[169], C.N.P. Gee[130], D.A.A. Geerts[106], Ch. Geich-Gimbel[21], K. Gellerstedt[147a,147b], C. Gemme[50a], A. Gemmell[53], M.H. Genest[55], S. Gentile[133a,133b], M. George[54], S. George[76], D. Gerbaudo[164], A. Gershon[154], H. Ghazlane[136b], N. Ghodbane[34], B. Giacobbe[20a], S. Giagu[133a,133b], V. Giangiobbe[12], P. Giannetti[123a,123b], F. Gianotti[30],

JHEP04(2014)031

B. Gibbard[25], S.M. Gibson[76], M. Gilchriese[15], T.P.S. Gillam[28], D. Gillberg[30], A.R. Gillman[130], D.M. Gingrich[3,d], N. Giokaris[9], M.P. Giordani[165a,165c], R. Giordano[103a,103b], F.M. Giorgi[16], P.F. Giraud[137], D. Giugni[90a], C. Giuliani[48], M. Giunta[94], B.K. Gjelsten[118], I. Gkialas[155,k], L.K. Gladilin[98], C. Glasman[81], J. Glatzer[30], A. Glazov[42], G.L. Glonti[64], M. Goblirsch-Kolb[100], J.R. Goddard[75], J. Godfrey[143], J. Godlewski[30], C. Goeringer[82], S. Goldfarb[88], T. Golling[177], D. Golubkov[129], A. Gomes[125a,125b,125d], L.S. Gomez Fajardo[42], R. Gonçalo[76], J. Goncalves Pinto Firmino Da Costa[42], L. Gonella[21], S. González de la Hoz[168], G. Gonzalez Parra[12], M.L. Gonzalez Silva[27], S. Gonzalez-Sevilla[49], L. Goossens[30], P.A. Gorbounov[96], H.A. Gordon[25], I. Gorelov[104], G. Gorfine[176], B. Gorini[30], E. Gorini[72a,72b], A. Gorišek[74], E. Gornicki[39], A.T. Goshaw[6], C. Gössling[43], M.I. Gostkin[64], M. Gouighri[136a], D. Goujdami[136c], M.P. Goulette[49], A.G. Goussiou[139], C. Goy[5], S. Gozpinar[23], H.M.X. Grabas[137], L. Graber[54], I. Grabowska-Bold[38a], P. Grafström[20a,20b], K-J. Grahn[42], J. Gramling[49], E. Gramstad[118], F. Grancagnolo[72a], S. Grancagnolo[16], V. Grassi[149], V. Gratchev[122], H.M. Gray[30], E. Graziani[135a], O.G. Grebenyuk[122], Z.D. Greenwood[78,l], K. Gregersen[36], I.M. Gregor[42], P. Grenier[144], J. Griffiths[8], N. Grigalashvili[64], A.A. Grillo[138], K. Grimm[71], S. Grinstein[12,m], Ph. Gris[34], Y.V. Grishkevich[98], J.-F. Grivaz[116], J.P. Grohs[44], A. Grohsjean[42], E. Gross[173], J. Grosse-Knetter[54], G.C. Grossi[134a,134b], J. Groth-Jensen[173], Z.J. Grout[150], K. Grybel[142], L. Guan[33b], F. Guescini[49], D. Guest[177], O. Gueta[154], C. Guicheney[34], E. Guido[50a,50b], T. Guillemin[116], S. Guindon[2], U. Gul[53], C. Gumpert[44], J. Gunther[127], J. Guo[35], S. Gupta[119], P. Gutierrez[112], N.G. Gutierrez Ortiz[53], C. Gutschow[77], N. Guttman[154], C. Guyot[137], C. Gwenlan[119], C.B. Gwilliam[73], A. Haas[109], C. Haber[15], H.K. Hadavand[8], N. Haddad[136e], P. Haefner[21], S. Hageboeck[21], Z. Hajduk[39], H. Hakobyan[178], M. Haleem[42], D. Hall[119], G. Halladjian[89], K. Hamacher[176], P. Hamal[114], K. Hamano[87], M. Hamer[54], A. Hamilton[146a], S. Hamilton[162], L. Han[33b], K. Hanagaki[117], K. Hanawa[156], M. Hance[15], P. Hanke[58a], J.R. Hansen[36], J.B. Hansen[36], J.D. Hansen[36], P.H. Hansen[36], K. Hara[161], A.S. Hard[174], T. Harenberg[176], S. Harkusha[91], D. Harper[88], R.D. Harrington[46], O.M. Harris[139], P.F. Harrison[171], F. Hartjes[106], A. Harvey[56], S. Hasegawa[102], Y. Hasegawa[141], S. Hassani[137], S. Haug[17], M. Hauschild[30], R. Hauser[89], M. Havranek[126], C.M. Hawkes[18], R.J. Hawkings[30], A.D. Hawkins[80], T. Hayashi[161], D. Hayden[89], C.P. Hays[119], H.S. Hayward[73], S.J. Haywood[130], S.J. Head[18], T. Heck[82], V. Hedberg[80], L. Heelan[8], S. Heim[121], T. Heim[176], B. Heinemann[15], L. Heinrich[109], S. Heisterkamp[36], J. Hejbal[126], L. Helary[22], C. Heller[99], M. Heller[30], S. Hellman[147a,147b], D. Hellmich[21], C. Helsens[30], J. Henderson[119], R.C.W. Henderson[71], C. Hengler[42], A. Henrichs[177], A.M. Henriques Correia[30], S. Henrot-Versille[116], C. Hensel[54], G.H. Herbert[16], Y. Hernández Jiménez[168], R. Herrberg-Schubert[16], G. Herten[48], R. Hertenberger[99], L. Hervas[30], G.G. Hesketh[77], N.P. Hessey[106], R. Hickling[75], E. Higón-Rodriguez[168], J.C. Hill[28], K.H. Hiller[42], S. Hillert[21], S.J. Hillier[18], I. Hinchliffe[15], E. Hines[121], M. Hirose[117], D. Hirschbuehl[176], J. Hobbs[149], N. Hod[106], M.C. Hodgkinson[140], P. Hodgson[140], A. Hoecker[30], M.R. Hoeferkamp[104], J. Hoffman[40], D. Hoffmann[84], J.I. Hofmann[58a], M. Hohlfeld[82], T.R. Holmes[15], T.M. Hong[121], L. Hooft van Huysduynen[109], J-Y. Hostachy[55], S. Hou[152], A. Hoummada[136a], J. Howard[119], J. Howarth[42], M. Hrabovsky[114], I. Hristova[16], J. Hrivnac[116], T. Hryn'ova[5], P.J. Hsu[82], S.-C. Hsu[139], D. Hu[35], X. Hu[25], Y. Huang[146c], Z. Hubacek[30], F. Hubaut[84], F. Huegging[21], T.B. Huffman[119], E.W. Hughes[35], G. Hughes[71], M. Huhtinen[30], T.A. Hülsing[82], M. Hurwitz[15], N. Huseynov[64,b], J. Huston[89], J. Huth[57], G. Iacobucci[49], G. Iakovidis[10], I. Ibragimov[142], L. Iconomidou-Fayard[116], J. Idarraga[116], E. Ideal[177], P. Iengo[103a], O. Igonkina[106], T. Iizawa[172], Y. Ikegami[65], K. Ikematsu[142], M. Ikeno[65], D. Iliadis[155], N. Ilic[159], Y. Inamaru[66], T. Ince[100], P. Ioannou[9], M. Iodice[135a], K. Iordanidou[9], V. Ippolito[133a,133b], A. Irles Quiles[168], C. Isaksson[167], M. Ishino[67], M. Ishitsuka[158], R. Ishmukhametov[110], C. Issever[119], S. Istin[19a], J.M. Iturbe Ponce[83], A.V. Ivashin[129], W. Iwanski[39], H. Iwasaki[65], J.M. Izen[41], V. Izzo[103a], B. Jackson[121], J.N. Jackson[73], M. Jackson[73], P. Jackson[1], M.R. Jaekel[30], V. Jain[2], K. Jakobs[48], S. Jakobsen[36], T. Jakoubek[126], J. Jakubek[127], D.O. Jamin[152], D.K. Jana[78], E. Jansen[77], H. Jansen[30], J. Janssen[21], M. Janus[171], G. Jarlskog[80], L. Jeanty[15], G.-Y. Jeng[151], I. Jen-La Plante[31],

JHEP04(2014)031

D. Jennens[87], P. Jenni[48,n], J. Jentzsch[43], C. Jeske[171], S. Jézéquel[5], H. Ji[174], W. Ji[82], J. Jia[149], Y. Jiang[33b], M. Jimenez Belenguer[42], S. Jin[33a], A. Jinaru[26a], O. Jinnouchi[158], M.D. Joergensen[36], D. Joffe[40], K.E. Johansson[147a], P. Johansson[140], K.A. Johns[7], K. Jon-And[147a,147b], G. Jones[171], R.W.L. Jones[71], T.J. Jones[73], P.M. Jorge[125a,125b], K.D. Joshi[83], J. Jovicevic[148], X. Ju[174], C.A. Jung[43], R.M. Jungst[30], P. Jussel[61], A. Juste Rozas[12,m], M. Kaci[168], A. Kaczmarska[39], M. Kado[116], H. Kagan[110], M. Kagan[144], E. Kajomovitz[45], S. Kama[40], N. Kanaya[156], M. Kaneda[30], S. Kaneti[28], T. Kanno[158], V.A. Kantserov[97], J. Kanzaki[65], B. Kaplan[109], A. Kapliy[31], D. Kar[53], K. Karakostas[10], N. Karastathis[10], M. Karnevskiy[82], S.N. Karpov[64], K. Karthik[109], V. Kartvelishvili[71], A.N. Karyukhin[129], L. Kashif[174], G. Kasieczka[58b], R.D. Kass[110], A. Kastanas[14], Y. Kataoka[156], A. Katre[49], J. Katzy[42], V. Kaushik[7], K. Kawagoe[69], T. Kawamoto[156], G. Kawamura[54], S. Kazama[156], V.F. Kazanin[108], M.Y. Kazarinov[64], R. Keeler[170], P.T. Keener[121], R. Kehoe[40], M. Keil[54], J.S. Keller[139], H. Keoshkerian[5], O. Kepka[126], B.P. Kerševan[74], S. Kersten[176], K. Kessoku[156], J. Keung[159], F. Khalil-zada[11], H. Khandanyan[147a,147b], A. Khanov[113], A. Khodinov[97], A. Khomich[58a], T.J. Khoo[28], G. Khoriauli[21], A. Khoroshilov[176], V. Khovanskiy[96], E. Khramov[64], J. Khubua[51b], H. Kim[147a,147b], S.H. Kim[161], N. Kimura[172], O. Kind[16], B.T. King[73], M. King[168], R.S.B. King[119], S.B. King[169], J. Kirk[130], A.E. Kiryunin[100], T. Kishimoto[66], D. Kisielewska[38a], F. Kiss[48], T. Kitamura[66], T. Kittelmann[124], K. Kiuchi[161], E. Kladiva[145b], M. Klein[73], U. Klein[73], K. Kleinknecht[82], P. Klimek[147a,147b], A. Klimentov[25], R. Klingenberg[43], J.A. Klinger[83], E.B. Klinkby[36], T. Klioutchnikova[30], P.F. Klok[105], E.-E. Kluge[58a], P. Kluit[106], S. Kluth[100], E. Kneringer[61], E.B.F.G. Knoops[84], A. Knue[53], T. Kobayashi[156], M. Kobel[44], M. Kocian[144], P. Kodys[128], S. Koenig[82], P. Koevesarki[21], T. Koffas[29], E. Koffeman[106], L.A. Kogan[119], S. Kohlmann[176], Z. Kohout[127], T. Kohriki[65], T. Koi[144], H. Kolanoski[16], I. Koletsou[5], J. Koll[89], A.A. Komar[95,*], Y. Komori[156], T. Kondo[65], K. Köneke[48], A.C. König[105], T. Kono[65,o], R. Konoplich[109,p], N. Konstantinidis[77], R. Kopeliansky[153], S. Koperny[38a], L. Köpke[82], A.K. Kopp[48], K. Korcyl[39], K. Kordas[155], A. Korn[77], A.A. Korol[108], I. Korolkov[12], E.V. Korolkova[140], V.A. Korotkov[129], O. Kortner[100], S. Kortner[100], V.V. Kostyukhin[21], S. Kotov[100], V.M. Kotov[64], A. Kotwal[45], C. Kourkoumelis[9], V. Kouskoura[155], A. Koutsman[160a], R. Kowalewski[170], T.Z. Kowalski[38a], W. Kozanecki[137], A.S. Kozhin[129], V. Kral[127], V.A. Kramarenko[98], G. Kramberger[74], D. Krasnopevtsev[97], M.W. Krasny[79], A. Krasznahorkay[30], J.K. Kraus[21], A. Kravchenko[25], S. Kreiss[109], M. Kretz[58c], J. Kretzschmar[73], K. Kreutzfeldt[52], P. Krieger[159], K. Kroeninger[54], H. Kroha[100], J. Kroll[121], J. Kroseberg[21], J. Krstic[13a], U. Kruchonak[64], H. Krüger[21], T. Kruker[17], N. Krumnack[63], Z.V. Krumshteyn[64], A. Kruse[174], M.C. Kruse[45], M. Kruskal[22], T. Kubota[87], S. Kuday[4a], S. Kuehn[48], A. Kugel[58c], A. Kuhl[138], T. Kuhl[42], V. Kukhtin[64], Y. Kulchitsky[91], S. Kuleshov[32b], M. Kuna[133a,133b], J. Kunkle[121], A. Kupco[126], H. Kurashige[66], Y.A. Kurochkin[91], R. Kurumida[66], V. Kus[126], E.S. Kuwertz[148], M. Kuze[158], J. Kvita[143], A. La Rosa[49], L. La Rotonda[37a,37b], L. Labarga[81], C. Lacasta[168], F. Lacava[133a,133b], J. Lacey[29], H. Lacker[16], D. Lacour[79], V.R. Lacuesta[168], E. Ladygin[64], R. Lafaye[5], B. Laforge[79], T. Lagouri[177], S. Lai[48], H. Laier[58a], E. Laisne[55], L. Lambourne[77], C.L. Lampen[7], W. Lampl[7], E. Lançon[137], U. Landgraf[48], M.P.J. Landon[75], V.S. Lang[58a], C. Lange[42], A.J. Lankford[164], F. Lanni[25], K. Lantzsch[30], A. Lanza[120a], S. Laplace[79], C. Lapoire[21], J.F. Laporte[137], T. Lari[90a], M. Lassnig[30], P. Laurelli[47], V. Lavorini[37a,37b], W. Lavrijsen[15], P. Laycock[73], B.T. Le[55], O. Le Dortz[79], E. Le Guirriec[84], E. Le Menedeu[12], T. LeCompte[6], F. Ledroit-Guillon[55], C.A. Lee[152], H. Lee[106], J.S.H. Lee[117], S.C. Lee[152], L. Lee[177], G. Lefebvre[79], M. Lefebvre[170], F. Legger[99], C. Leggett[15], A. Lehan[73], M. Lehmacher[21], G. Lehmann Miotto[30], X. Lei[7], A.G. Leister[177], M.A.L. Leite[24d], R. Leitner[128], D. Lellouch[173], B. Lemmer[54], K.J.C. Leney[77], T. Lenz[106], G. Lenzen[176], B. Lenzi[30], R. Leone[7], K. Leonhardt[44], S. Leontsinis[10], C. Leroy[94], C.G. Lester[28], C.M. Lester[121], J. Levêque[5], D. Levin[88], L.J. Levinson[173], A. Lewis[119], G.H. Lewis[109], A.M. Leyko[21], M. Leyton[41], B. Li[33b,q], B. Li[84], H. Li[149], H.L. Li[31], S. Li[45], X. Li[88], Z. Liang[119,r], H. Liao[34], B. Liberti[134a], P. Lichard[30], K. Lie[166], J. Liebal[21], W. Liebig[14], C. Limbach[21], A. Limosani[87], M. Limper[62], S.C. Lin[152,s], F. Linde[106], B.E. Lindquist[149], J.T. Linnemann[89], E. Lipeles[121], A. Lipniacka[14], M. Lisovyi[42],

JHEP04(2014)031

T.M. Liss[166], D. Lissauer[25], A. Lister[169], A.M. Litke[138], B. Liu[152], D. Liu[152], J.B. Liu[33b], K. Liu[33b,t], L. Liu[88], M. Liu[45], M. Liu[33b], Y. Liu[33b], M. Livan[120a,120b], S.S.A. Livermore[119], A. Lleres[55], J. Llorente Merino[81], S.L. Lloyd[75], F. Lo Sterzo[152], E. Lobodzinska[42], P. Loch[7], W.S. Lockman[138], T. Loddenkoetter[21], F.K. Loebinger[83], A.E. Loevschall-Jensen[36], A. Loginov[177], C.W. Loh[169], T. Lohse[16], K. Lohwasser[48], M. Lokajicek[126], V.P. Lombardo[5], J.D. Long[88], R.E. Long[71], L. Lopes[125a], D. Lopez Mateos[57], B. Lopez Paredes[140], J. Lorenz[99], N. Lorenzo Martinez[116], M. Losada[163], P. Loscutoff[15], M.J. Losty[160a,*], X. Lou[41], A. Lounis[116], J. Love[6], P.A. Love[71], A.J. Lowe[144,e], F. Lu[33a], H.J. Lubatti[139], C. Luci[133a,133b], A. Lucotte[55], D. Ludwig[42], F. Luehring[60], W. Lukas[61], L. Luminari[133a], O. Lundberg[147a,147b], B. Lund-Jensen[148], M. Lungwitz[82], D. Lynn[25], R. Lysak[126], E. Lytken[80], H. Ma[25], L.L. Ma[33d], G. Maccarrone[47], A. Macchiolo[100], B. Maček[74], J. Machado Miguens[125a,125b], D. Macina[30], R. Mackeprang[36], D. Madaffari[84], R. Madar[48], H.J. Maddocks[71], W.F. Mader[44], A. Madsen[167], M. Maeno[8], T. Maeno[25], E. Magradze[54], K. Mahboubi[48], J. Mahlstedt[106], S. Mahmoud[73], C. Maiani[137], C. Maidantchik[24a], A. Maio[125a,125b,125d], S. Majewski[115], Y. Makida[65], N. Makovec[116], P. Mal[137,u], B. Malaescu[79], Pa. Malecki[39], V.P. Maleev[122], F. Malek[55], U. Mallik[62], D. Malon[6], C. Malone[144], S. Maltezos[10], V.M. Malyshev[108], S. Malyukov[30], J. Mamuzic[13b], B. Mandelli[30], L. Mandelli[90a], I. Mandić[74], R. Mandrysch[62], J. Maneira[125a,125b], A. Manfredini[100], L. Manhaes de Andrade Filho[24b], J.A. Manjarres Ramos[160b], A. Mann[99], P.M. Manning[138], A. Manousakis-Katsikakis[9], B. Mansoulie[137], R. Mantifel[86], L. Mapelli[30], L. March[168], J.F. Marchand[29], F. Marchese[134a,134b], G. Marchiori[79], M. Marcisovsky[126], C.P. Marino[170], C.N. Marques[125a], F. Marroquim[24a], S.P. Marsden[83], Z. Marshall[15], L.F. Marti[17], S. Marti-Garcia[168], B. Martin[30], B. Martin[89], J.P. Martin[94], T.A. Martin[171], V.J. Martin[46], B. Martin dit Latour[49], H. Martinez[137], M. Martinez[12,m], S. Martin-Haugh[130], A.C. Martyniuk[77], M. Marx[139], F. Marzano[133a], A. Marzin[30], L. Masetti[82], T. Mashimo[156], R. Mashinistov[95], J. Masik[83], A.L. Maslennikov[108], I. Massa[20a,20b], N. Massol[5], P. Mastrandrea[149], A. Mastroberardino[37a,37b], T. Masubuchi[156], P. Matricon[116], H. Matsunaga[156], T. Matsushita[66], P. Mättig[176], S. Mättig[42], J. Mattmann[82], J. Maurer[84], S.J. Maxfield[73], D.A. Maximov[108,f], R. Mazini[152], L. Mazzaferro[134a,134b], G. Mc Goldrick[159], S.P. Mc Kee[88], A. McCarn[88], R.L. McCarthy[149], T.G. McCarthy[29], N.A. McCubbin[130], K.W. McFarlane[56,*], J.A. Mcfayden[77], G. Mchedlidze[54], T. Mclaughlan[18], S.J. McMahon[130], R.A. McPherson[170,i], A. Meade[85], J. Mechnich[106], M. Mechtel[176], M. Medinnis[42], S. Meehan[31], R. Meera-Lebbai[112], S. Mehlhase[36], A. Mehta[73], K. Meier[58a], C. Meineck[99], B. Meirose[80], C. Melachrinos[31], B.R. Mellado Garcia[146c], F. Meloni[90a,90b], L. Mendoza Navas[163], A. Mengarelli[20a,20b], S. Menke[100], E. Meoni[162], K.M. Mercurio[57], S. Mergelmeyer[21], N. Meric[137], P. Mermod[49], L. Merola[103a,103b], C. Meroni[90a], F.S. Merritt[31], H. Merritt[110], A. Messina[30,v], J. Metcalfe[25], A.S. Mete[164], C. Meyer[82], C. Meyer[31], J-P. Meyer[137], J. Meyer[30], R.P. Middleton[130], S. Migas[73], L. Mijović[137], G. Mikenberg[173], M. Mikestikova[126], M. Mikuž[74], D.W. Miller[31], C. Mills[46], A. Milov[173], D.A. Milstead[147a,147b], D. Milstein[173], A.A. Minaenko[129], M. Miñano Moya[168], I.A. Minashvili[64], A.I. Mincer[109], B. Mindur[38a], M. Mineev[64], Y. Ming[174], L.M. Mir[12], G. Mirabelli[133a], T. Mitani[172], J. Mitrevski[99], V.A. Mitsou[168], S. Mitsui[65], A. Miucci[49], P.S. Miyagawa[140], J.U. Mjörnmark[80], T. Moa[147a,147b], K. Mochizuki[84], V. Moeller[28], S. Mohapatra[35], W. Mohr[48], S. Molander[147a,147b], R. Moles-Valls[168], K. Mönig[42], C. Monini[55], J. Monk[36], E. Monnier[84], J. Montejo Berlingen[12], F. Monticelli[70], S. Monzani[133a,133b], R.W. Moore[3], C. Mora Herrera[49], A. Moraes[53], N. Morange[62], J. Morel[54], D. Moreno[82], M. Moreno Llácer[54], P. Morettini[50a], M. Morgenstern[44], M. Morii[57], S. Moritz[82], A.K. Morley[148], G. Mornacchi[30], J.D. Morris[75], L. Morvaj[102], H.G. Moser[100], M. Mosidze[51b], J. Moss[110], R. Mount[144], E. Mountricha[25], S.V. Mouraviev[95,*], E.J.W. Moyse[85], S.G. Muanza[84], R.D. Mudd[18], F. Mueller[58a], J. Mueller[124], K. Mueller[21], T. Mueller[28], T. Mueller[82], D. Muenstermann[49], Y. Munwes[154], J.A. Murillo Quijada[18], W.J. Murray[171,c], E. Musto[153], A.G. Myagkov[129,w], M. Myska[126], O. Nackenhorst[54], J. Nadal[54], K. Nagai[61], R. Nagai[158], Y. Nagai[84], K. Nagano[65], A. Nagarkar[110], Y. Nagasaka[59], M. Nagel[100], A.M. Nairz[30], Y. Nakahama[30], K. Nakamura[65], T. Nakamura[156], I. Nakano[111], H. Namasivayam[41], G. Nanava[21], R. Narayan[58b], T. Nattermann[21], T. Naumann[42],

JHEP04(2014)031

G. Navarro[163], R. Nayyar[7], H.A. Neal[88], P.Yu. Nechaeva[95], T.J. Neep[83], A. Negri[120a,120b], G. Negri[30], M. Negrini[20a], S. Nektarijevic[49], A. Nelson[164], T.K. Nelson[144], S. Nemecek[126], P. Nemethy[109], A.A. Nepomuceno[24a], M. Nessi[30,x], M.S. Neubauer[166], M. Neumann[176], A. Neusiedl[82], R.M. Neves[109], P. Nevski[25], F.M. Newcomer[121], P.R. Newman[18], D.H. Nguyen[6], R.B. Nickerson[119], R. Nicolaidou[137], B. Nicquevert[30], J. Nielsen[138], N. Nikiforou[35], A. Nikiforov[16], V. Nikolaenko[129,w], I. Nikolic-Audit[79], K. Nikolics[49], K. Nikolopoulos[18], P. Nilsson[8], Y. Ninomiya[156], A. Nisati[133a], R. Nisius[100], T. Nobe[158], L. Nodulman[6], M. Nomachi[117], I. Nomidis[155], S. Norberg[112], M. Nordberg[30], J. Novakova[128], S. Nowak[100], M. Nozaki[65], L. Nozka[114], K. Ntekas[10], A.-E. Nuncio-Quiroz[21], G. Nunes Hanninger[87], T. Nunnemann[99], E. Nurse[77], F. Nuti[87], B.J. O'Brien[46], F. O'grady[7], D.C. O'Neil[143], V. O'Shea[53], F.G. Oakham[29,d], H. Oberlack[100], J. Ocariz[79], A. Ochi[66], M.I. Ochoa[77], S. Oda[69], S. Odaka[65], H. Ogren[60], A. Oh[83], S.H. Oh[45], C.C. Ohm[30], H. Ohman[167], T. Ohshima[102], W. Okamura[117], H. Okawa[25], Y. Okumura[31], T. Okuyama[156], A. Olariu[26a], A.G. Olchevski[64], S.A. Olivares Pino[46], D. Oliveira Damazio[25], E. Oliver Garcia[168], D. Olivito[121], A. Olszewski[39], J. Olszowska[39], A. Onofre[125a,125e], P.U.E. Onyisi[31,y], C.J. Oram[160a], M.J. Oreglia[31], Y. Oren[154], D. Orestano[135a,135b], N. Orlando[72a,72b], C. Oropeza Barrera[53], R.S. Orr[159], B. Osculati[50a,50b], R. Ospanov[121], G. Otero y Garzon[27], H. Otono[69], M. Ouchrif[136d], E.A. Ouellette[170], F. Ould-Saada[118], A. Ouraou[137], K.P. Oussoren[106], Q. Ouyang[33a], A. Ovcharova[15], M. Owen[83], V.E. Ozcan[19a], N. Ozturk[8], K. Pachal[119], A. Pacheco Pages[12], C. Padilla Aranda[12], S. Pagan Griso[15], E. Paganis[140], C. Pahl[100], F. Paige[25], P. Pais[85], K. Pajchel[118], G. Palacino[160b], S. Palestini[30], D. Pallin[34], A. Palma[125a,125b], J.D. Palmer[18], Y.B. Pan[174], E. Panagiotopoulou[10], J.G. Panduro Vazquez[76], P. Pani[106], N. Panikashvili[88], S. Panitkin[25], D. Pantea[26a], Th.D. Papadopoulou[10], K. Papageorgiou[155,k], A. Paramonov[6], D. Paredes Hernandez[34], M.A. Parker[28], F. Parodi[50a,50b], J.A. Parsons[35], U. Parzefall[48], E. Pasqualucci[133a], S. Passaggio[50a], A. Passeri[135a], F. Pastore[135a,135b,*], Fr. Pastore[76], G. Pásztor[49,z], S. Pataraia[176], N.D. Patel[151], J.R. Pater[83], S. Patricelli[103a,103b], T. Pauly[30], J. Pearce[170], M. Pedersen[118], S. Pedraza Lopez[168], R. Pedro[125a,125b], S.V. Peleganchuk[108], D. Pelikan[167], H. Peng[33b], B. Penning[31], J. Penwell[60], D.V. Perepelitsa[35], E. Perez Codina[160a], M.T. Pérez García-Estañ[168], V. Perez Reale[35], L. Perini[90a,90b], H. Pernegger[30], R. Perrino[72a], R. Peschke[42], V.D. Peshekhonov[64], K. Peters[30], R.F.Y. Peters[83], B.A. Petersen[87], J. Petersen[30], T.C. Petersen[36], E. Petit[42], A. Petridis[147a,147b], C. Petridou[155], E. Petrolo[133a], F. Petrucci[135a,135b], M. Petteni[143], R. Pezoa[32b], P.W. Phillips[130], G. Piacquadio[144], E. Pianori[171], A. Picazio[49], E. Piccaro[75], M. Piccinini[20a,20b], S.M. Piec[42], R. Piegaia[27], D.T. Pignotti[110], J.E. Pilcher[31], A.D. Pilkington[77], J. Pina[125a,125b,125d], M. Pinamonti[165a,165c,aa], A. Pinder[119], J.L. Pinfold[3], A. Pingel[36], B. Pinto[125a], C. Pizio[90a,90b], M.-A. Pleier[25], V. Pleskot[128], E. Plotnikova[64], P. Plucinski[147a,147b], S. Poddar[58a], F. Podlyski[34], R. Poettgen[82], L. Poggioli[116], D. Pohl[21], M. Pohl[49], G. Polesello[120a], A. Policicchio[37a,37b], R. Polifka[159], A. Polini[20a], C.S. Pollard[45], V. Polychronakos[25], K. Pommès[30], L. Pontecorvo[133a], B.G. Pope[89], G.A. Popeneciu[26b], D.S. Popovic[13a], A. Poppleton[30], X. Portell Bueso[12], G.E. Pospelov[100], S. Pospisil[127], K. Potamianos[15], I.N. Potrap[64], C.J. Potter[150], C.T. Potter[115], G. Poulard[30], J. Poveda[60], V. Pozdnyakov[64], R. Prabhu[77], P. Pralavorio[84], A. Pranko[15], S. Prasad[30], R. Pravahan[8], S. Prell[63], D. Price[83], J. Price[73], L.E. Price[6], D. Prieur[124], M. Primavera[72a], M. Proissl[46], K. Prokofiev[109], F. Prokoshin[32b], E. Protopapadaki[137], S. Protopopescu[25], J. Proudfoot[6], M. Przybycien[38a], H. Przysiezniak[5], E. Ptacek[115], E. Pueschel[85], D. Puldon[149], M. Purohit[25,ab], P. Puzo[116], Y. Pylypchenko[62], J. Qian[88], A. Quadt[54], D.R. Quarrie[15], W.B. Quayle[165a,165b], D. Quilty[53], A. Qureshi[160b], V. Radeka[25], V. Radescu[42], S.K. Radhakrishnan[149], P. Radloff[115], F. Ragusa[90a,90b], G. Rahal[179], S. Rajagopalan[25], M. Rammensee[30], M. Rammes[142], A.S. Randle-Conde[40], C. Rangel-Smith[79], K. Rao[164], F. Rauscher[99], T.C. Rave[48], T. Ravenscroft[53], M. Raymond[30], A.L. Read[118], D.M. Rebuzzi[120a,120b], A. Redelbach[175], G. Redlinger[25], R. Reece[138], K. Reeves[41], L. Rehnisch[16], A. Reinsch[115], H. Reisin[27], M. Relich[164], C. Rembser[30], Z.L. Ren[152], A. Renaud[116], M. Rescigno[133a], S. Resconi[90a], B. Resende[137], P. Reznicek[128], R. Rezvani[94], R. Richter[100],

JHEP04(2014)031

M. Ridel[79], P. Rieck[16], M. Rijssenbeek[149], A. Rimoldi[120a,120b], L. Rinaldi[20a], E. Ritsch[61], I. Riu[12], F. Rizatdinova[113], E. Rizvi[75], S.H. Robertson[86,i], A. Robichaud-Veronneau[119], D. Robinson[28], J.E.M. Robinson[83], A. Robson[53], C. Roda[123a,123b], D. Roda Dos Santos[126], L. Rodrigues[30], S. Roe[30], O. Røhne[118], S. Rolli[162], A. Romaniouk[97], M. Romano[20a,20b], G. Romeo[27], E. Romero Adam[168], N. Rompotis[139], L. Roos[79], E. Ros[168], S. Rosati[133a], K. Rosbach[49], A. Rose[150], M. Rose[76], P.L. Rosendahl[14], O. Rosenthal[142], V. Rossetti[147a,147b], E. Rossi[103a,103b], L.P. Rossi[50a], R. Rosten[139], M. Rotaru[26a], I. Roth[173], J. Rothberg[139], D. Rousseau[116], C.R. Royon[137], A. Rozanov[84], Y. Rozen[153], X. Ruan[146c], F. Rubbo[12], I. Rubinskiy[42], V.I. Rud[98], C. Rudolph[44], M.S. Rudolph[159], F. Rühr[7], A. Ruiz-Martinez[63], Z. Rurikova[48], N.A. Rusakovich[64], A. Ruschke[99], J.P. Rutherfoord[7], N. Ruthmann[48], P. Ruzicka[126], Y.F. Ryabov[122], M. Rybar[128], G. Rybkin[116], N.C. Ryder[119], A.F. Saavedra[151], S. Sacerdoti[27], A. Saddique[3], I. Sadeh[154], H.F-W. Sadrozinski[138], R. Sadykov[64], F. Safai Tehrani[133a], H. Sakamoto[156], Y. Sakurai[172], G. Salamanna[75], A. Salamon[134a], M. Saleem[112], D. Salek[106], P.H. Sales De Bruin[139], D. Salihagic[100], A. Salnikov[144], J. Salt[168], B.M. Salvachua Ferrando[6], D. Salvatore[37a,37b], F. Salvatore[150], A. Salvucci[105], A. Salzburger[30], D. Sampsonidis[155], A. Sanchez[103a,103b], J. Sánchez[168], V. Sanchez Martinez[168], H. Sandaker[14], H.G. Sander[82], M.P. Sanders[99], M. Sandhoff[176], T. Sandoval[28], C. Sandoval[165a,165b], R. Sandstroem[100], D.P.C. Sankey[130], A. Sansoni[47], C. Santoni[34], R. Santonico[134a,134b], H. Santos[125a], I. Santoyo Castillo[150], K. Sapp[124], A. Sapronov[64], J.G. Saraiva[125a,125d], B. Sarrazin[21], G. Sartisohn[176], O. Sasaki[65], Y. Sasaki[156], I. Satsounkevitch[91], G. Sauvage[5,*], E. Sauvan[5], P. Savard[159,d], D.O. Savu[30], C. Sawyer[119], L. Sawyer[78,l], D.H. Saxon[53], J. Saxon[121], C. Sbarra[20a], A. Sbrizzi[3], T. Scanlon[30], D.A. Scannicchio[164], M. Scarcella[151], J. Schaarschmidt[173], P. Schacht[100], D. Schaefer[121], R. Schaefer[42], A. Schaelicke[46], S. Schaepe[21], S. Schaetzel[58b], U. Schäfer[82], A.C. Schaffer[116], D. Schaile[99], R.D. Schamberger[149], V. Scharf[58a], V.A. Schegelsky[122], D. Scheirich[128], M. Schernau[164], M.I. Scherzer[35], C. Schiavi[50a,50b], J. Schieck[99], C. Schillo[48], M. Schioppa[37a,37b], S. Schlenker[30], E. Schmidt[48], K. Schmieden[30], C. Schmitt[82], C. Schmitt[99], S. Schmitt[58b], B. Schneider[17], Y.J. Schnellbach[73], U. Schnoor[44], L. Schoeffel[137], A. Schoening[58b], B.D. Schoenrock[89], A.L.S. Schorlemmer[54], M. Schott[82], D. Schouten[160a], J. Schovancova[25], M. Schram[86], S. Schramm[159], M. Schreyer[175], C. Schroeder[82], N. Schuh[82], M.J. Schultens[21], H.-C. Schultz-Coulon[58a], H. Schulz[16], M. Schumacher[48], B.A. Schumm[138], Ph. Schune[137], A. Schwartzman[144], Ph. Schwegler[100], Ph. Schwemling[137], R. Schwienhorst[89], J. Schwindling[137], T. Schwindt[21], M. Schwoerer[5], F.G. Sciacca[17], E. Scifo[116], G. Sciolla[23], W.G. Scott[130], F. Scuri[123a,123b], F. Scutti[21], J. Searcy[88], G. Sedov[42], E. Sedykh[122], S.C. Seidel[104], A. Seiden[138], F. Seifert[127], J.M. Seixas[24a], G. Sekhniaidze[103a], S.J. Sekula[40], K.E. Selbach[46], D.M. Seliverstov[122], G. Sellers[73], M. Seman[145b], N. Semprini-Cesari[20a,20b], C. Serfon[30], L. Serin[116], L. Serkin[54], T. Serre[84], R. Seuster[160a], H. Severini[112], F. Sforza[100], A. Sfyrla[30], E. Shabalina[54], M. Shamim[115], L.Y. Shan[33a], J.T. Shank[22], Q.T. Shao[87], M. Shapiro[15], P.B. Shatalov[96], K. Shaw[165a,165c], P. Sherwood[77], S. Shimizu[66], C.O. Shimmin[164], M. Shimojima[101], T. Shin[56], M. Shiyakova[64], A. Shmeleva[95], M.J. Shochet[31], D. Short[119], S. Shrestha[63], E. Shulga[97], M.A. Shupe[7], S. Shushkevich[42], P. Sicho[126], D. Sidorov[113], A. Sidoti[133a], F. Siegert[44], Dj. Sijacki[13a], O. Silbert[173], J. Silva[125a,125d], Y. Silver[154], D. Silverstein[144], S.B. Silverstein[147a], V. Simak[127], O. Simard[5], Lj. Simic[13a], S. Simion[116], E. Simioni[82], B. Simmons[77], R. Simoniello[90a,90b], M. Simonyan[36], P. Sinervo[159], N.B. Sinev[115], V. Sipica[142], G. Siragusa[175], A. Sircar[78], A.N. Sisakyan[64,*], S.Yu. Sivoklokov[98], J. Sjölin[147a,147b], T.B. Sjursen[14], L.A. Skinnari[15], H.P. Skottowe[57], K.Yu. Skovpen[108], P. Skubic[112], M. Slater[18], T. Slavicek[127], K. Sliwa[162], V. Smakhtin[173], B.H. Smart[46], L. Smestad[118], S.Yu. Smirnov[97], Y. Smirnov[97], L.N. Smirnova[98,ac], O. Smirnova[80], K.M. Smith[53], M. Smizanska[71], K. Smolek[127], A.A. Snesarev[95], G. Snidero[75], J. Snow[112], S. Snyder[25], R. Sobie[170,i], F. Socher[44], J. Sodomka[127], A. Soffer[154], D.A. Soh[152,r], C.A. Solans[30], M. Solar[127], J. Solc[127], E.Yu. Soldatov[97], U. Soldevila[168], E. Solfaroli Camillocci[133a,133b], A.A. Solodkov[129], O.V. Solovyanov[129], V. Solovyev[122], P. Sommer[48], H.Y. Song[33b], N. Soni[1], A. Sood[15], V. Sopko[127], B. Sopko[127], M. Sosebee[8], R. Soualah[165a,165c], P. Soueid[94], A.M. Soukharev[108], D. South[42], S. Spagnolo[72a,72b],

JHEP04(2014)031

F. Spanò[76], W.R. Spearman[57], R. Spighi[20a], G. Spigo[30], M. Spousta[128], T. Spreitzer[159], B. Spurlock[8], R.D. St. Denis[53], J. Stahlman[121], R. Stamen[58a], E. Stanecka[39], R.W. Stanek[6], C. Stanescu[135a], M. Stanescu-Bellu[42], M.M. Stanitzki[42], S. Stapnes[118], E.A. Starchenko[129], J. Stark[55], P. Staroba[126], P. Starovoitov[42], R. Staszewski[39], P. Stavina[145a,*], G. Steele[53], P. Steinberg[25], I. Stekl[127], B. Stelzer[143], H.J. Stelzer[30], O. Stelzer-Chilton[160a], H. Stenzel[52], S. Stern[100], G.A. Stewart[53], J.A. Stillings[21], M.C. Stockton[86], M. Stoebe[86], K. Stoerig[48], G. Stoicea[26a], S. Stonjek[100], A.R. Stradling[8], A. Straessner[44], J. Strandberg[148], S. Strandberg[147a,147b], A. Strandlie[118], E. Strauss[144], M. Strauss[112], P. Strizenec[145b], R. Ströhmer[175], D.M. Strom[115], R. Stroynowski[40], S.A. Stucci[17], B. Stugu[14], I. Stumer[25,*], N.A. Styles[42], D. Su[144], J. Su[124], HS. Subramania[3], R. Subramaniam[78], A. Succurro[12], Y. Sugaya[117], C. Suhr[107], M. Suk[127], V.V. Sulin[95], S. Sultansoy[4c], T. Sumida[67], X. Sun[55], J.E. Sundermann[48], K. Suruliz[140], G. Susinno[37a,37b], M.R. Sutton[150], Y. Suzuki[65], M. Svatos[126], S. Swedish[169], M. Swiatlowski[144], I. Sykora[145a], T. Sykora[128], D. Ta[89], K. Tackmann[42], J. Taenzer[159], A. Taffard[164], R. Tafirout[160a], N. Taiblum[154], Y. Takahashi[102], H. Takai[25], R. Takashima[68], H. Takeda[66], T. Takeshita[141], Y. Takubo[65], M. Talby[84], A.A. Talyshev[108,f], J.Y.C. Tam[175], M.C. Tamsett[78,ad], K.G. Tan[87], J. Tanaka[156], R. Tanaka[116], S. Tanaka[132], S. Tanaka[65], A.J. Tanasijczuk[143], K. Tani[66], N. Tannoury[84], S. Tapprogge[82], S. Tarem[153], F. Tarrade[29], G.F. Tartarelli[90a], P. Tas[128], M. Tasevsky[126], T. Tashiro[67], E. Tassi[37a,37b], A. Tavares Delgado[125a,125b], Y. Tayalati[136d], C. Taylor[77], F.E. Taylor[93], G.N. Taylor[87], W. Taylor[160b], F.A. Teischinger[30], M. Teixeira Dias Castanheira[75], P. Teixeira-Dias[76], K.K. Temming[48], H. Ten Kate[30], P.K. Teng[152], S. Terada[65], K. Terashi[156], J. Terron[81], S. Terzo[100], M. Testa[47], R.J. Teuscher[159,i], J. Therhaag[21], T. Theveneaux-Pelzer[34], S. Thoma[48], J.P. Thomas[18], J. Thomas-Wilsker[76], E.N. Thompson[35], P.D. Thompson[18], P.D. Thompson[159], A.S. Thompson[53], L.A. Thomsen[36], E. Thomson[121], M. Thomson[28], W.M. Thong[87], R.P. Thun[88,*], F. Tian[35], M.J. Tibbetts[15], V.O. Tikhomirov[95,ae], Yu.A. Tikhonov[108,f], S. Timoshenko[97], E. Tiouchichine[84], P. Tipton[177], S. Tisserant[84], T. Todorov[5], S. Todorova-Nova[128], B. Toggerson[164], J. Tojo[69], S. Tokár[145a], K. Tokushuku[65], K. Tollefson[89], L. Tomlinson[83], M. Tomoto[102], L. Tompkins[31], K. Toms[104], N.D. Topilin[64], E. Torrence[115], H. Torres[143], E. Torró Pastor[168], J. Toth[84,z], F. Touchard[84], D.R. Tovey[140], H.L. Tran[116], T. Trefzger[175], L. Tremblet[30], A. Tricoli[30], I.M. Trigger[160a], S. Trincaz-Duvoid[79], M.F. Tripiana[70], N. Triplett[25], W. Trischuk[159], B. Trocmé[55], C. Troncon[90a], M. Trottier-McDonald[143], M. Trovatelli[135a,135b], P. True[89], M. Trzebinski[39], A. Trzupek[39], C. Tsarouchas[30], J.C-L. Tseng[119], P.V. Tsiareshka[91], D. Tsionou[137], G. Tsipolitis[10], N. Tsirintanis[9], S. Tsiskaridze[12], V. Tsiskaridze[48], E.G. Tskhadadze[51a], I.I. Tsukerman[96], V. Tsulaia[15], S. Tsuno[65], D. Tsybychev[149], A. Tua[140], A. Tudorache[26a], V. Tudorache[26a], A.N. Tuna[121], S.A. Tupputi[20a,20b], S. Turchikhin[98,ac], D. Turecek[127], I. Turk Cakir[4d], R. Turra[90a,90b], P.M. Tuts[35], A. Tykhonov[74], M. Tylmad[147a,147b], M. Tyndel[130], K. Uchida[21], I. Ueda[156], R. Ueno[29], M. Ughetto[84], M. Ugland[14], M. Uhlenbrock[21], F. Ukegawa[161], G. Unal[30], A. Undrus[25], G. Unel[164], F.C. Ungaro[48], Y. Unno[65], D. Urbaniec[35], P. Urquijo[21], G. Usai[8], A. Usanova[61], L. Vacavant[84], V. Vacek[127], B. Vachon[86], N. Valencic[106], S. Valentinetti[20a,20b], A. Valero[168], L. Valery[34], S. Valkar[128], E. Valladolid Gallego[168], S. Vallecorsa[49], J.A. Valls Ferrer[168], R. Van Berg[121], P.C. Van Der Deijl[106], R. van der Geer[106], H. van der Graaf[106], R. Van Der Leeuw[106], D. van der Ster[30], N. van Eldik[30], P. van Gemmeren[6], J. Van Nieuwkoop[143], I. van Vulpen[106], M.C. van Woerden[30], M. Vanadia[133a,133b], W. Vandelli[30], A. Vaniachine[6], P. Vankov[42], F. Vannucci[79], G. Vardanyan[178], R. Vari[133a], E.W. Varnes[7], T. Varol[85], D. Varouchas[15], A. Vartapetian[8], K.E. Varvell[151], V.I. Vassilakopoulos[56], F. Vazeille[34], T. Vazquez Schroeder[54], J. Veatch[7], F. Veloso[125a,125c], S. Veneziano[133a], A. Ventura[72a,72b], D. Ventura[85], M. Venturi[48], N. Venturi[159], A. Venturini[23], V. Vercesi[120a], M. Verducci[139], W. Verkerke[106], J.C. Vermeulen[106], A. Vest[44], M.C. Vetterli[143,d], O. Viazlo[80], I. Vichou[166], T. Vickey[146c,af], O.E. Vickey Boeriu[146c], G.H.A. Viehhauser[119], S. Viel[169], R. Vigne[30], M. Villa[20a,20b], M. Villaplana Perez[168], E. Vilucchi[47], M.G. Vincter[29], V.B. Vinogradov[64], J. Virzi[15], O. Vitells[173], I. Vivarelli[150], F. Vives Vaque[3], S. Vlachos[10], D. Vladoiu[99],

JHEP04(2014)031

M. Vlasak[127], A. Vogel[21], P. Vokac[127], G. Volpi[47], M. Volpi[87], H. von der Schmitt[100], H. von Radziewski[48], E. von Toerne[21], V. Vorobel[128], M. Vos[168], R. Voss[30], J.H. Vossebeld[73], N. Vranjes[137], M. Vranjes Milosavljevic[106], V. Vrba[126], M. Vreeswijk[106], T. Vu Anh[48], R. Vuillermet[30], I. Vukotic[31], Z. Vykydal[127], W. Wagner[176], P. Wagner[21], S. Wahrmund[44], J. Wakabayashi[102], J. Walder[71], R. Walker[99], W. Walkowiak[142], R. Wall[177], P. Waller[73], B. Walsh[177], C. Wang[152], C. Wang[45], F. Wang[174], H. Wang[15], H. Wang[40], J. Wang[42], J. Wang[33a], K. Wang[86], R. Wang[104], S.M. Wang[152], T. Wang[21], X. Wang[177], A. Warburton[86], C.P. Ward[28], D.R. Wardrope[77], M. Warsinsky[48], A. Washbrook[46], C. Wasicki[42], I. Watanabe[66], P.M. Watkins[18], A.T. Watson[18], I.J. Watson[151], M.F. Watson[18], G. Watts[139], S. Watts[83], B.M. Waugh[77], S. Webb[83], M.S. Weber[17], S.W. Weber[175], J.S. Webster[31], A.R. Weidberg[119], P. Weigell[100], J. Weingarten[54], C. Weiser[48], H. Weits[106], P.S. Wells[30], T. Wenaus[25], D. Wendland[16], Z. Weng[152,r], T. Wengler[30], S. Wenig[30], N. Wermes[21], M. Werner[48], P. Werner[30], M. Wessels[58a], J. Wetter[162], K. Whalen[29], A. White[8], M.J. White[1], R. White[32b], S. White[123a,123b], D. Whiteson[164], D. Wicke[176], F.J. Wickens[130], W. Wiedenmann[174], M. Wielers[80,c], P. Wienemann[21], C. Wiglesworth[36], L.A.M. Wiik-Fuchs[21], P.A. Wijeratne[77], A. Wildauer[100], M.A. Wildt[42,ag], H.G. Wilkens[30], J.Z. Will[99], H.H. Williams[121], S. Williams[28], C. Willis[89], S. Willocq[85], J.A. Wilson[18], A. Wilson[88], I. Wingerter-Seez[5], S. Winkelmann[48], F. Winklmeier[115], M. Wittgen[144], T. Wittig[43], J. Wittkowski[99], S.J. Wollstadt[82], M.W. Wolter[39], H. Wolters[125a,125c], B.K. Wosiek[39], J. Wotschack[30], M.J. Woudstra[83], K.W. Wozniak[39], M. Wright[53], S.L. Wu[174], X. Wu[49], Y. Wu[88], E. Wulf[35], T.R. Wyatt[83], B.M. Wynne[46], S. Xella[36], M. Xiao[137], D. Xu[33a], L. Xu[33b,ah], B. Yabsley[151], S. Yacoob[146b,ai], M. Yamada[65], H. Yamaguchi[156], Y. Yamaguchi[156], A. Yamamoto[65], K. Yamamoto[63], S. Yamamoto[156], T. Yamamura[156], T. Yamanaka[156], K. Yamauchi[102], Y. Yamazaki[66], Z. Yan[22], H. Yang[33e], H. Yang[174], U.K. Yang[83], Y. Yang[110], S. Yanush[92], L. Yao[33a], W-M. Yao[15], Y. Yasu[65], E. Yatsenko[42], K.H. Yau Wong[21], J. Ye[40], S. Ye[25], A.L. Yen[57], E. Yildirim[42], M. Yilmaz[4b], R. Yoosoofmiya[124], K. Yorita[172], R. Yoshida[6], K. Yoshihara[156], C. Young[144], C.J.S. Young[30], S. Youssef[22], D.R. Yu[15], J. Yu[8], J.M. Yu[88], J. Yu[113], L. Yuan[66], A. Yurkewicz[107], B. Zabinski[39], R. Zaidan[62], A.M. Zaitsev[129,w], A. Zaman[149], S. Zambito[23], L. Zanello[133a,133b], D. Zanzi[100], A. Zaytsev[25], C. Zeitnitz[176], M. Zeman[127], A. Zemla[38a], K. Zengel[23], O. Zenin[129], T. Ženiš[145a], D. Zerwas[116], G. Zevi della Porta[57], D. Zhang[88], F. Zhang[174], H. Zhang[89], J. Zhang[6], L. Zhang[152], X. Zhang[33d], Z. Zhang[116], Z. Zhao[33b], A. Zhemchugov[64], J. Zhong[119], B. Zhou[88], L. Zhou[35], N. Zhou[164], C.G. Zhu[33d], H. Zhu[33a], J. Zhu[88], Y. Zhu[33b], X. Zhuang[33a], A. Zibell[99], D. Zieminska[60], N.I. Zimine[64], C. Zimmermann[82], R. Zimmermann[21], S. Zimmermann[21], S. Zimmermann[48], Z. Zinonos[54], M. Ziolkowski[142], R. Zitoun[5], G. Zobernig[174], A. Zoccoli[20a,20b], M. zur Nedden[16], G. Zurzolo[103a,103b], V. Zutshi[107], L. Zwalinski[30]

[1] School of Chemistry and Physics, University of Adelaide, Adelaide, Australia
[2] Physics Department, SUNY Albany, Albany NY, United States of America
[3] Department of Physics, University of Alberta, Edmonton AB, Canada
[4] [(a)] Department of Physics, Ankara University, Ankara; [(b)] Department of Physics, Gazi University, Ankara; [(c)] Division of Physics, TOBB University of Economics and Technology, Ankara; [(d)] Turkish Atomic Energy Authority, Ankara, Turkey
[5] LAPP, CNRS/IN2P3 and Université de Savoie, Annecy-le-Vieux, France
[6] High Energy Physics Division, Argonne National Laboratory, Argonne IL, United States of America
[7] Department of Physics, University of Arizona, Tucson AZ, United States of America
[8] Department of Physics, The University of Texas at Arlington, Arlington TX, United States of America
[9] Physics Department, University of Athens, Athens, Greece
[10] Physics Department, National Technical University of Athens, Zografou, Greece
[11] Institute of Physics, Azerbaijan Academy of Sciences, Baku, Azerbaijan
[12] Institut de Física d'Altes Energies and Departament de Física de la Universitat Autònoma de Barcelona, Barcelona, Spain

JHEP04(2014)031

[13] [(a)] Institute of Physics, University of Belgrade, Belgrade; [(b)] Vinca Institute of Nuclear Sciences, University of Belgrade, Belgrade, Serbia
[14] Department for Physics and Technology, University of Bergen, Bergen, Norway
[15] Physics Division, Lawrence Berkeley National Laboratory and University of California, Berkeley CA, United States of America
[16] Department of Physics, Humboldt University, Berlin, Germany
[17] Albert Einstein Center for Fundamental Physics and Laboratory for High Energy Physics, University of Bern, Bern, Switzerland
[18] School of Physics and Astronomy, University of Birmingham, Birmingham, United Kingdom
[19] [(a)] Department of Physics, Bogazici University, Istanbul; [(b)] Department of Physics, Dogus University, Istanbul; [(c)] Department of Physics Engineering, Gaziantep University, Gaziantep, Turkey
[20] [(a)] INFN Sezione di Bologna; [(b)] Dipartimento di Fisica e Astronomia, Università di Bologna, Bologna, Italy
[21] Physikalisches Institut, University of Bonn, Bonn, Germany
[22] Department of Physics, Boston University, Boston MA, United States of America
[23] Department of Physics, Brandeis University, Waltham MA, United States of America
[24] [(a)] Universidade Federal do Rio De Janeiro COPPE/EE/IF, Rio de Janeiro; [(b)] Federal University of Juiz de Fora (UFJF), Juiz de Fora; [(c)] Federal University of Sao Joao del Rei (UFSJ), Sao Joao del Rei; [(d)] Instituto de Fisica, Universidade de Sao Paulo, Sao Paulo, Brazil
[25] Physics Department, Brookhaven National Laboratory, Upton NY, United States of America
[26] [(a)] National Institute of Physics and Nuclear Engineering, Bucharest; [(b)] National Institute for Research and Development of Isotopic and Molecular Technologies, Physics Department, Cluj Napoca; [(c)] University Politehnica Bucharest, Bucharest; [(d)] West University in Timisoara, Timisoara, Romania
[27] Departamento de Física, Universidad de Buenos Aires, Buenos Aires, Argentina
[28] Cavendish Laboratory, University of Cambridge, Cambridge, United Kingdom
[29] Department of Physics, Carleton University, Ottawa ON, Canada
[30] CERN, Geneva, Switzerland
[31] Enrico Fermi Institute, University of Chicago, Chicago IL, United States of America
[32] [(a)] Departamento de Física, Pontificia Universidad Católica de Chile, Santiago; [(b)] Departamento de Física, Universidad Técnica Federico Santa María, Valparaíso, Chile
[33] [(a)] Institute of High Energy Physics, Chinese Academy of Sciences, Beijing; [(b)] Department of Modern Physics, University of Science and Technology of China, Anhui; [(c)] Department of Physics, Nanjing University, Jiangsu; [(d)] School of Physics, Shandong University, Shandong; [(e)] Physics Department, Shanghai Jiao Tong University, Shanghai, China
[34] Laboratoire de Physique Corpusculaire, Clermont Université and Université Blaise Pascal and CNRS/IN2P3, Clermont-Ferrand, France
[35] Nevis Laboratory, Columbia University, Irvington NY, United States of America
[36] Niels Bohr Institute, University of Copenhagen, Kobenhavn, Denmark
[37] [(a)] INFN Gruppo Collegato di Cosenza, Laboratori Nazionali di Frascati; [(b)] Dipartimento di Fisica, Università della Calabria, Rende, Italy
[38] [(a)] AGH University of Science and Technology, Faculty of Physics and Applied Computer Science, Krakow; [(b)] Marian Smoluchowski Institute of Physics, Jagiellonian University, Krakow, Poland
[39] The Henryk Niewodniczanski Institute of Nuclear Physics, Polish Academy of Sciences, Krakow, Poland
[40] Physics Department, Southern Methodist University, Dallas TX, United States of America
[41] Physics Department, University of Texas at Dallas, Richardson TX, United States of America
[42] DESY, Hamburg and Zeuthen, Germany
[43] Institut für Experimentelle Physik IV, Technische Universität Dortmund, Dortmund, Germany
[44] Institut für Kern- und Teilchenphysik, Technische Universität Dresden, Dresden, Germany
[45] Department of Physics, Duke University, Durham NC, United States of America
[46] SUPA - School of Physics and Astronomy, University of Edinburgh, Edinburgh, United Kingdom

JHEP04(2014)031

[47] INFN Laboratori Nazionali di Frascati, Frascati, Italy
[48] Fakultät für Mathematik und Physik, Albert-Ludwigs-Universität, Freiburg, Germany
[49] Section de Physique, Université de Genève, Geneva, Switzerland
[50] [(a)] INFN Sezione di Genova; [(b)] Dipartimento di Fisica, Università di Genova, Genova, Italy
[51] [(a)] E. Andronikashvili Institute of Physics, Iv. Javakhishvili Tbilisi State University, Tbilisi; [(b)] High Energy Physics Institute, Tbilisi State University, Tbilisi, Georgia
[52] II Physikalisches Institut, Justus-Liebig-Universität Giessen, Giessen, Germany
[53] SUPA - School of Physics and Astronomy, University of Glasgow, Glasgow, United Kingdom
[54] II Physikalisches Institut, Georg-August-Universität, Göttingen, Germany
[55] Laboratoire de Physique Subatomique et de Cosmologie, Université Joseph Fourier and CNRS/IN2P3 and Institut National Polytechnique de Grenoble, Grenoble, France
[56] Department of Physics, Hampton University, Hampton VA, United States of America
[57] Laboratory for Particle Physics and Cosmology, Harvard University, Cambridge MA, United States of America
[58] [(a)] Kirchhoff-Institut für Physik, Ruprecht-Karls-Universität Heidelberg, Heidelberg; [(b)] Physikalisches Institut, Ruprecht-Karls-Universität Heidelberg, Heidelberg; [(c)] ZITI Institut für technische Informatik, Ruprecht-Karls-Universität Heidelberg, Mannheim, Germany
[59] Faculty of Applied Information Science, Hiroshima Institute of Technology, Hiroshima, Japan
[60] Department of Physics, Indiana University, Bloomington IN, United States of America
[61] Institut für Astro- und Teilchenphysik, Leopold-Franzens-Universität, Innsbruck, Austria
[62] University of Iowa, Iowa City IA, United States of America
[63] Department of Physics and Astronomy, Iowa State University, Ames IA, United States of America
[64] Joint Institute for Nuclear Research, JINR Dubna, Dubna, Russia
[65] KEK, High Energy Accelerator Research Organization, Tsukuba, Japan
[66] Graduate School of Science, Kobe University, Kobe, Japan
[67] Faculty of Science, Kyoto University, Kyoto, Japan
[68] Kyoto University of Education, Kyoto, Japan
[69] Department of Physics, Kyushu University, Fukuoka, Japan
[70] Instituto de Física La Plata, Universidad Nacional de La Plata and CONICET, La Plata, Argentina
[71] Physics Department, Lancaster University, Lancaster, United Kingdom
[72] [(a)] INFN Sezione di Lecce; [(b)] Dipartimento di Matematica e Fisica, Università del Salento, Lecce, Italy
[73] Oliver Lodge Laboratory, University of Liverpool, Liverpool, United Kingdom
[74] Department of Physics, Jožef Stefan Institute and University of Ljubljana, Ljubljana, Slovenia
[75] School of Physics and Astronomy, Queen Mary University of London, London, United Kingdom
[76] Department of Physics, Royal Holloway University of London, Surrey, United Kingdom
[77] Department of Physics and Astronomy, University College London, London, United Kingdom
[78] Louisiana Tech University, Ruston LA, United States of America
[79] Laboratoire de Physique Nucléaire et de Hautes Energies, UPMC and Université Paris-Diderot and CNRS/IN2P3, Paris, France
[80] Fysiska institutionen, Lunds universitet, Lund, Sweden
[81] Departamento de Fisica Teorica C-15, Universidad Autonoma de Madrid, Madrid, Spain
[82] Institut für Physik, Universität Mainz, Mainz, Germany
[83] School of Physics and Astronomy, University of Manchester, Manchester, United Kingdom
[84] CPPM, Aix-Marseille Université and CNRS/IN2P3, Marseille, France
[85] Department of Physics, University of Massachusetts, Amherst MA, United States of America
[86] Department of Physics, McGill University, Montreal QC, Canada
[87] School of Physics, University of Melbourne, Victoria, Australia
[88] Department of Physics, The University of Michigan, Ann Arbor MI, United States of America
[89] Department of Physics and Astronomy, Michigan State University, East Lansing MI, United States of America
[90] [(a)] INFN Sezione di Milano; [(b)] Dipartimento di Fisica, Università di Milano, Milano, Italy

JHEP04(2014)031

[91] B.I. Stepanov Institute of Physics, National Academy of Sciences of Belarus, Minsk, Republic of Belarus
[92] National Scientific and Educational Centre for Particle and High Energy Physics, Minsk, Republic of Belarus
[93] Department of Physics, Massachusetts Institute of Technology, Cambridge MA, United States of America
[94] Group of Particle Physics, University of Montreal, Montreal QC, Canada
[95] P.N. Lebedev Institute of Physics, Academy of Sciences, Moscow, Russia
[96] Institute for Theoretical and Experimental Physics (ITEP), Moscow, Russia
[97] Moscow Engineering and Physics Institute (MEPhI), Moscow, Russia
[98] D.V.Skobeltsyn Institute of Nuclear Physics, M.V.Lomonosov Moscow State University, Moscow, Russia
[99] Fakultät für Physik, Ludwig-Maximilians-Universität München, München, Germany
[100] Max-Planck-Institut für Physik (Werner-Heisenberg-Institut), München, Germany
[101] Nagasaki Institute of Applied Science, Nagasaki, Japan
[102] Graduate School of Science and Kobayashi-Maskawa Institute, Nagoya University, Nagoya, Japan
[103] [(a)] INFN Sezione di Napoli; [(b)] Dipartimento di Scienze Fisiche, Università di Napoli, Napoli, Italy
[104] Department of Physics and Astronomy, University of New Mexico, Albuquerque NM, United States of America
[105] Institute for Mathematics, Astrophysics and Particle Physics, Radboud University Nijmegen/Nikhef, Nijmegen, Netherlands
[106] Nikhef National Institute for Subatomic Physics and University of Amsterdam, Amsterdam, Netherlands
[107] Department of Physics, Northern Illinois University, DeKalb IL, United States of America
[108] Budker Institute of Nuclear Physics, SB RAS, Novosibirsk, Russia
[109] Department of Physics, New York University, New York NY, United States of America
[110] Ohio State University, Columbus OH, United States of America
[111] Faculty of Science, Okayama University, Okayama, Japan
[112] Homer L. Dodge Department of Physics and Astronomy, University of Oklahoma, Norman OK, United States of America
[113] Department of Physics, Oklahoma State University, Stillwater OK, United States of America
[114] Palacký University, RCPTM, Olomouc, Czech Republic
[115] Center for High Energy Physics, University of Oregon, Eugene OR, United States of America
[116] LAL, Université Paris-Sud and CNRS/IN2P3, Orsay, France
[117] Graduate School of Science, Osaka University, Osaka, Japan
[118] Department of Physics, University of Oslo, Oslo, Norway
[119] Department of Physics, Oxford University, Oxford, United Kingdom
[120] [(a)] INFN Sezione di Pavia; [(b)] Dipartimento di Fisica, Università di Pavia, Pavia, Italy
[121] Department of Physics, University of Pennsylvania, Philadelphia PA, United States of America
[122] Petersburg Nuclear Physics Institute, Gatchina, Russia
[123] [(a)] INFN Sezione di Pisa; [(b)] Dipartimento di Fisica E. Fermi, Università di Pisa, Pisa, Italy
[124] Department of Physics and Astronomy, University of Pittsburgh, Pittsburgh PA, United States of America
[125] [(a)] Laboratorio de Instrumentacao e Fisica Experimental de Particulas - LIP, Lisboa; [(b)] Faculdade de Ciências, Universidade de Lisboa, Lisboa; [(c)] Department of Physics, University of Coimbra, Coimbra; [(d)] Centro de Física Nuclear da Universidade de Lisboa, Lisboa; [(e)] Departamento de Fisica, Universidade do Minho, Braga, Portugal; [(f)] Departamento de Fisica Teorica y del Cosmos and CAFPE, Universidad de Granada, Granada, Spain; [(g)] Dep Fisica and CEFITEC of Faculdade de Ciencias e Tecnologia, Universidade Nova de Lisboa, Caparica, Portugal
[126] Institute of Physics, Academy of Sciences of the Czech Republic, Praha, Czech Republic
[127] Czech Technical University in Prague, Praha, Czech Republic
[128] Faculty of Mathematics and Physics, Charles University in Prague, Praha, Czech Republic

JHEP04(2014)031

[129] State Research Center Institute for High Energy Physics, Protvino, Russia
[130] Particle Physics Department, Rutherford Appleton Laboratory, Didcot, United Kingdom
[131] Physics Department, University of Regina, Regina SK, Canada
[132] Ritsumeikan University, Kusatsu, Shiga, Japan
[133] [a] INFN Sezione di Roma; [b] Dipartimento di Fisica, Sapienza Università di Roma, Roma, Italy
[134] [a] INFN Sezione di Roma Tor Vergata; [b] Dipartimento di Fisica, Università di Roma Tor Vergata, Roma, Italy
[135] [a] INFN Sezione di Roma Tre; [b] Dipartimento di Matematica e Fisica, Università Roma Tre, Roma, Italy
[136] [a] Faculté des Sciences Ain Chock, Réseau Universitaire de Physique des Hautes Energies - Université Hassan II, Casablanca; [b] Centre National de l'Energie des Sciences Techniques Nucleaires, Rabat; [c] Faculté des Sciences Semlalia, Université Cadi Ayyad, LPHEA-Marrakech; [d] Faculté des Sciences, Université Mohamed Premier and LPTPM, Oujda; [e] Faculté des sciences, Université Mohammed V-Agdal, Rabat, Morocco
[137] DSM/IRFU (Institut de Recherches sur les Lois Fondamentales de l'Univers), CEA Saclay (Commissariat à l'Energie Atomique et aux Energies Alternatives), Gif-sur-Yvette, France
[138] Santa Cruz Institute for Particle Physics, University of California Santa Cruz, Santa Cruz CA, United States of America
[139] Department of Physics, University of Washington, Seattle WA, United States of America
[140] Department of Physics and Astronomy, University of Sheffield, Sheffield, United Kingdom
[141] Department of Physics, Shinshu University, Nagano, Japan
[142] Fachbereich Physik, Universität Siegen, Siegen, Germany
[143] Department of Physics, Simon Fraser University, Burnaby BC, Canada
[144] SLAC National Accelerator Laboratory, Stanford CA, United States of America
[145] [a] Faculty of Mathematics, Physics & Informatics, Comenius University, Bratislava; [b] Department of Subnuclear Physics, Institute of Experimental Physics of the Slovak Academy of Sciences, Kosice, Slovak Republic
[146] [a] Department of Physics, University of Cape Town, Cape Town; [b] Department of Physics, University of Johannesburg, Johannesburg; [c] School of Physics, University of the Witwatersrand, Johannesburg, South Africa
[147] [a] Department of Physics, Stockholm University; [b] The Oskar Klein Centre, Stockholm, Sweden
[148] Physics Department, Royal Institute of Technology, Stockholm, Sweden
[149] Departments of Physics & Astronomy and Chemistry, Stony Brook University, Stony Brook NY, United States of America
[150] Department of Physics and Astronomy, University of Sussex, Brighton, United Kingdom
[151] School of Physics, University of Sydney, Sydney, Australia
[152] Institute of Physics, Academia Sinica, Taipei, Taiwan
[153] Department of Physics, Technion: Israel Institute of Technology, Haifa, Israel
[154] Raymond and Beverly Sackler School of Physics and Astronomy, Tel Aviv University, Tel Aviv, Israel
[155] Department of Physics, Aristotle University of Thessaloniki, Thessaloniki, Greece
[156] International Center for Elementary Particle Physics and Department of Physics, The University of Tokyo, Tokyo, Japan
[157] Graduate School of Science and Technology, Tokyo Metropolitan University, Tokyo, Japan
[158] Department of Physics, Tokyo Institute of Technology, Tokyo, Japan
[159] Department of Physics, University of Toronto, Toronto ON, Canada
[160] [a] TRIUMF, Vancouver BC; [b] Department of Physics and Astronomy, York University, Toronto ON, Canada
[161] Faculty of Pure and Applied Sciences, University of Tsukuba, Tsukuba, Japan
[162] Department of Physics and Astronomy, Tufts University, Medford MA, United States of America
[163] Centro de Investigaciones, Universidad Antonio Narino, Bogota, Colombia
[164] Department of Physics and Astronomy, University of California Irvine, Irvine CA, United States of America

JHEP04(2014)031

[165] [(a)] INFN Gruppo Collegato di Udine, Sezione di Trieste; [(b)] ICTP, Trieste; [(c)] Dipartimento di Chimica, Fisica e Ambiente, Università di Udine, Udine, Italy
[166] Department of Physics, University of Illinois, Urbana IL, United States of America
[167] Department of Physics and Astronomy, University of Uppsala, Uppsala, Sweden
[168] Instituto de Física Corpuscular (IFIC) and Departamento de Física Atómica, Molecular y Nuclear and Departamento de Ingeniería Electrónica and Instituto de Microelectrónica de Barcelona (IMB-CNM), University of Valencia and CSIC, Valencia, Spain
[169] Department of Physics, University of British Columbia, Vancouver BC, Canada
[170] Department of Physics and Astronomy, University of Victoria, Victoria BC, Canada
[171] Department of Physics, University of Warwick, Coventry, United Kingdom
[172] Waseda University, Tokyo, Japan
[173] Department of Particle Physics, The Weizmann Institute of Science, Rehovot, Israel
[174] Department of Physics, University of Wisconsin, Madison WI, United States of America
[175] Fakultät für Physik und Astronomie, Julius-Maximilians-Universität, Würzburg, Germany
[176] Fachbereich C Physik, Bergische Universität Wuppertal, Wuppertal, Germany
[177] Department of Physics, Yale University, New Haven CT, United States of America
[178] Yerevan Physics Institute, Yerevan, Armenia
[179] Centre de Calcul de l'Institut National de Physique Nucléaire et de Physique des Particules (IN2P3), Villeurbanne, France

[a] Also at Department of Physics, King's College London, London, United Kingdom
[b] Also at Institute of Physics, Azerbaijan Academy of Sciences, Baku, Azerbaijan
[c] Also at Particle Physics Department, Rutherford Appleton Laboratory, Didcot, United Kingdom
[d] Also at TRIUMF, Vancouver BC, Canada
[e] Also at Department of Physics, California State University, Fresno CA, United States of America
[f] Also at Novosibirsk State University, Novosibirsk, Russia
[g] Also at CPPM, Aix-Marseille Université and CNRS/IN2P3, Marseille, France
[h] Also at Università di Napoli Parthenope, Napoli, Italy
[i] Also at Institute of Particle Physics (IPP), Canada
[j] Also at Department of Physics and Astronomy, Michigan State University, East Lansing MI, United States of America
[k] Also at Department of Financial and Management Engineering, University of the Aegean, Chios, Greece
[l] Also at Louisiana Tech University, Ruston LA, United States of America
[m] Also at Institucio Catalana de Recerca i Estudis Avancats, ICREA, Barcelona, Spain
[n] Also at CERN, Geneva, Switzerland
[o] Also at Ochadai Academic Production, Ochanomizu University, Tokyo, Japan
[p] Also at Manhattan College, New York NY, United States of America
[q] Also at Institute of Physics, Academia Sinica, Taipei, Taiwan
[r] Also at School of Physics and Engineering, Sun Yat-sen University, Guangzhou, China
[s] Also at Academia Sinica Grid Computing, Institute of Physics, Academia Sinica, Taipei, Taiwan
[t] Also at Laboratoire de Physique Nucléaire et de Hautes Energies, UPMC and Université Paris-Diderot and CNRS/IN2P3, Paris, France
[u] Also at School of Physical Sciences, National Institute of Science Education and Research, Bhubaneswar, India
[v] Also at Dipartimento di Fisica, Sapienza Università di Roma, Roma, Italy
[w] Also at Moscow Institute of Physics and Technology State University, Dolgoprudny, Russia
[x] Also at section de Physique, Université de Genève, Geneva, Switzerland
[y] Also at Department of Physics, The University of Texas at Austin, Austin TX, United States of America
[z] Also at Institute for Particle and Nuclear Physics, Wigner Research Centre for Physics, Budapest, Hungary
[aa] Also at International School for Advanced Studies (SISSA), Trieste, Italy

JHEP04(2014)031

[ab] Also at Department of Physics and Astronomy, University of South Carolina, Columbia SC, United States of America
[ac] Also at Faculty of Physics, M.V.Lomonosov Moscow State University, Moscow, Russia
[ad] Also at Physics Department, Brookhaven National Laboratory, Upton NY, United States of America
[ae] Also at Moscow Engineering and Physics Institute (MEPhI), Moscow, Russia
[af] Also at Department of Physics, Oxford University, Oxford, United Kingdom
[ag] Also at Institut für Experimentalphysik, Universität Hamburg, Hamburg, Germany
[ah] Also at Department of Physics, The University of Michigan, Ann Arbor MI, United States of America
[ai] Also at Discipline of Physics, University of KwaZulu-Natal, Durban, South Africa
[*] Deceased

JHEP04(2014)031